PETROGRAPHY AND GEOCEHMISTRY OF ANHYDRITE UNITS FROM THE CANADIAN SALT COMPANY MINE, PUGWASH, CUMBERLAND COUNTY, NOVA SCOTIA

by

Peter A. Rose

Thesis submitted in partial fulfillment of the requirements for a Bachelor of Science with Honours in geology.

Dalhousie University

March 4 , 1987

Distribution License

DalSpace requires agreement to this non-exclusive distribution license before your item can appear on DalSpace.

NON-EXCLUSIVE DISTRIBUTION LICENSE

You (the author(s) or copyright owner) grant to Dalhousie University the non-exclusive right to reproduce and distribute your submission worldwide in any medium.

You agree that Dalhousie University may, without changing the content, reformat the submission for the purpose of preservation.

You also agree that Dalhousie University may keep more than one copy of this submission for purposes of security, back-up and preservation.

You agree that the submission is your original work, and that you have the right to grant the rights contained in this license. You also agree that your submission does not, to the best of your knowledge, infringe upon anyone's copyright.

If the submission contains material for which you do not hold copyright, you agree that you have obtained the unrestricted permission of the copyright owner to grant Dalhousie University the rights required by this license, and that such third-party owned material is clearly identified and acknowledged within the text or content of the submission.

If the submission is based upon work that has been sponsored or supported by an agency or organization other than Dalhousie University, you assert that you have fulfilled any right of review or other obligations required by such contract or agreement.

Dalhousie University will clearly identify your name(s) as the author(s) or owner(s) of the submission, and will not make any alteration to the content of the files that you have submitted.

If you have questions regarding this license please contact the repository manager at dalspace@dal.ca.

Grant the distribution license by signing and dating below.

_____ _____

Name of signatory Date

Table of Contents

List of Figures

List of Plates

Abstract

Evaporitic rocks exposed in the workings of the Canadian Salt Company Mine at Pugwash, Nova Scotia consist of massive, nodular and stylolitic anhydrite and clear white, reddish brown to black halite with minor occurences of carnallite and sylvite. The anhydrite and halite occur both as thick beds and as thinly bedded intervals transitional to each other. The beds exposed in the mine are intensely deformed and are generally steeply dipping (i.e. 60-70 degrees).

The division of anhydrite into well defined units has been the subject of some debate. Based on macroscopic observations anhydrite has been divided by different authors into two, three and even ten distinct units. At the present time the most likely division of the anhydrites appears to be a threefold one.

Representative core samples have been collected from four diamond drill holes from the 192 m (630 ft.) and 250 m (830 ft.) levels of the mine. The drill holes were carefully chosen in an attempt to represent type sections through three macroscopically different anhydrite bodies. This study proves the validity of the current division of anhydrite into three units using techniques such as petrographic microscopy and geochemistry. Based on mineralogies and textures observed in thin sections and on differences in chemical composition, three anhydrite units are recognized. Each of the three anhydrite units has been subjected to a complex sequence of diagenetic processes. Mineral replacements such as calcite psueudomorphs after anhydrite and diagenetic products such as borate nodules and elemental sulfur make the present appearance of the three units very different. The shaft anhydrite was probably deposited in shallow water and may have been subjected to periodic subaerial exposure. The borate anhydrite was probably deposited under more saline conditions than the shaft anhydrite.

Acknowledgements

I would like to thank Dr. Paul Schenk for his kind help and encouragement. I am deeply indebted to Dave Carter of the Nova Scotia Department of Mines and Energy. He suggested the project, provided thin sections and geochemical data and kindly permitted the use of computers, microscopes and photographic equipment at the Nova Scotia Department of Mines and Energy. In addition he provided helpful suggestions and criticism throughout the project. Bob Boehner of the Department of Mines provided excellent advice on geochemical data. Linda Richard also provided valuable help with geochemistry. Ryo Matsumoto helped to stain core chips and provided several useful suggestions. I am also grateful for the help of my mother, Jean Rose, who recovered my thesis after it was stolen from my car.

I. INTRODUCTION

I.i Purpose of Study

This thesis provides a detailed description of anhydrite occurrences exposed in the workings of the Canadian Salt Company Mine at Pugwash, Nova Scotia. Portions of this work will be included in a more comprehensive study of the deposit by D. C. Carter, Nova Scotia Department of Mines and Energy, Mineral Resources Division.

The thesis has three major objectives: 1) to provide detailed petrographic descriptions of anhydrite thin sections from three anhydrite units that have been separated macroscpically; 2) to determine if it is possible to microscopically distinguish these three anhydrite units; and 3) to investigate the geochemistry of 74 anhydrite samples from the deposit. This thesis should make three contributions: 1) aid in understanding the complicated stratigraphy of the Pugwash evaporite deposit; 2) form a basis for the future study of anhydrite in the deposit; and 3) provide information useful to the future development and planning of the Pugwash Salt Mine.

I.ii Location and Access

The evaporite deposit at Pugwash is located in northeastern Cumberland County to the south and west of the town of Pugwash (NTS 11E/13E) (see Figure 1-1 and 1-2). Paved roads leading into Pugwash include Route 6 from Pictou to Amherst, Route 321 approximately 30 km east of Oxford and Route 368 from Wentworth.

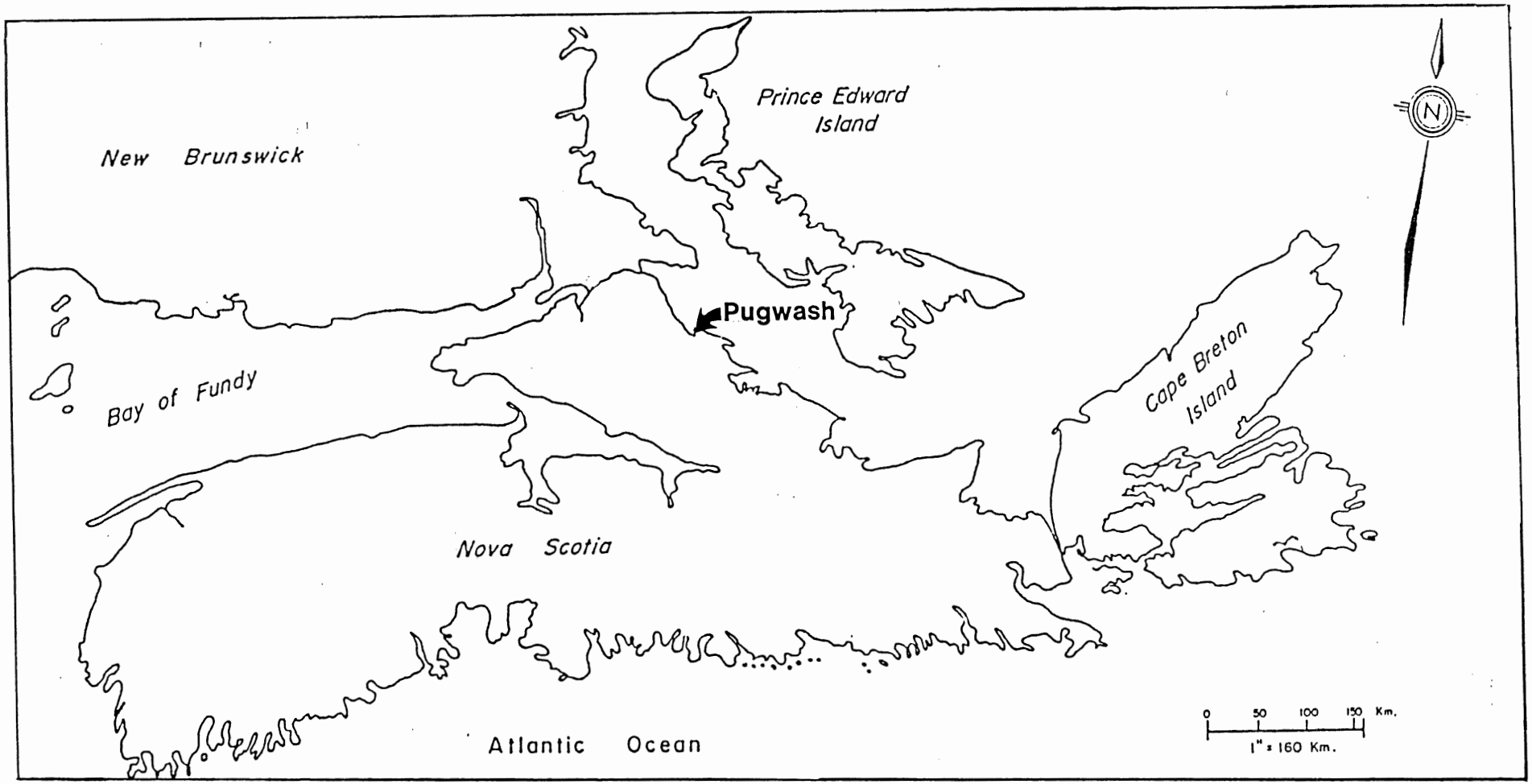

Figure 1-1. Location map showing the study area in relation to the Maritime provinces.

I.iii Research Methods

This study of anydrite from the Pugwash Mine is based on core from four diamond drill holes (Figure 1-3, 1-4 and 1-5). Samples collected from these four holes will be used to represent type sections through what may be three distinct anhydrite units. D. C. Carter of the Nova Scotia Department of Mines and Energy collected the samples during the 1986 field season.

104 thin sections were cut and 74 samples were chemically analysed. Thin sections were described and classified according to the scheme of Maiklem et al. (1969). Geochemical data were statistically analyzed.

I.iv General Geology of the Windsor Group

The Windsor Group in Nova Scotia consists of interbedded marine and nonmarine sediments deposited in a complex subsiding basin system. The only demonstrable marine incursion into this basin occurred during the Visean with the deposition of marine carbonates, evaporites, and siltstones (Bell, 1929; Schenk , 1967; McCutcheon, 1981; Carter and Pickerill, 1985). This basin has been referred to as the Fundy Basin, Fundy Epieugeosyncline (Bell, 1929, 1958) Fundy Aulocogene (Keppie, 1977), Magdalen Basin (Keppie 1982a,b) and Maritimes Basin (Roliff, 1962; Knight, 1983).

The Windsor Group generally consists of more than 50% evaporites, mainly anhydrite, gypsum, and halite with minor but in places economic potash deposits. Evaporites occur as thick and

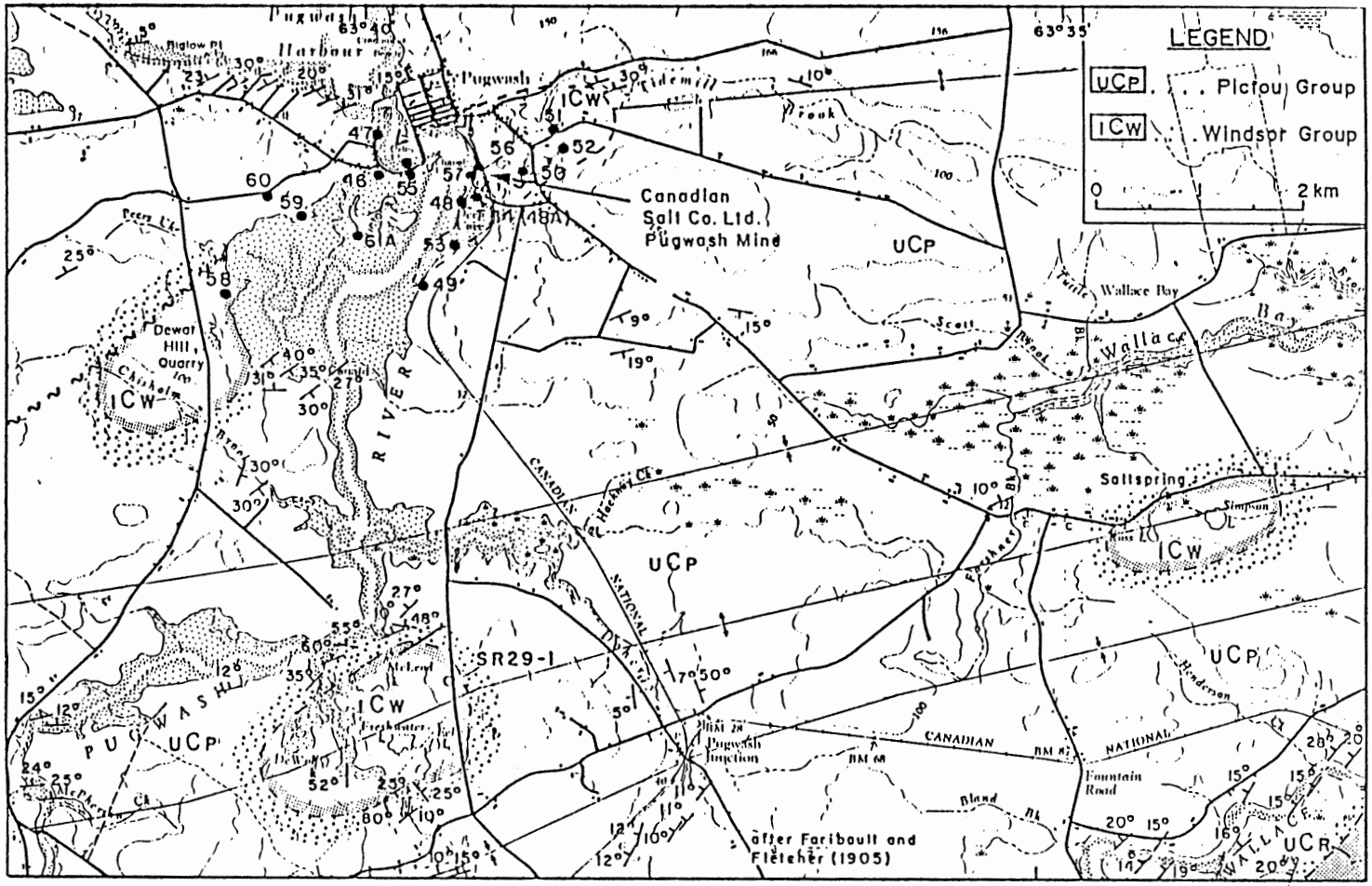

Figure 1-2. Pugwash area: geology and location map (after Faribault and Fletcher, 1905).

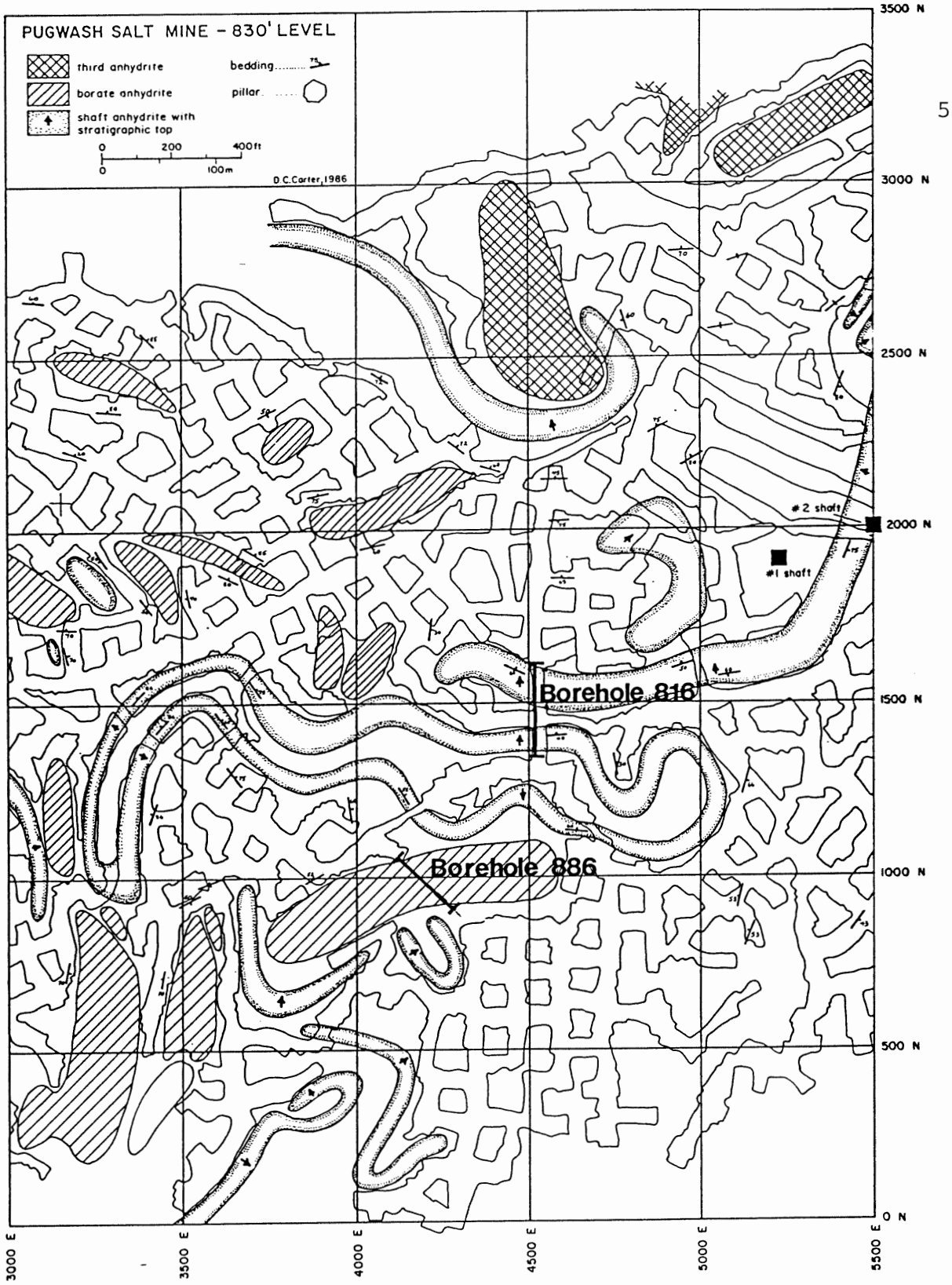

Figure 1-3. Location of boreholes P-886 and P-816, 250 m level (830 feet), Pugwash Salt Mine (Carter, 1986).

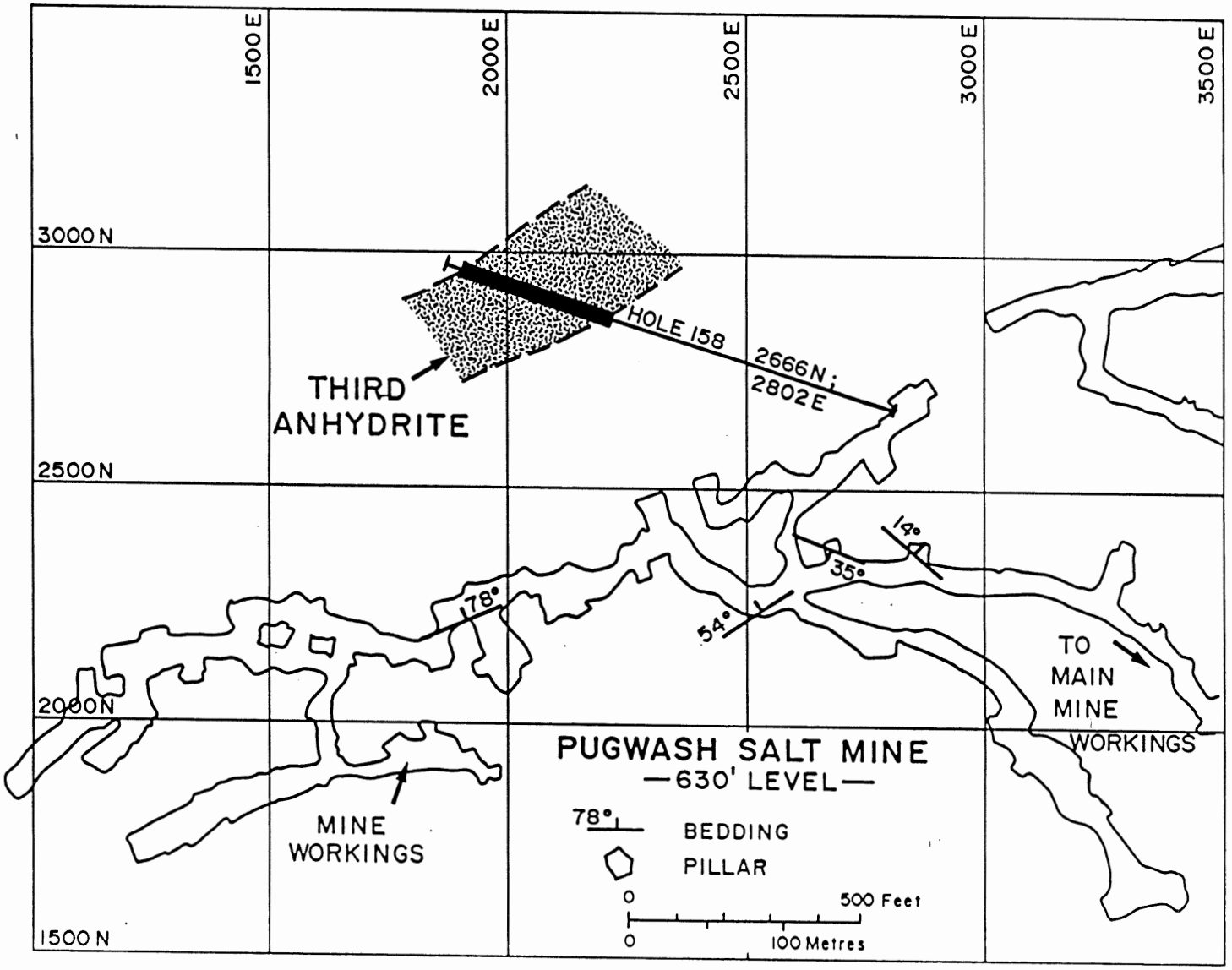

Figure 1-4. Location of borehole P-158, 192 m level (630 Foot), Pugwash Salt Mine.

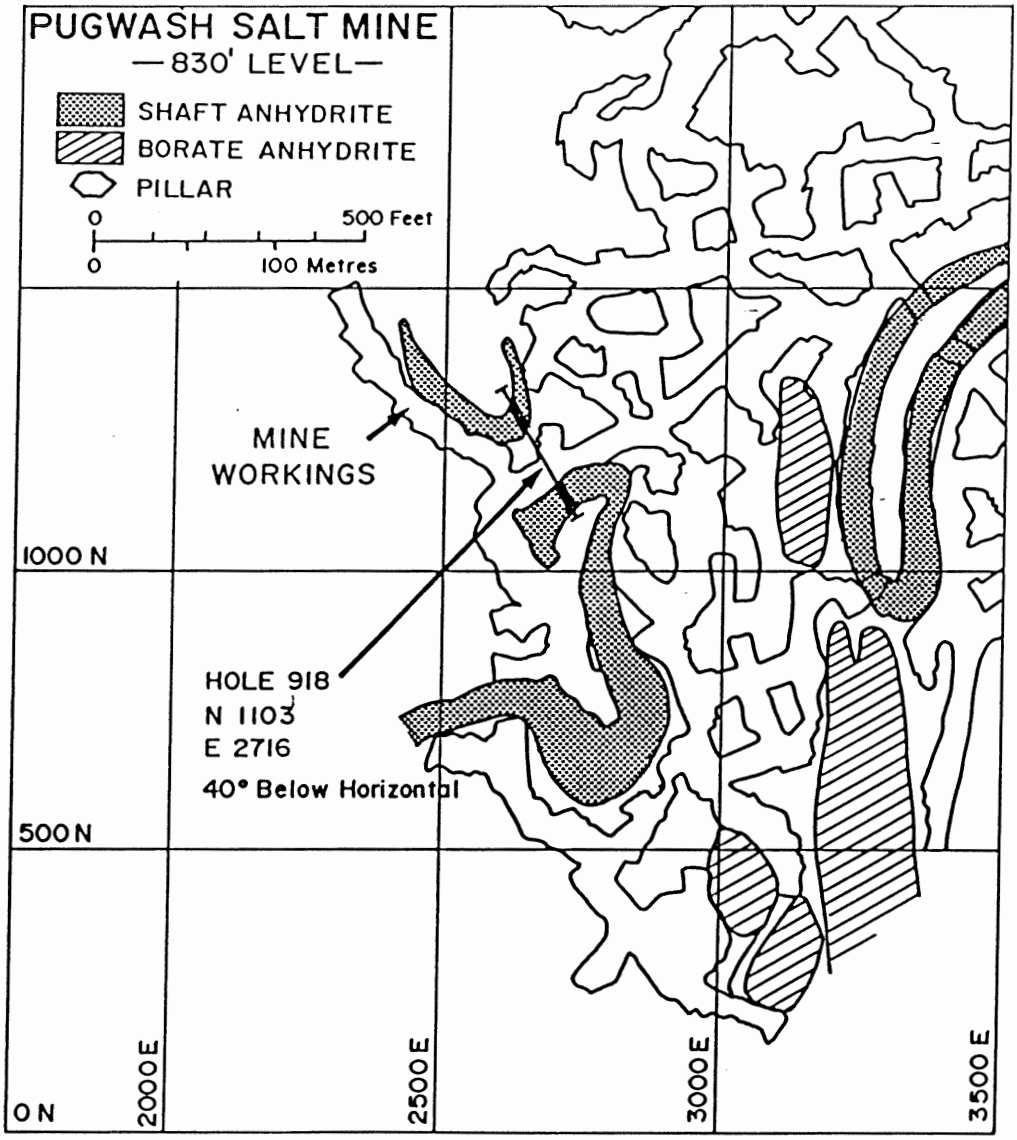

Figure 1-5. Location of borehole P-918, 250 m level (830 foot), Pugwash Salt Mine.

thin beds interbedded and closely associated with fossiliferous marine limestone and dolostone, and red and green terrigenous siliciclastic sediments (Boehner, 1986).

I. v. Geology of the Windsor Group in the Pugwash Area

The evaporite deposit at Pugwash occurs at the eastern end of the east-west trending Cumberland Basin, the largest Carboniferous structural basin in Nova Scotia. Strata range in age from Stephanian to Tournaisian and consist mainly of fine- and coarse-grained alluvial-fluvial continental siliciclastics with marine evaporites and marine carbonates. This complex sequence was deposited to the north of the Cobequid Highlands following the Acadian Orogeny (Boehner et al., 1985).

The first detailed geological mapping of the Pugwash area was by Faribault and Fletcher (1905) (Fig. 1-2). Their map as well as that of Evans (1972), shows Windsor Group strata (including limestone, shale and gypsum) exposed in the Pugwash area in an elliptical-shaped diapir. The ellipse of Windsor Group sediments is approximately 5km long by 1km wide. Seismic work has indicated that the diapir extends to great depths of 4000m (15,000 ft.) (personal communication, D. C Carter, 1987). The axis of the ellipse trends northeast-southwest. Windsor Group rocks are bounded by an unconformable overlap of Pennsylvanian sedimentary strata. The major axis of the ellipse of Windsor Group sediments is roughly coincident with the trace of the axial plane of a major anticline in the Pennsylvanian Cumberland Group.

The ellipse of Windsor Group rocks is the core of this anticline.

The extent and shape of the deposit of Windsor Group sediments in the vicinity of Pugwash was well documented by Bell (1944). Strata of the Pictou Group unconformably overlie those of the Windsor Group. The presence of karst or sinkhole topography near the Pugwash deposit indicates that gypsum underlies much of the eastern and central part of the Windsor Group sediments.

I. vi. History of the Pugwash Deposit

Initial geologic investigations around Pugwash suggested that the area was not suitable for salt or potash exploration (Hayes, 1931). Bell (1941) confirmed this, concluding that most of the Windsor Group strata was located beneath the Pugwash River estuary.

The first indication of salt at Pugwash came in October, 1953 when drilling for a water well intersected salt at 45 m (150 ft.). Following the discovery ten more holes were drilled in the area of the Pugwash inner harbour, on the northeastern end of the Pugwash structure. Seven holes cut significant thicknesses of salt and consequently development of the deposit began. The Malagash Salt Company constructed a shaft to 219.5 m (720 ft.) with a development level at 192 m (630 ft.). The mine officially opened on November 4, 1959, with reserve estimates of 181.4 Mt (Boehner, 1986). The Canadian Salt Company Limited took over the operation in 1961. In 1962 a second shaft was constructed approximately 75 m (250 ft.) northeast of the first (Boehner,

1986). Later development underground constructed levels at 250 m (830 ft.) and 229 m (730 ft.). During 1967 construction began on a decline to the 305 m (1000 ft.) level.

Mining of the Pugwash deposit initially used a regular grid room-and-pillar method. This mining method was selected based on interpretation of drill hole data which suggested a simple, horizontally stratified deposit. Underground development revealed the deposit to be very complex, consisting of a number of steeply-dipping, sub-vertical anhydrite units interbedded with halite. Eventually the mining method was modified to avoid areas of anhydrite waste rock. The modified room-and- pillar method removes salt from between anhydrite layers. Drifts 9 m (30 ft.) high by 15 m (50 ft.) wide are constructed parallel to anhydrite beds and are separated by pillars 23 m (75 ft.) wide. Crosscuts link neighboring drifts for ventilation (Boehner, 1986). Figure 1-3 shows an example of the modified mining pattern and its relationship to the irregular shape and distribution of the anhydrite units (Carter, 1985, 1986).

I. vii. Previous Work

Once mining had created adequate exposure, the evaporite sequence was subjected to a number of studies. Aumento (1964) made a detailed mineralogiocal study of carnallitite occurrences within the mine. Barr (1966) studied the bromine content of salts in the mine as part of an investigation into the possibilities of potash deposits in Nova Scotia. Evans (1965, 1967, 1972, 1974)

discussed the structure, stratigraphy, and depositional history of the evaporite minerals forming the Pugwash deposit. Goodman (1985) discussed features of the Pugwash deposit and the Ojibway deposit, located in Windsor, Ontario, attempting to establish a common origin for the two deposits. Later investigations had the benefit of additional exposure on the 229 m (730 ft.) and 250 m (830 ft.) levels. Carter (1985, 1986) has made preliminary investigations on the sedimentology, stratigraphy and structure of the deposit incorporating data from the 192 m (630 ft.), 229 m (730 ft.), 250 m (830 ft.) levels, exploratory data from the 305 m (1000 ft.) level and observations from approximately 12,200m (40,000 ft.) of drill core. Preliminary reports indicate that the Pugwash deposit represents a true piercement diapir and that the present deposit may be a remnant of the original (Carter, 1986).

II. STRATIGRAPHY

II.i Introduction

This chapter is a descriptive account of the stratigraphy of anhydrite units exposed in the workings of the Pugwash Mine, which has been reconstructed from detailed mapping of mine workings and examination of drill core. Extreme deformation has precluded measurement of original thicknesses, but structural relationships, sedimentary structures, and internal markers allow reconstruction of stratigraphy.

The evaporite sequence exposed in the Pugwash Mine consists of interbedded halite and anhydrite with minor sylvite and carnallite (see Fig. 2-1). Although the sequence is structurally complex, it is possible to identify and correlate individual anhydrite units. Mine exposures and drill core indicate three lithologically distinct anhydrite units (Carter, 1985, 1986). The shaft anhydrite unit occupies the core of the diapir and is conidered to be the oldest unit. The third anyhdrite is in contact with Pennsylvanian clastics near the edge of the diapir and is interpreted to be the youngest. The borate anhydrite unit is of intermediate age. Earlier work at a time of more limited mine exposure (incomplete 630 ft. level) suggested two anhydrite units (Evans, 1972). Recently, Goodman (1985) suggested ten anhydrite units. Internal characteristics and stratigraphic positions provide the basis for the threefold division of Carter (1985, 1986).

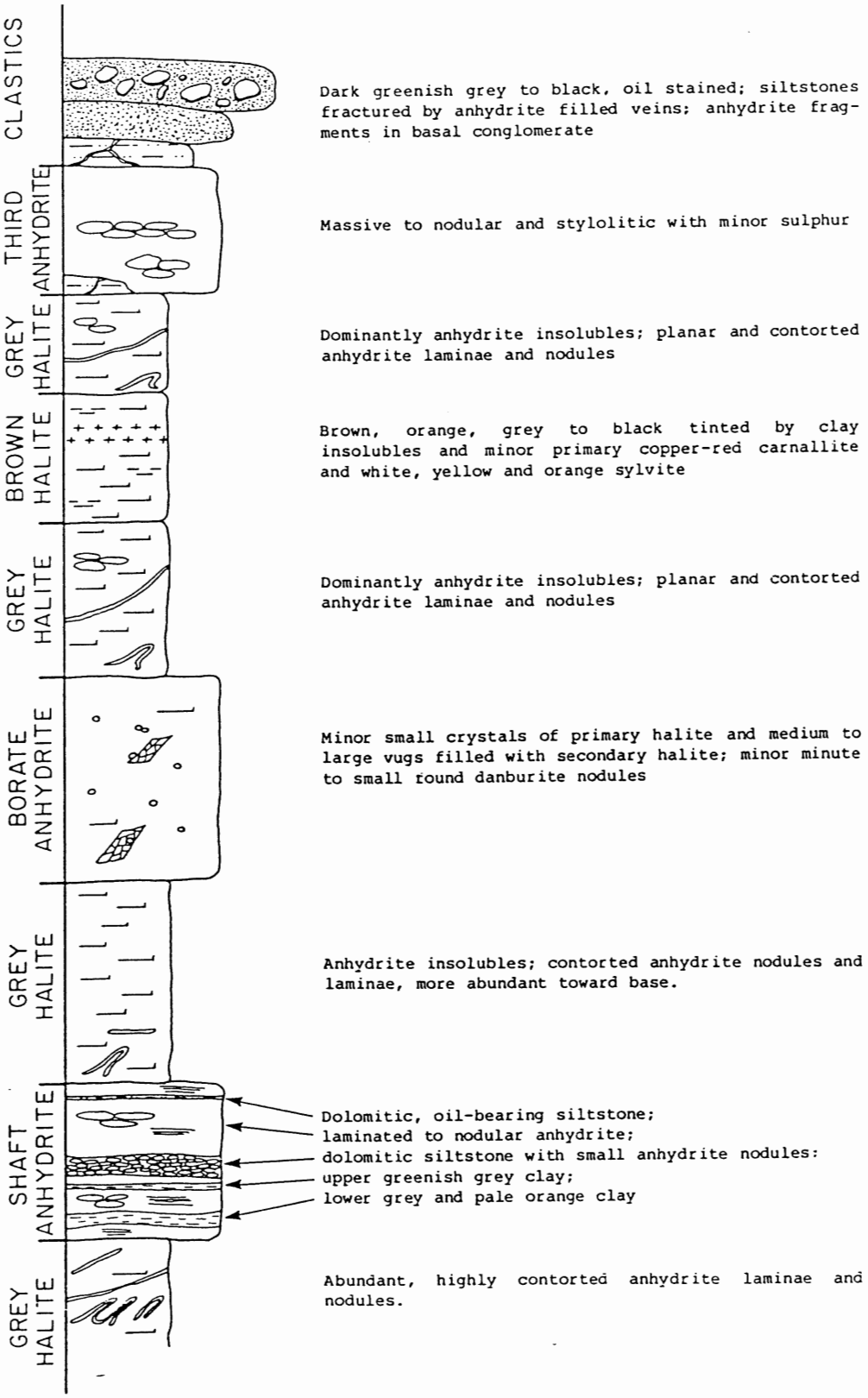

Figure 2-1. Idealized stratigraphy of ther Pugwash evaporite deposit. No vertical scale implied (Carter, 1986).

The three anhydrite units have the following characteristics from bottom to top: 1) the shaft or main anhydrite (Evans, 1972; Carter, 1985,1986) consists of laminated to nodular anhydrite with distinct carbonate and clay beds; 2) the borate anhydrite (Carter, 1985, 1986) consists of massive to nodular anhydrite with borate nodules; and 3) the third anhydrite (Carter,1986) consists of massive to nodular anhydrite with small quantities of elemental sulphur; similar to the borate anhydrite but without borate nodules.

II.i. Shaft Anhydrite Unit

The shaft anhydrite is the lowermost unit and consists of laminated to nodular anhydrite with internal markers (see Fig. 2-2). Mapping on the three mine levels shows that this unit consists of elongate, ribbon-like bodies 15 to 18 m thick (50 to 60 ft.). Stratigraphic top is indicated by dewatering features and anticlinal closures of halite by anhydrite beds.

Distinguishing features include four separate lithological marker horizons. Two clay markers (C2 and C1) underlie two carbonate markers (D1 and D) (Carter, 1986). The D1 and D marker beds have previously been termed "dolomitic" by Carter (1985, 1986). Petrographic studies and staining of core chips with Alizarin Red-S solution in a 0.2 % HCl solution indicates that calcite forms more than 95% of carbonate in these beds. Each marker has distinct characteristics. The C2 clay, the lowermost marker, is grey to pale orange and approximately 0.5m thick. The

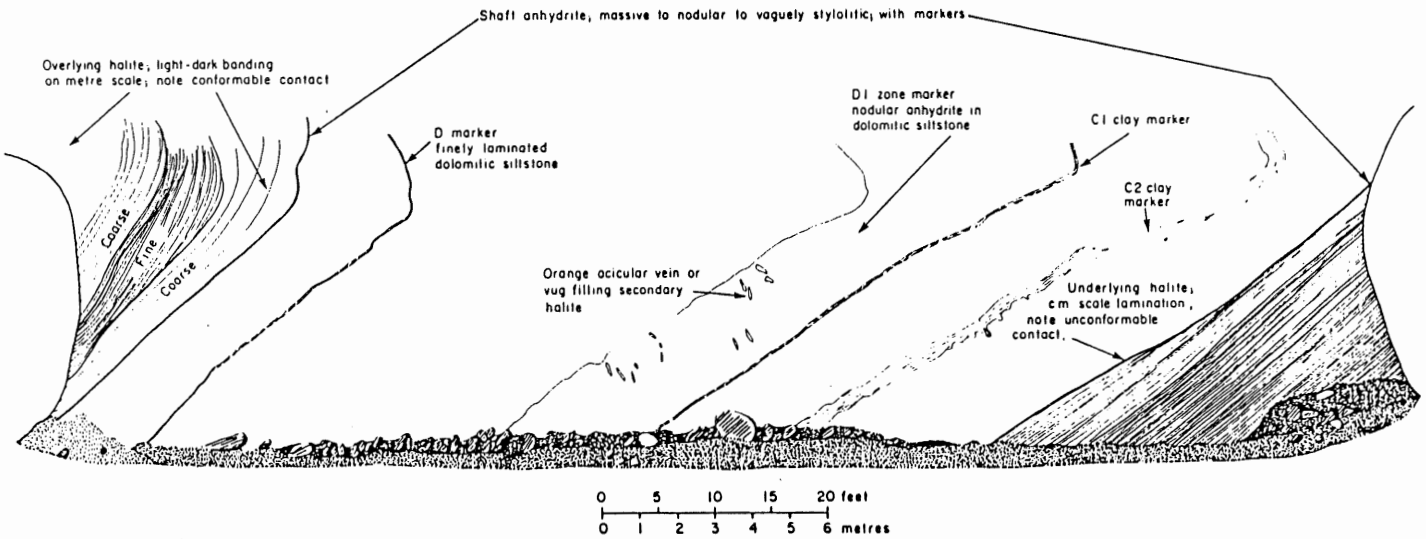

Figure 2-2. Stratigraphy of the shaft anhydrite unit exposed in a wall section on the 830 ft. level. Note conformable contact with halite and internal markers (Carter, 1985).

overlying C1 marker is generally thicker and consists of laminated to bedded greenish-grey clay. The thickness of both clays varies laterally in the form of pinch and swell structures. These structures are probably the result of compaction and/or deformation. The overlying D1 marker is not a single layer but defines a zone a few metres thick consisting of small anhydrite nodules in laminated carbonate. The D1 marker zone has secondary salt filling vugs and veins. The overlying D marker bed consists of finely laminated carbonate. It is similar to the D1 marker but is oil-bearing, has dark brown siltstone fragments, larger (0.5-0.75cm) anhydrite nodules, and discrete laminae of dark salt.

The shaft anhydrite contains no primary salt. Secondary salt is usually orange in colour, acicular in texture and vein- and vug-filling in habit.

II.iii. Borate Anhydrite Unit

The borate anhydrite, the middle unit is ovate and irregular shaped in plan and consists of massive to nodular anhydrite. Overall size of individual borate anhydrite bodies generally increases with depth. Stratigraphic tops and lineations are unknown.

The distinguishing feature of this unit is the occurrence of borate nodules (see Fig. 2-3). Occurrences of danburite nodules are scattered in the borate anhydrite on all levels of the mine. The borate mineral has been identified by x-ray diffraction as danburite ($CaB_2Si_2O_8$) (Carter, 1985). Nodules range in size from

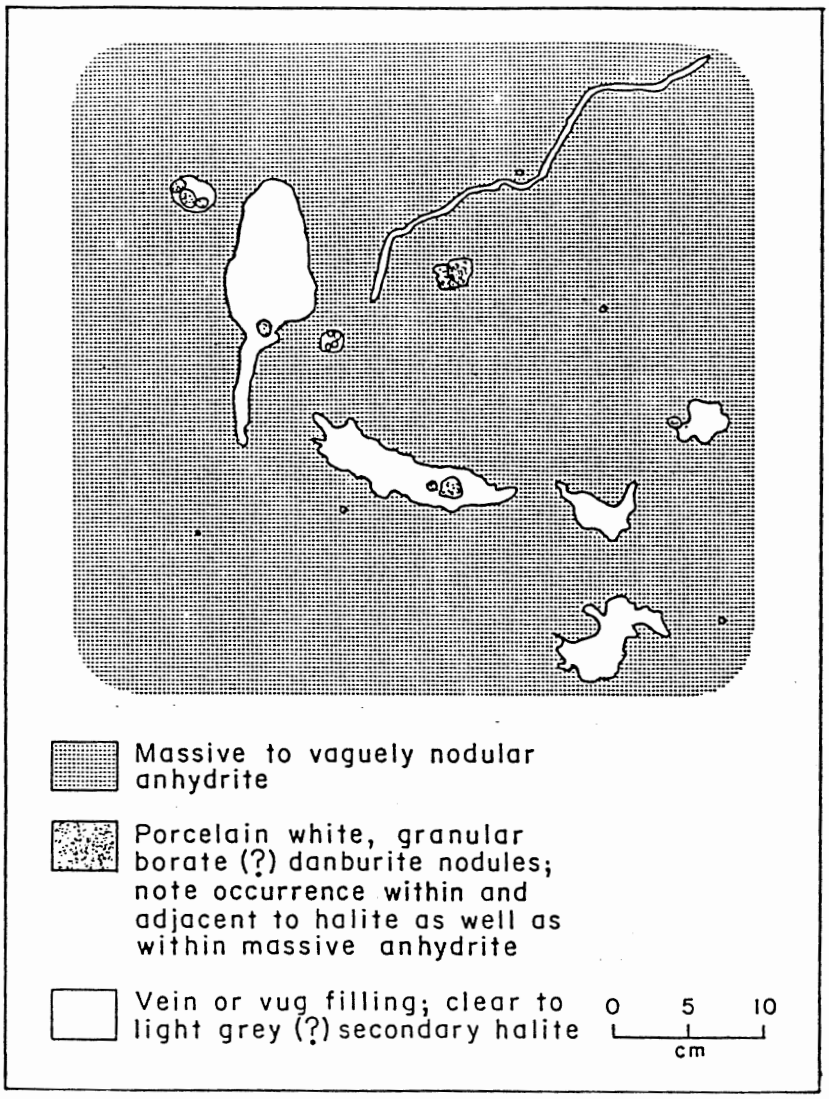

Figure 2-3. Detailed sketch of the borate anhydrite unit exposed on the 250 m level. Stratigraphic top unknown. Note absence of lineation and varied occurrence of borate nodules (Carter, 1985).

approximately 0.5 mm to 1 cm, are porcelain white to light grey in colour and consist of very fine-grained aggregates of danburite crystals. Most are spherical, but some of the larger ones have colliform shapes indicating growth from multiple centers. They occur in massive to nodular anhydrite and within or at the edges of vugs or veins filled with secondary halite. Danburite nodules displace carbonate and anhydrite laminations, indicating primary formation, and occur in secondary halite, indicating a secondary, late-stage origin. The danburite nodules are the result of primary development modified by secondary diagenetic processes.

Halite occurrences in the borate anhydrite are both primary and secondary. Primary halite consists of minor small crystals. Secondary halite fills medium to large (10-15 cm) vugs and fractures.

II.iv. Third Anhydrite Unit

The third anhydrite, the uppermost unit, consists of massive to nodular and stylolitic anhydrite and is similar to the borate anhydrite but lacks danburite nodules. It is irregular to ovate and elongate in plan section.

This unit is often difficult to recognize due to its similarity to the borate anhydrite. All observations are from drill core, where the third anhydrite is located near the edge of the diapir, above the borate anhydrite. In nodular portions of this unit, elemental sulphur replaces organic material that rims

the anhydrite nodules. This feature is not observed in the borate anhydrite.

III. PETROGRAPHY

III. i. Introduction

This chapter is a discussion of petrographic features observed in the shaft, borate, and third anhydrite units. Petrographic study is perhaps the most important aspect of this thesis. Investigation of thin sections proved extremely useful in the attempt to distinguish the three anhydrite units. The final determination of whether or not the shaft and especially the borate and third anhydrites are distinct and/or separate units will hinge on the data presented in this chapter.

Petrographic study involved the description of 104 polished thin sections and the examination of core chips stained with Alizarin Red-S solution in a 0.2 % HCl solution. Textural descriptions are based on the classification scheme of Maiklem et al. (1969). This classification scheme was originally proposed in an attempt to standardize anhydrite terminology. It considered the structure and texture of anhydrite. Structural types are classified by: 1) external form; 2) anhydrite to matrix relationship; 3) bedding; and 4) distortion. The textural types are classified by: 1) size; 2) shape; and 3) spatial relationship of crystals within anhydrite masses (Maiklem et al., 1969). Textural classification proved very useful during petrographic studies. Based on crystal size and shape, anhdyrite observed in thin section was classified as equidimensional (blocky, microcrystalline), or elongate (lath-shaped, subfelted, felted

and aligned-felted).

Thin sections were cut at approximately 3 m intervals depending on the continuity of lithologies. In layers with numerous lithology changes, frequency of sample collection was increased to 1-2m intervals. Stratigraphic top could only be determined in borehole P-918 from the shaft anhydrite unit. Samples from drill cores were collected to represent type sections through each anhydrite unit. Samples for thin sections were gathered from four drill cores: 1) P-816: 13 thin section from the shaft anhydrite representing approximately 43 m; 2) P-918: 27 sections from the shaft anhydrite representing approximately 18m; 3) P-886: 28 sections from the borate anhydrite representing approximately 76m; and 4) P-158: 28 sections from the third anhydrite representing 13m. Hole P-158 was drilled on the 192 m (630 ft.) level. All other holes were drilled on the 250m (830 ft.) level.

Study of thin sections indicates that each unit has distinctinve mineralogy and textures. This is important because the borate and third anhydrite are often very difficult to distinguish on a macroscopic scale. An earlier discussion of petrography of the shaft anhydrite by Evans (1972) is considered essentially correct but in the following discussion more detailed descriptions and notes of some newly recognized features are given. Evans (1972) distinguished the borate anhydrite but did not discuss this unit. He did not mention the third anhydrite unit.

The shaft anhydrite is polymineralic and exhibits three main textures. The borate anhydrite contains fewer minerals and it has two main textures. The third anhydrite has the highest anhydrite content and one main texture. Replacement and growth of secondary minerals as a result of diagenesis has extensively altered the original composition of all three anhydrite units.

III. ii. Petrography of the Shaft Anyhdrite

Anhydrite in the shaft unit is intimately associated with: 1) carbonate material (calcite and minor dolomite); and 2) organic layers (possibly cyanobacteria). Pyrite is an important accessory mineral. Laminae of silt-sized quartz and fossiliferous material are also noted.

The three main textural types are: 1) laminated carbonate (mainly calcite) and organic matter with displacive anhydrite nodules; 2) laminated anhydrite with regular alternations of anhydrite and organic material; and 3) nodular anhydrite rimmed with carbonate and organic matter. A fourth textural relationship observed on a limited scale was laminated quartz silt with organic matter and small spindle shaped anhydrite nodules (Plate 3-1 to 3-4)..

Laminated carbonate with anhydrite

The laminated carbonate has four major components: anhydrite, calcite, organic matter and pyrite (Plate 3-1).

Calcite is the dominant mineral of this textural type. It is

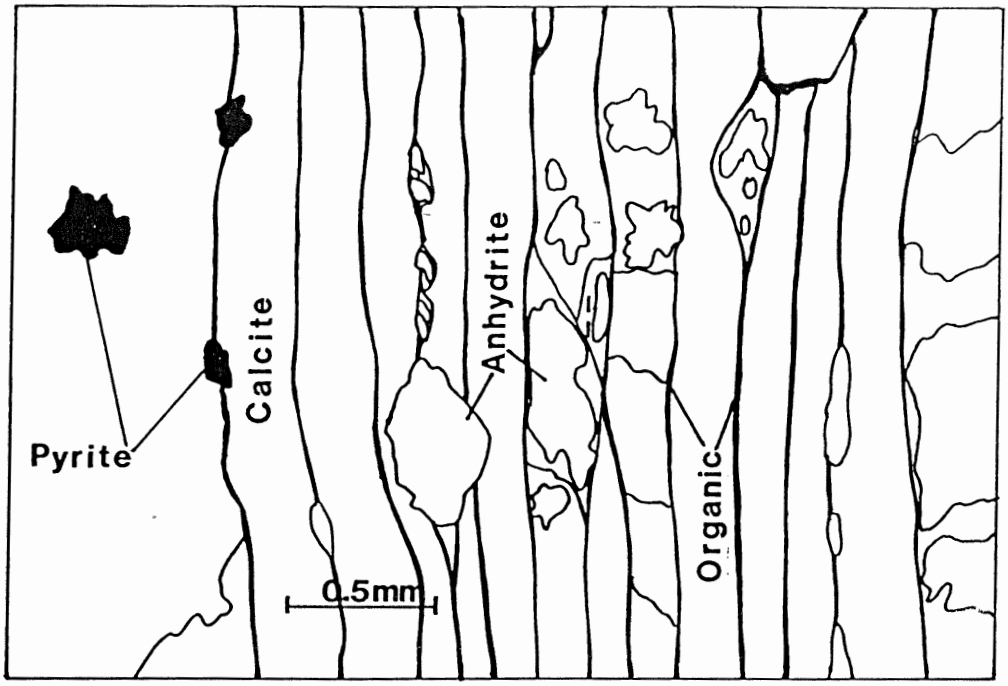
Pyrite
Calcite
Anhydrite
Organic
0.5mm

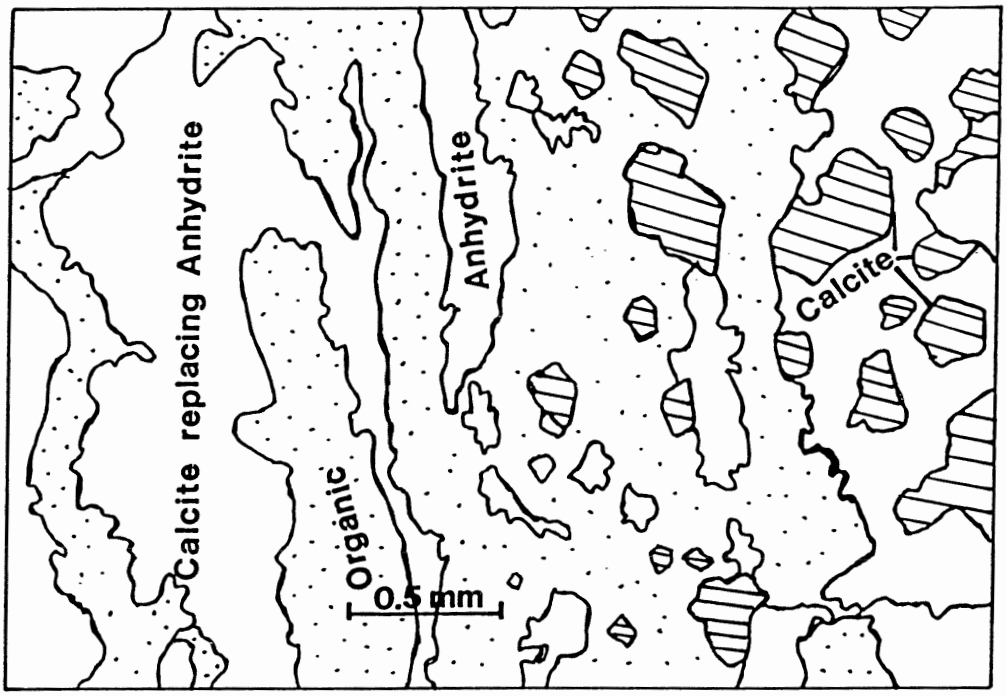
Calcite replacing Anhydrite
Organic
Anhydrite
Calcite
0.5 mm

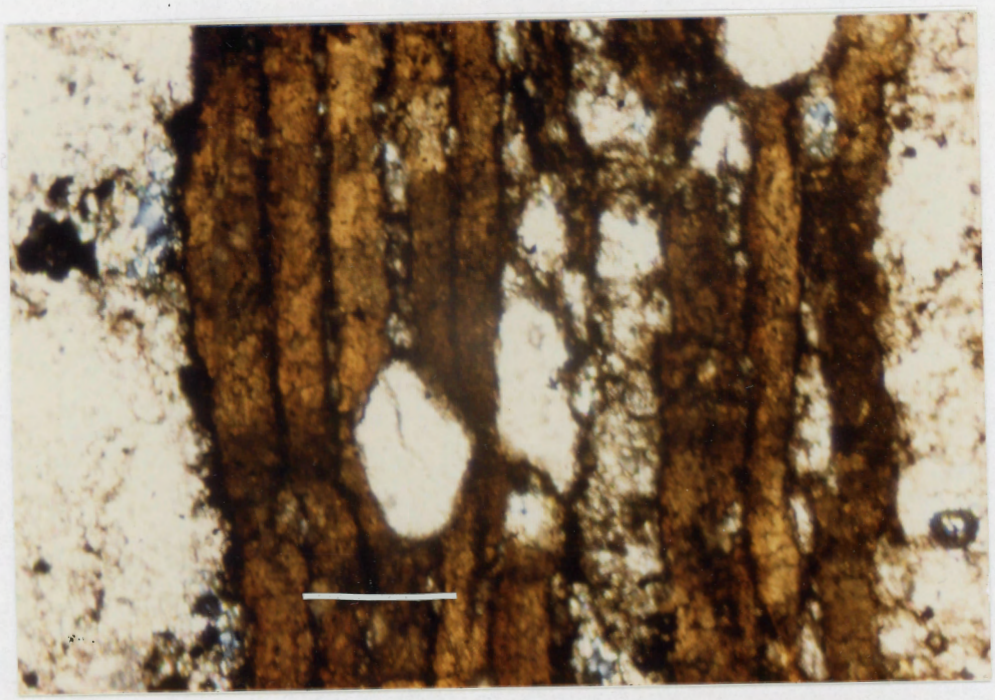

Plate 3-1 - Thin section P-918-67; Shaft anhydrite unit; Laminated carbonate with anhydrite nodules; note recrystallized, brown calcite and dark organic layers; crossed nicols; bar scale is 0.5 mm.

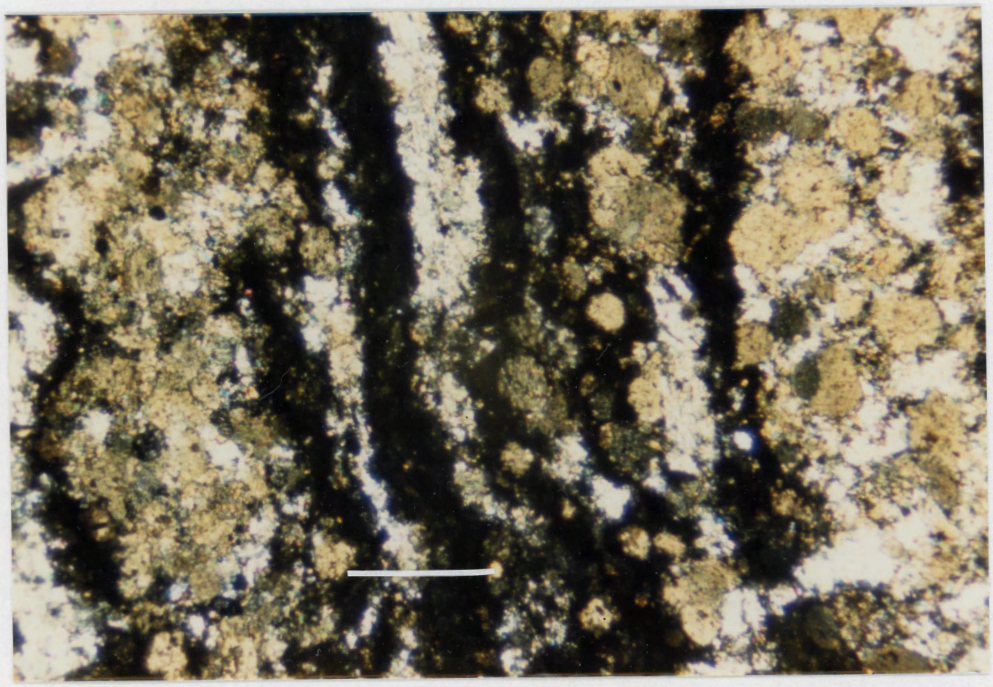

Plate 3-2 - Thin section P-918-12; Shaft anhydrite unit; laminated anhydrite; note calcite that replaces anhydrite and dark organic layers; crossed nicols; bar scale is 0.5 mm.

medium to dark brown in colour due to inclusions of organic material. It exhibits anhedral, intergrown grain boundaries and appears to have been extensively recrystallized. This type of calcite occurs as thin laminations (< 0.5 mm) alternating with dark, brownish-black organic material. Secondary calcite lacks organic inclusions and appears as subhedral to euhedral grains that are pinkish-brown in plane polarized light. This type of calcite replaces anhydrite nodules and overgrows euhedral anhydrite crystals. Grain size is variable ranging from about 0.005 mm up to 2 mm.

Anhydrite occurs in two forms: 1) nodular pseudomorphs after gypsum that displace carbonate and organic laminae; and 2) blocky, euhedral, secondary anhydrite. Anhydrite is interpreted to form pseudomorphs after gypsum because many nodules have the outline of tabular and spindle shaped gypsum crystals. In plane polarized light this anhydrite is coloured very pale brown from inclusions of carbonate and organic matter. Euhedral anhydrite is considered secondary for two reasons: 1) it crosscuts laminations and anhydrite nodules that pseudomorph gypsum, and; 2) it is clear in plane polarized light (lacks inclusions of carbonate and organic material).

Organic material occurs as thin, filamentous laminae, and is closely associated with grains of pyrite. Organic material often contains angular to subrounded clasts of silt-sized quartz.

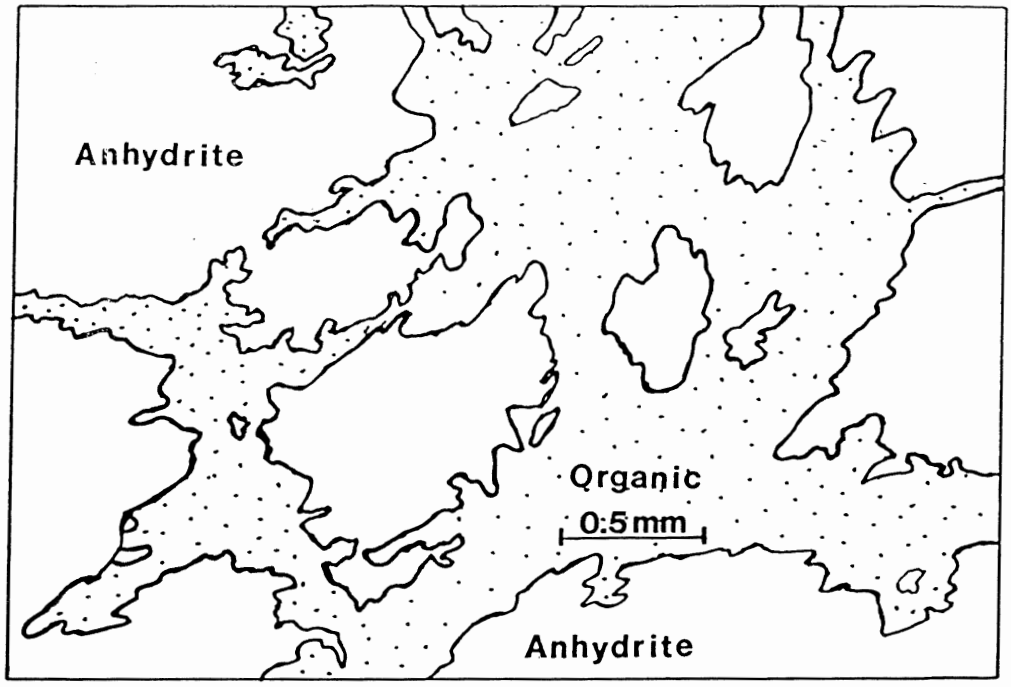
Anhydrite
Organic
0.5mm
Anhydrite

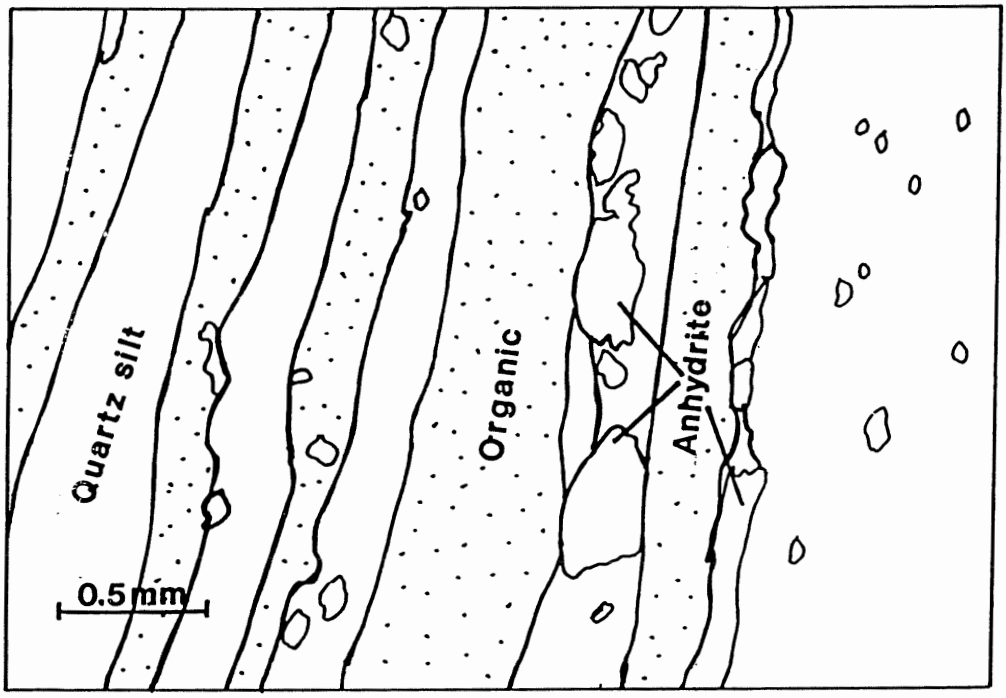
Quartz silt
Organic
Anhydrite
0.5mm

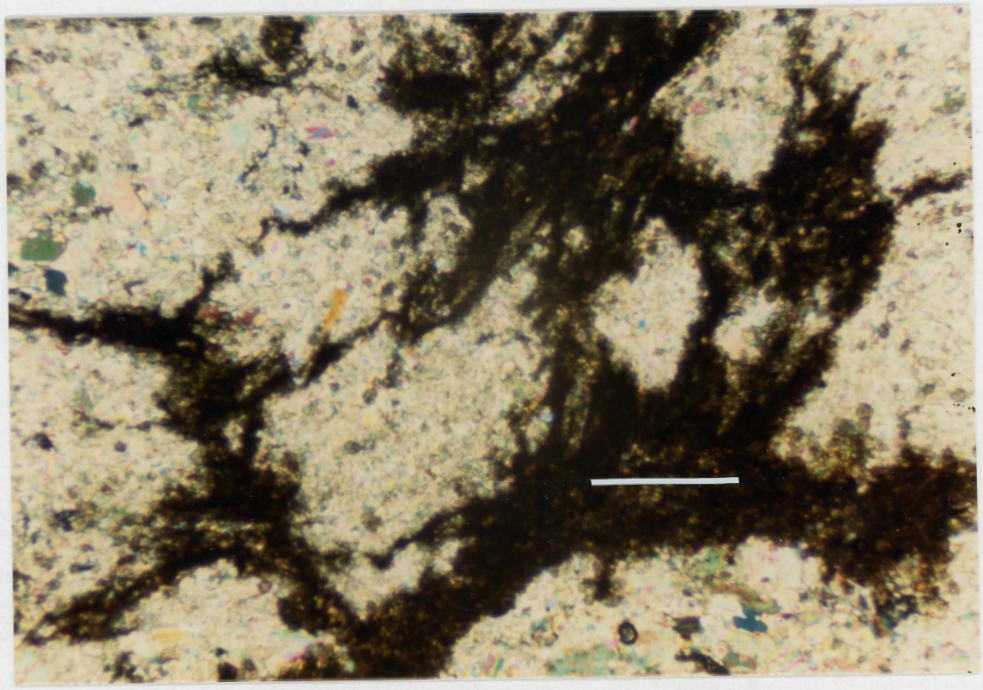

Plate 3-3 - Thin section P-816-60; Shaft anhydrite unit; Nodular anhydrite; note nodular anhydrite that displaces carbonate and organic material; crossed nicols; bar scale is 0.5 mm.

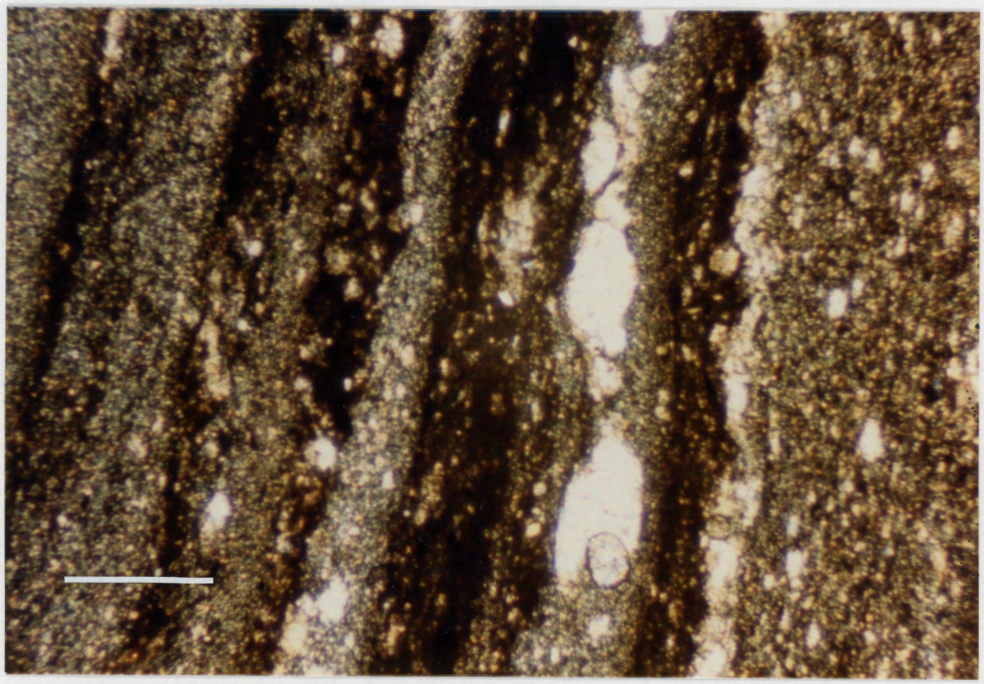

Plate 3-4 - Thin section P-918-25.5; Shaft anhydrite unit; Laminated quartz silt with organic and anhydrite; note laminated quartz silt and organic material with spindle-shaped, displacive anhydrite nodules (pseudomorphs after gypsum); crossed nicols; bar scale is 0.5 mm.

Laminated anhydrite

The laminated anhydrite consists of four major components: anhydrite, calcite, organic matter and pyrite (Plate 3-2).

Anhydrite is the most abundant mineral. It appears both as thin laminae alternating with organic matter and as nodules displacing organic laminae. Calcite occurs as inclusions in anhydrite nodules and also is observed as euhedral overgrowths replacing anhydrite. In addition some anhydrite nodules with a felted texture are observed to be partially replaced by calcite. Calcite generally consists of subhedral to euhedral grains and is pale brown in plane polarized light. The overgrowth and replacement relationships indicate: 1) primary calcite was replaced by anhydrite; and 2) some of this replacment anhydrite was later calcitized. Calcite replacing anhydrite is much lighter in colour than that in the laminated carbonate (due to the lack of organic material). Much of the organic matter has been converted to and/or is asscoiated with pyrite and appears very dark. In some laminated portions anhydrite forms poorly developed entrolithic folds. The laminated anhydrite fabric was formed by coalescing nodules and the pervasive replacement of carbonate by anhydrite and the displacment of organic material by anhydrite growth. Interference of nodules may have caused deformation and formed the entrolithic folds.

Nodular Anhydrite

Components are the same in nodular and laminated portions,

but anhydrite forms a much higher percentage of the rock in the nodular portions (Plate 3-3).

Nodules consist of microcrystalline to blocky anhydrite with thin films of organic material separating adjacent nodules. In portions where the nodular texture has not completely developed, some nodules have cores of pale calcite with inclusions of anhydrite and rims of corroded dolomite rhombs.

III. iii. Petrography of the Borate Anhydrite

The borate anhydrite unit is made up of four main components: 1) anhydrite; 2) halite; 3) organic matter; and 4) carbonate (calcite with minor dolomite). Minor constiuents include the borate mineral danburite, and pyrite.

Anhydrite in this unit exhibits two main textural types: 1) nodular; and 2) massive. Nodular anhydrite is the dominant textural type.

Nodular Anhydrite

Nodular anhydrite consists of microcrystalline to blocky nodules showing displacive growth within carbonate and organic laminae. Carbonate consists mainly of calcite. Some massive calcite laminae are observed, but they are irregular, thin, and often stained reddish brown by organic material. Calcite has been recrystallized as in the shaft anhydrite unit. Corroded calcite rhombs occur within some nodules indicating that there was a period of calcite replacement by anhydrite. Dolomite rhombs are

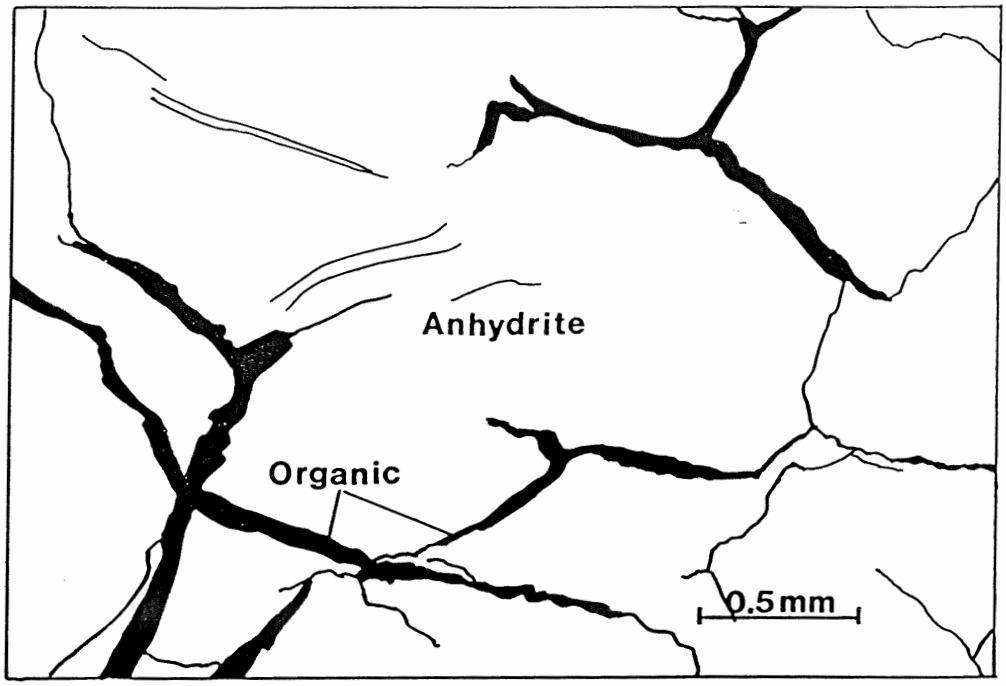
Anhydrite
Organic
0.5mm

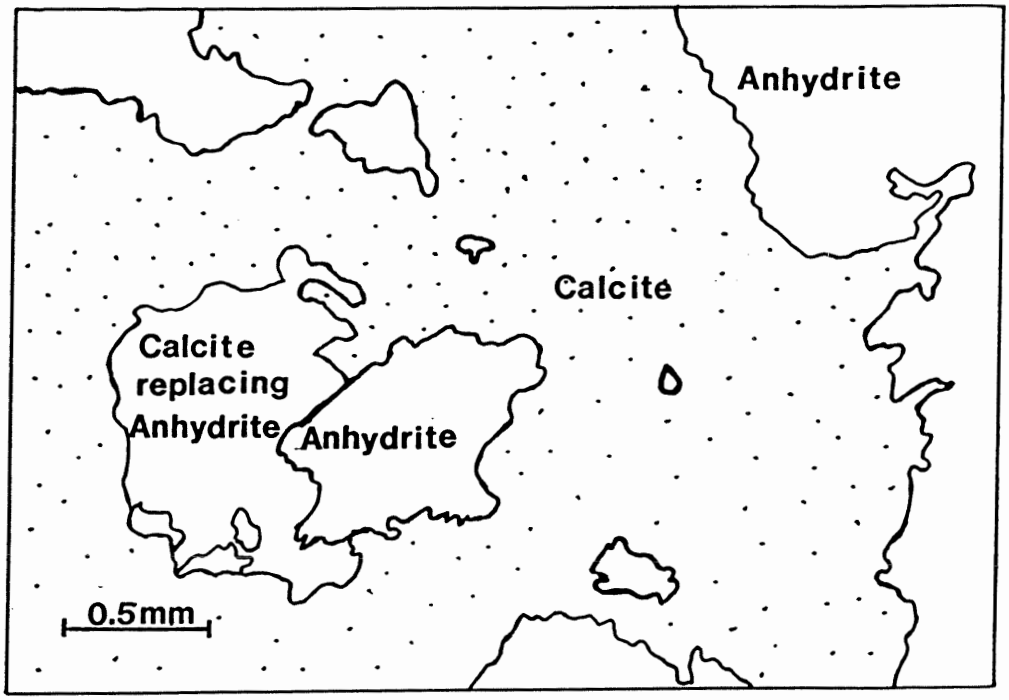
Anhydrite
Calcite
Calcite
replacing
Anhydrite
Anhydrite
0.5mm

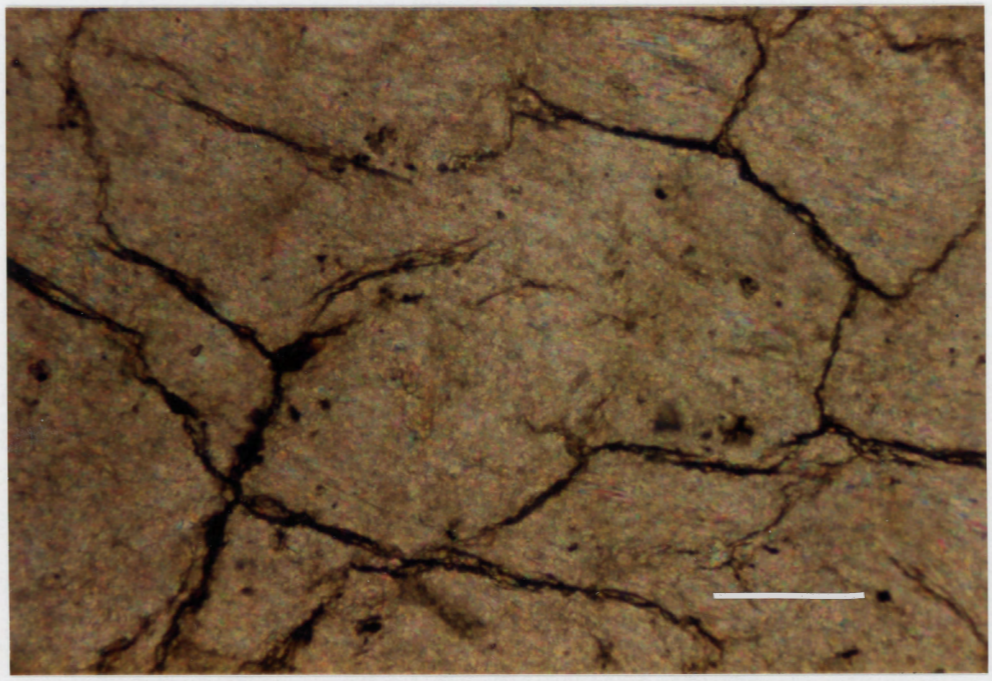

Plate 3-5 - Thin section 886-160; Borate anhydrite unit; Stylolitic anhydrite; note stylolitic texture with "tooth-and socket" intergrowth of nodules; anhydrite nodules rimmed by organic material; crossed nicols; bar scale is 0.5 mm.

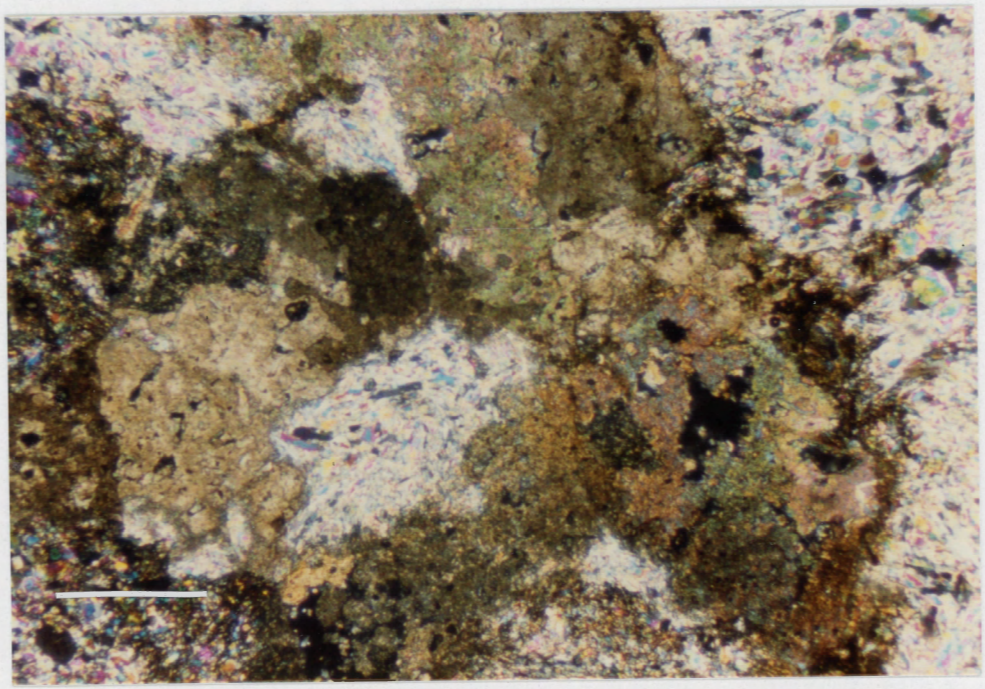

Plate 3-6 - Thin section 886-140; Borate anhydrite unit; Nodular anhydrite and carbonate; note anhydrite nodule that displaces carbonate and organic material and calcite that replaces anhydrite; crossed nicols; bar scale is 0.5 mm.

euhedral and light brown in plane polarized light and are associated with halite-filled vugs. Organic matter displaced by the growth of anhydrite nodules is often very distorted. It appears to have deformed very easily, and has been altered by the effects of differential compaction. It consists of thin, dark brown to black material and contains minor silt-sized quartz grains and pyrite. Some nodular anhydrite shows a stylolitic texture, with the characteristic tooth and socket intergrowth of nodules (Plates 3-5 and 3-6).

Massive Anhydrite

Massive anhydrite is less common than and usually closely associated with nodular anhydrite. In massive portions the groundmass consists of microcrystalline anyhdrite with common fibroradiate clusters consisting of aggregates of fibrous, lath-shaped anhydrite. Lath-shaped crystals grouped in fibroradiate arrangements are clear in plane polarized light and show very high birefringence (Plate 3-7).

Secondary halite is a major component in both nodular and massive portions of the borate anhydrite. The cutting process has removed halite from most thin sections leaving irregular shaped vugs. Halite in core chips consists of masses of clear, cubic crystals. Recrystallized anhydrite occurs in both nodular and massive textures. It is clear in plane polarized light and consists of euhedral, blocky crystals. The euhedral nature and lack of carbonate and organic inclusions suggest a secondary

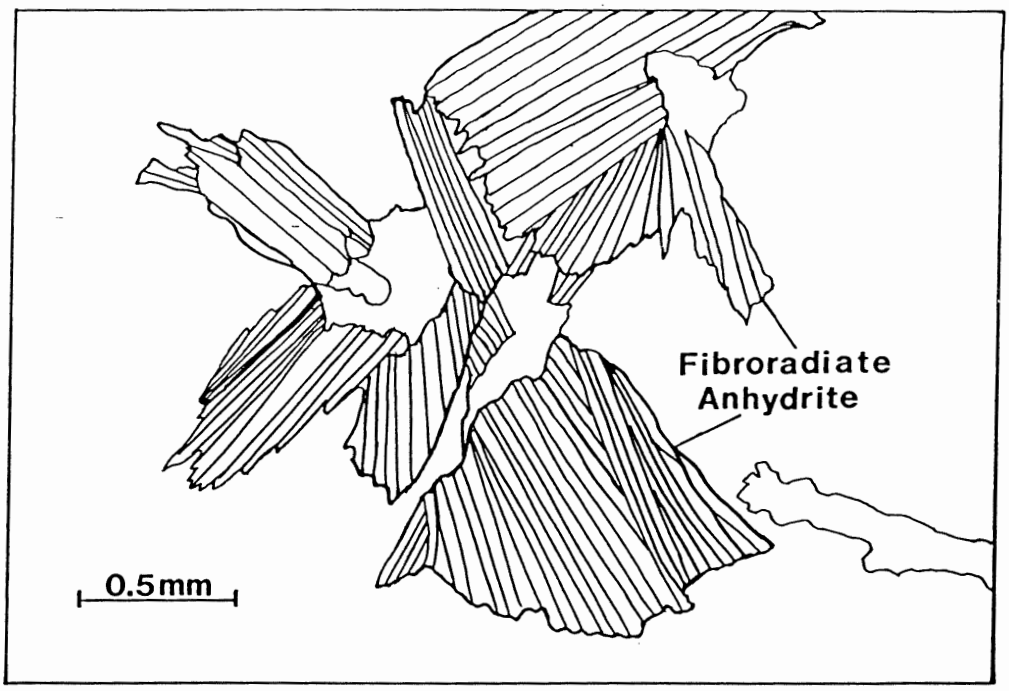
Fibroradiate
Anhydrite
0.5mm

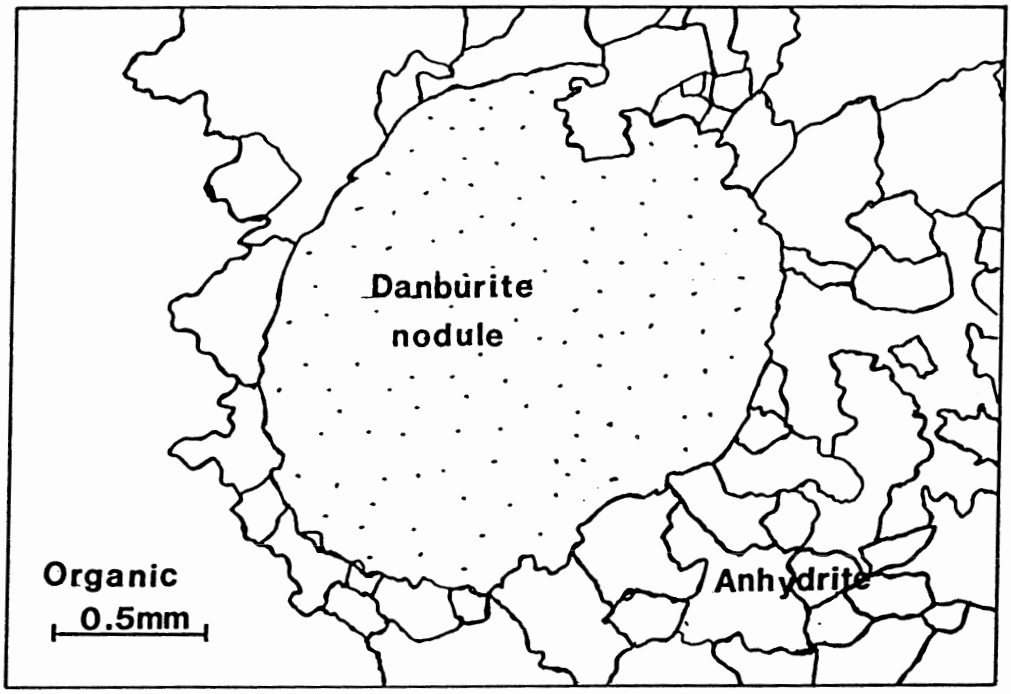
Danburite
nodule
Organic
0.5mm
Anhydrite

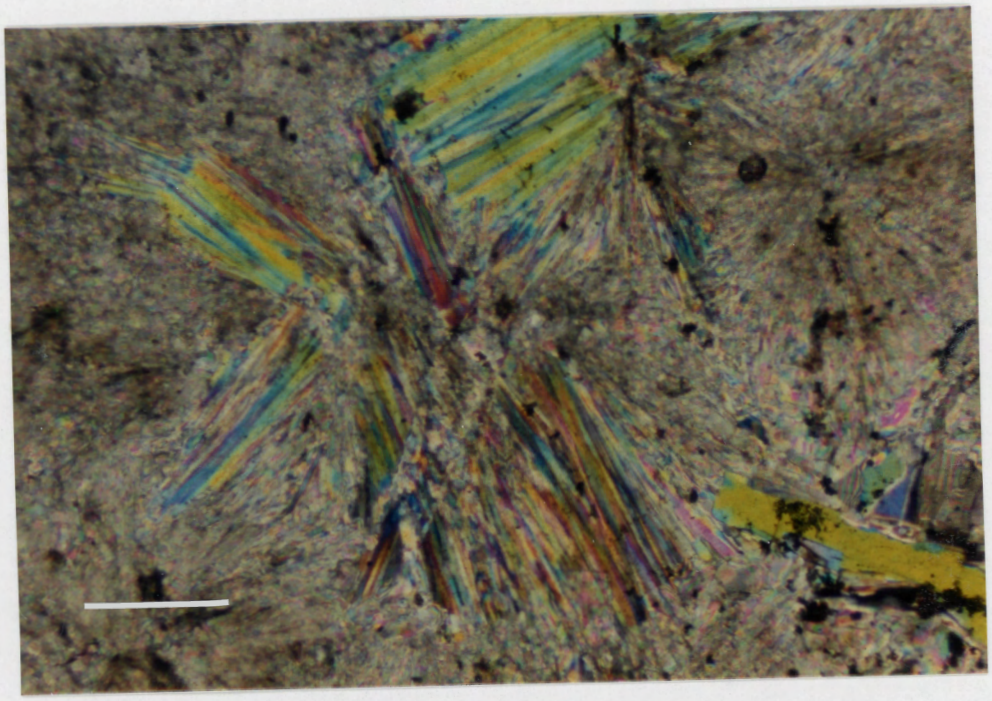

Plate 3-7 - Thin section 886-170; Borate anhydrite unit; Fibroradiate anhydrite; note fibroradiate clusters of anhydrite crystals in a microcrystalline anhydrite groundmass; crossed nicols; bar scale is 0.5 mm.

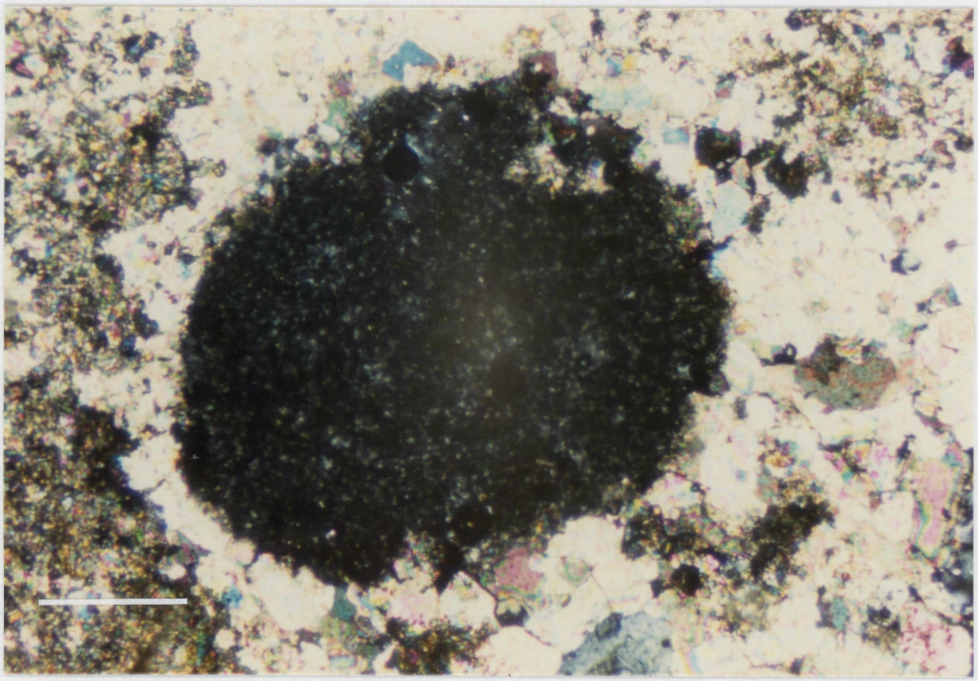

Plate 3-8 - Thin section 886-160; Borate anhydrite unit; note fine-grained danburite nodule that displaces anhydrite and organic material; also note recrystallized anhydrite around nodule; crossed nicols; bar scale is 0.5 mm.

origin. Also, in some recrystallized areas there is a halo of fine-grained, organic/carbonate material around the periphery of the secondary anhydrite. A likely source for this material would be the organics and carbonate within primary anhydrite that has been replaced.

The occurrence of borate nodules is unique to this unit. As was previously mentioned the borate nodules have been identified as danburite by X-ray diffraction (Carter, 1985). In thin section the nodules are oval to colliform shaped, dark greyish-black in plane polarized light and consist of aggregates of very fine grained crystals of danburite. Under high magnification, indivdual crystals appear tabular to acicular. Borate nodules show displacive growth within organic laminae and anhydrite (Plate 3-8). Borate nodules occur within anhydrite, at the border of halite filled vugs and within secondary halite. This suggests that the nodules are late diagenetic products. The colliform shape of some nodules suggests growth from multiple centers.

III. iv. Petrography of the Third Anyhdrite

The third anhydrite unit consists mainly of anhydrite. Organic material occurs in very minor amounts. It has been compacted to very thin laminations by the growth of anhydrite nodules. Carbonate and pyrite have not been observed. Anhydrite in the third unit is much coarser grained than in the borate unit. Portions with massive to weakly aligned laths are transitional to zones of very coarse, well-aligned laths that

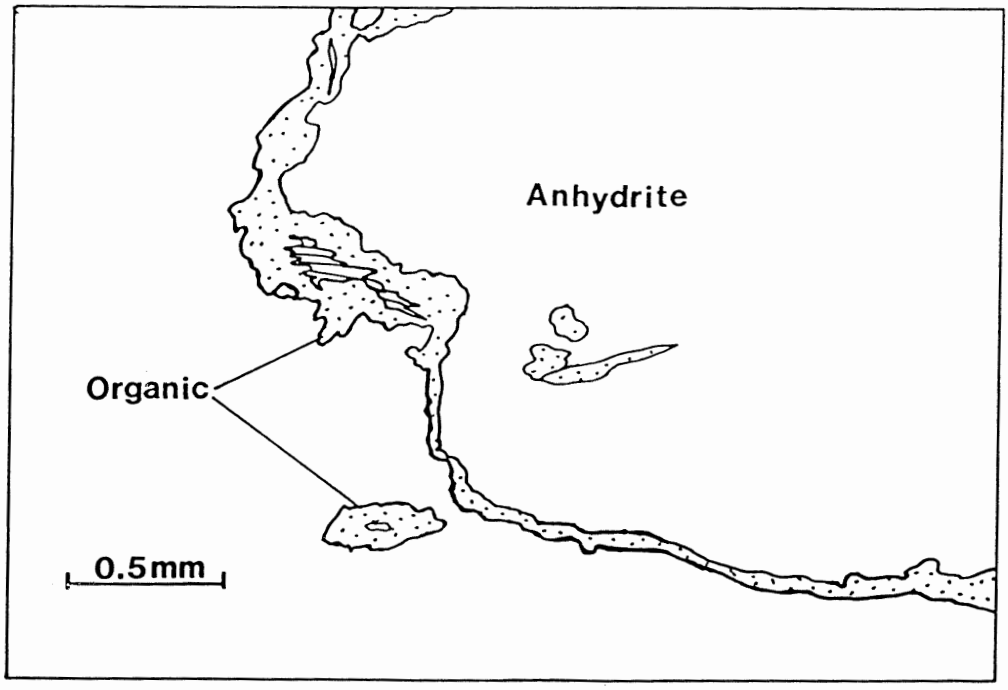
Anhydrite
Organic
0.5mm

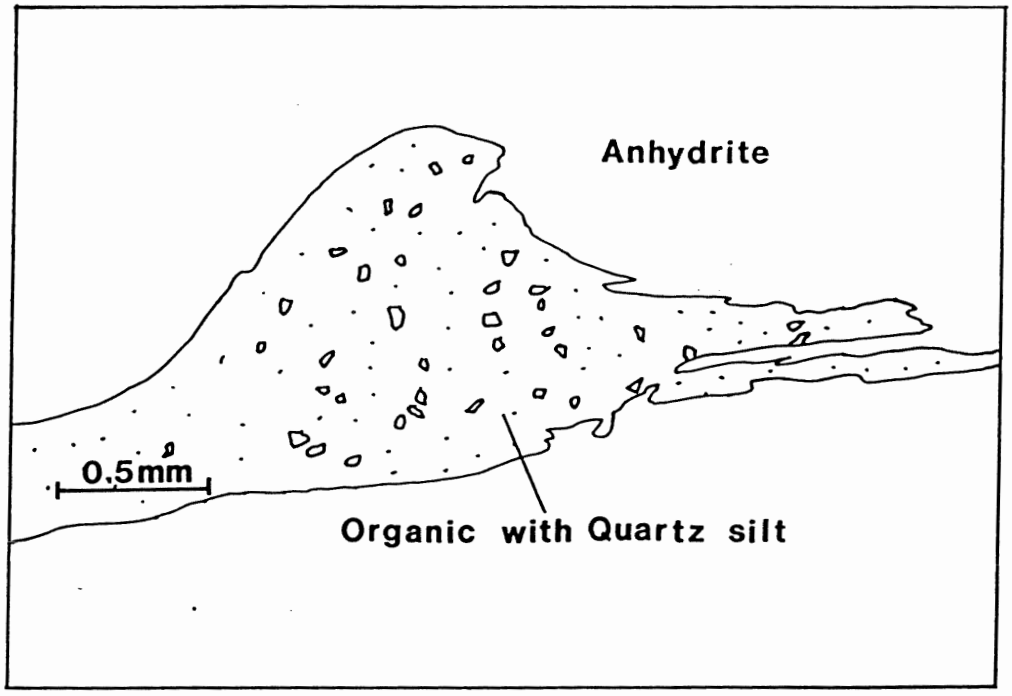
Anhydrite
0.5mm
Organic with Quartz silt

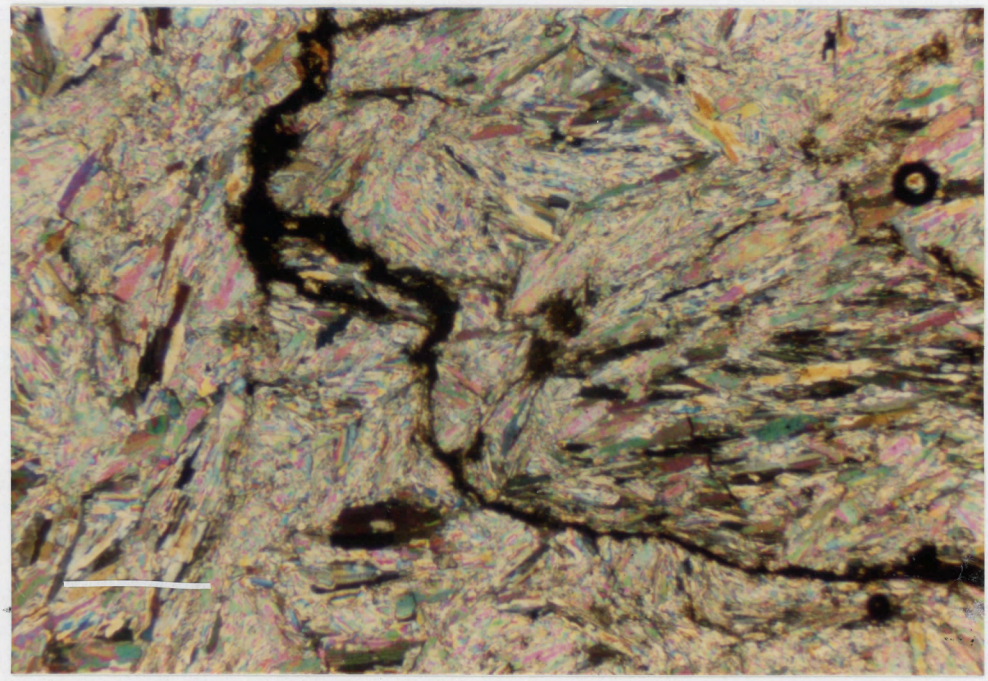

Plate 3-9 - Thin section 158-91; Third anhydrite unit; Nodular anhydrite; note coarse textured anhydrite nodule that displaces organic material; crossed nicols; bar scale is 0.5 mm.

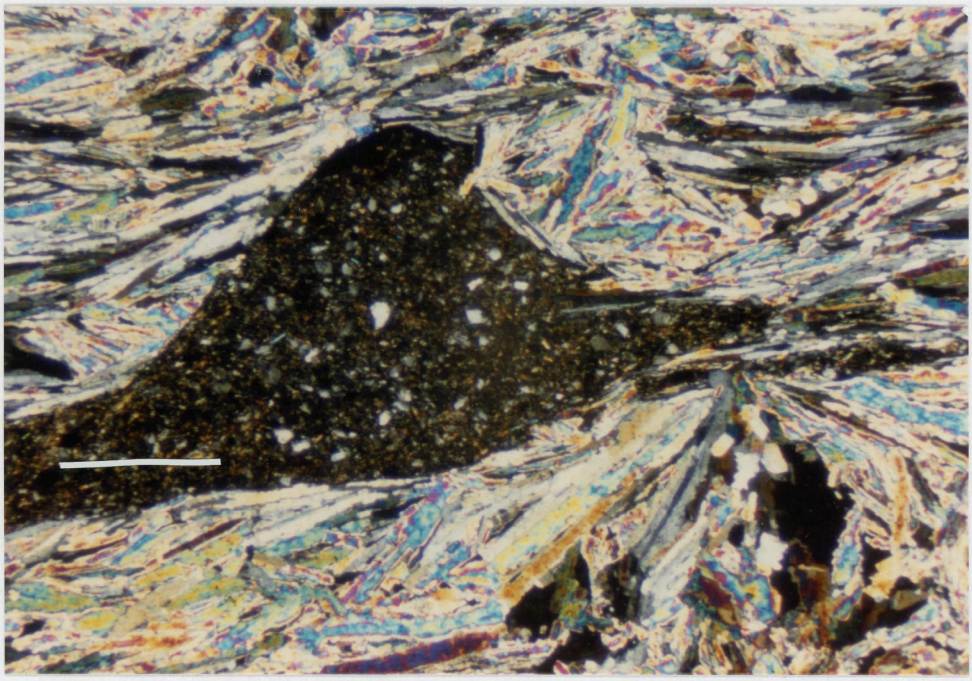

Plate 3-10 - Thin section 158-80; Third anhydrite unit; Nodular anhydrite; note coarse, nodular anhydrite that displaces organic material with angular clasts of silt-sized quartz; crossed nicols; bar scale is 0.1 mm.

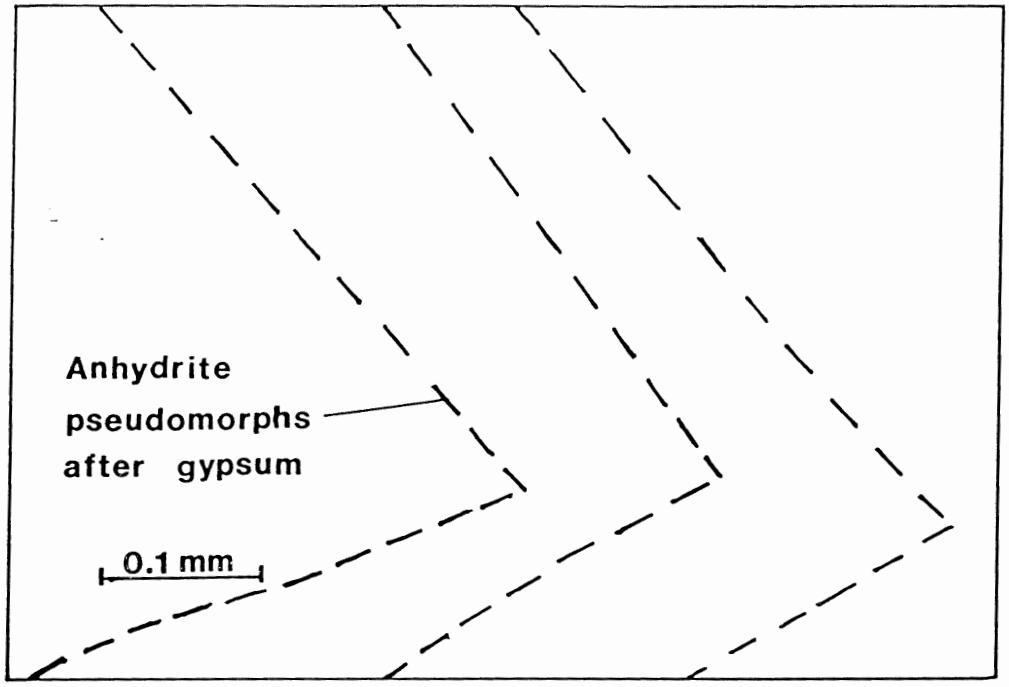
Anhydrite
pseudomorphs
after gypsum
0.1 mm

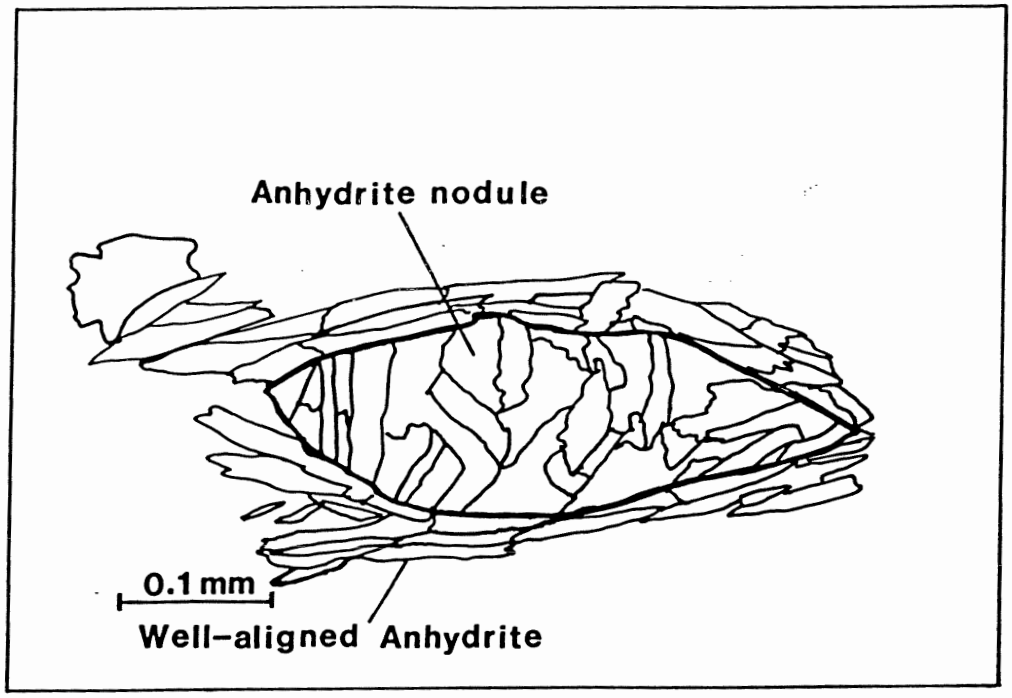
Anhydrite nodule
0.1 mm
Well-aligned Anhydrite

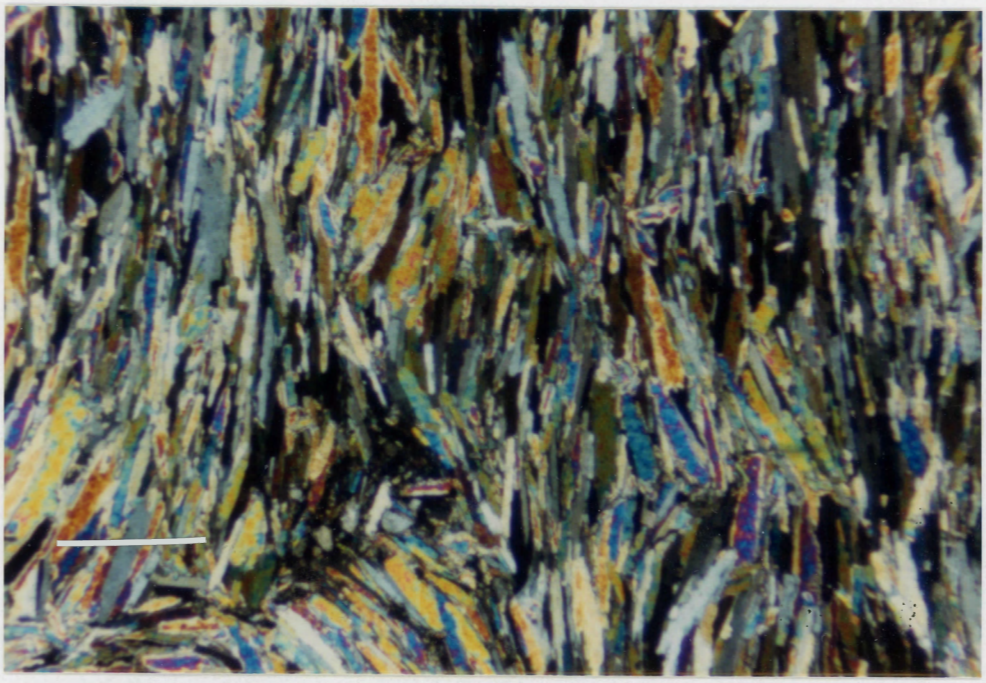

Plate 3-11 - Thin section 158-76; Third anhydrite unit; Nodular anhydrite; note anhydrite pseudomorphs after gypsum; crossed nicols; bar scale is 0.1 mm.

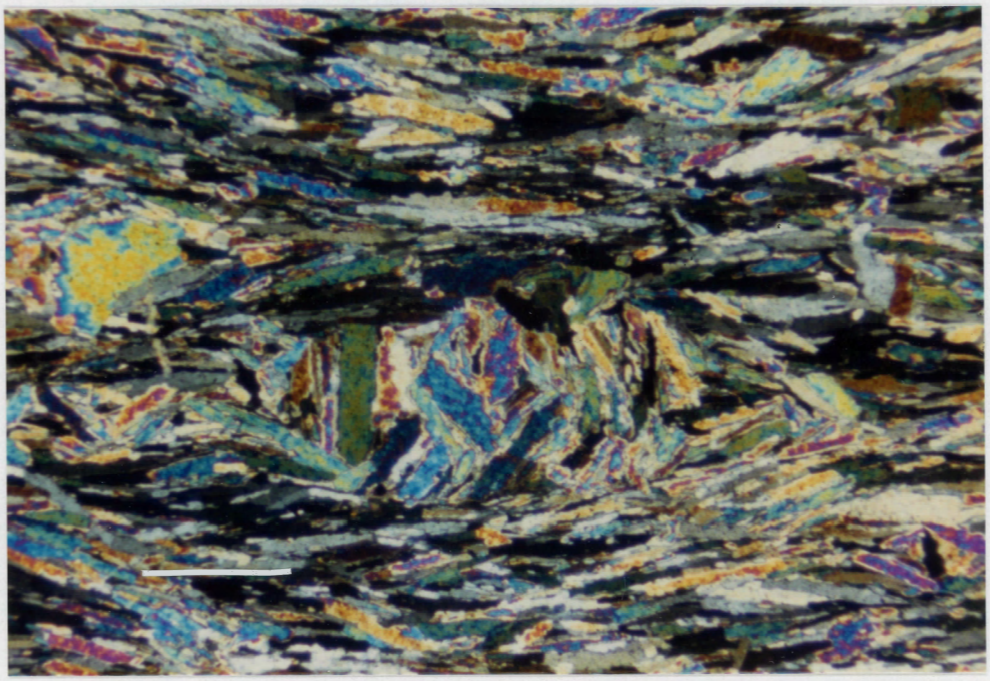

Plate 3-12 - Thin section 158-93; Third anhydrite unit; note anhydrite nodule rimmed by well-aligned, coarse anhydrite laths; crossed nicols; bar scale is 0.1 mm.

appear to pseudomorph gypsum. Another unique feature is the occurence of anhydrite nodules surrounded by very well-aligned, coarse anhydrite laths. Textures are mainly nodular with minor massive anhydrite (Plates 3-9 to 3-12).

In nodular portions organic material has been almost completely replaced or displaced and consists of very thin films separating nodules. It contains minor angular to subrounded silt-size quartz clasts. Elemental sulphur was not observed in thin sections. It is probable that the sulphur was removed by the heat generated during the cutting of thin sections. Also, geochemical data indicate that sulphur is minor in the third anhydrite unit.

III. v. Comparison of microscopic features

Petrographic observations indicate that each unit has distinctive features. Mineralogy may be used to separate the shaft anhydrite unit from others. The shaft anhydrite, with abundant carbonate and organics, and lesser pyrite and fossiliferous material, is easily distinguished from the borate and third anhydrites. The borate and third anhydrites are somewhat more difficult to separate mineralogically. Both consist mainly of anhydrite, with only minor organic material. These units are more readily separated on the basis of textures. Textural features provide the best means of determining whether or not the units represent separate entities. Fibroradiate textures observed in the borate anhydrite are very distinct and are not observed in the third anhydrite. These textures formed

through recrystallization. The coarse, well-aligned fabric observed in the third anhydrite is also very distinct and is not present in the borate unit. This fabric occurs where anhydrite laths pseudomorph gypsum.

III. vi. Conclusions

Based on mineralogic and textural features observed in thin sections it is possible to recognize three distict anhydrite units. The borate and third anhydrite that are often difficult to separate on a megascopic scale are readily differentiated on a microscopic scale.

IV. GEOCHEMISTRY

IV. i. Introduction

This chapter is a discussion of geochemistry in the shaft, borate, and third anhydrite units. Samples that provide geochemical data were not originally collected with statistical analysis in mind. The samples were obtained in an attempt to discover anomalies in the three anhydrite units and to determine values of elemental sulphur in the third anhydrite unit. Thus sample numbers are relatively small. Geochemical data were statistically analyzed for three reasons: 1) to highlight analytical results; 2) to identify statistical similarities and/or differences between the units; and 3) to show correlations within each unit.

IV. ii. Analytical Methods

Data consist of 74 whole rock analyses, with 15 samples from the shaft anhydrite unit, 30 samples from the borate anhydrite unit, and 29 samples from the third anhydrite unit. All analyses were done at the Technical University of Nova Scotia under contract with the Nova Scotia Department of Mines and Energy. Samples consisted of one-half of a split core approximately 3-5cm in length, pulverized in a shatter box to 100 mesh size and stored in an airtight plastic vial. A split and reference sample were included in each group of twenty samples in order to check the reliability of analytical results. Each individual sample was

analyzed for combined water, moisture content, SO_3, CaO, Cl, MnO, Fe_2O_3, MgO, Na_2O, K_2O, Sr. Selected samples were analyzed for organic carbon and native sulphur. Gravimetric methods determined quantities of moisture content, combined water, sulphate and elemental sulphur. Titration determined quantities of CaO and Cl. Concentrations of MnO, Fe_2O_3, MgO, Na_2O, K_2O and Sr were measured by progressively dissolving samples in hydrochloric, nitric, hydrofluoric, and perchloric acid. Residues were then processed with the Thermo Jerrel-Ash Video 12E Atomic Absorption Spectrophotometer. Dissolution of samples in hydrochloric acid, and heating residues in an induction furnace determined the concentration of organic carbon.

IV. iii. Statistical Methods

Degree of precision was checked for all analytical data. For each element in the duplicate pair or split sample, precision (T) was calculated as a percentage:

$$T = \frac{V1 - V2}{\overline{V1,2}} \times 100\%$$

V1 = first value of element in first member of split

V2 = value of element in second member of split

$\overline{V1,2}$ = mean of V1 and V2

T = tolerance of precision

Precision for all elements was acceptable considering that each of the three anhydrite units contained thirty or less samples. There were no established precision limits for any of elements so tolerance of precision was carefully considered for each pair of splits. Only combined water and moisture content analyses had unacceptably high T values. Four samples were retested with improved results.

In addition, analytical results for control reference samples were used to determine acceptibility of data. The results of analyses on reference samples were compared to previous analyses. Only five analyses of reference samples were available (twenty are recommended). In order for results to be accepted they had to be within +/- 2.5 standard deviations of the mean. All results were within these limits.

Prior to statistical analysis, data were checked for problems of constant sum closure (Skala, 1979; Butler and Woronow, 1986). Closure occurs when component parts of the same object are expressed as percentages of the same whole. An increase in one component will necessarily cause a decrease in one or more other components because the sum of all the components remains constant. Closure significantly affects correlation coefficients. A correlation coefficient between a pair of closed components is affected by the linear association between the components and by closure itself. Standard statistical methods cannot separate these two sources (Butler and Woronow, 1986). Atchison (1984 a,b) has developed techniques that

appear to provide a basis for assessing relationships between the components. These methods involve the comparison of: 1) composition data (data in the form of percentages); 2) logarithms of composition data; and 3) log centered data (data produced by subtracting the geometric mean from each of the component logarithms). Correlation coefficients are checked for each form of data. Significant changes in correlation coefficients indicate that closure influences the data set. Checking analytical data for the three anhydrite units, as prescribed by Atchison (1984 a, b), indicates that closure is not a problem because correlation coefficients generated by each of the three methods mentioned above are within 0.001 of each other.

Geochemical data was analyzed on an IBM PC-XT using a statistical software package: "Systat Version 2.1." Mean, maximum, minimum, standard deviation, range and variance were determined for each variable. In addition Pearson and Spearman correlation matrices were determined. For elements showing significant correlations X-Y plots were printed. A "DOS Basic" program was used to calculate Student t-tests.

IV. iv. Results of Basic Statistics

Figures 3-1 to 3-4 summarize arithmetic mean and ranges of chemical data for each anhydrite unit. Complete results of individual analyses are provided in Appendix I. Each unit has distinct geochemical characteristics. Interpretation of results must consider the possibility of introduction of errors by small

sample populations (for example the shaft anhydrite unit with n = 15). Results for combined water and moisture content are not included in the discussion because analysis gave results very close to detection limits.

SO_3

Figure 3-1 illustrates variations in means and ranges of SO_3 between the three units. The third anhydrite has 24 % more SO_3 than the shaft anhydrite and 15 % more SO_3 than the borate anhydrite. The range of SO_3 values in the shaft anhydrite is more than 6 times that in the third anhydrite. The range of SO_3 values in the borate anhydrite is more than 4 times that in the third anhydrite. Significant differences in mean SO_3 values and ranges are caused by variability in anhydrite content. The shaft anhydrite has the lowest anhydrite content and the third anhydrite has the highest. The borate anhydrite is intermediate.

CaO

Figure 3-1 illustrates variation in means and ranges of CaO between the three units. The shaft anhydrite has 8 % more CaO than the borate anhydrite and the third anhydrite has 10 % more CaO than the borate anhydrite. The range of CaO values in the borate anhydrite is more than 4 times that of the shaft and slightly less than 3 times that of the third. Differences in CaO values are related to different in calcium sulfate contents in the three anhydrite units.

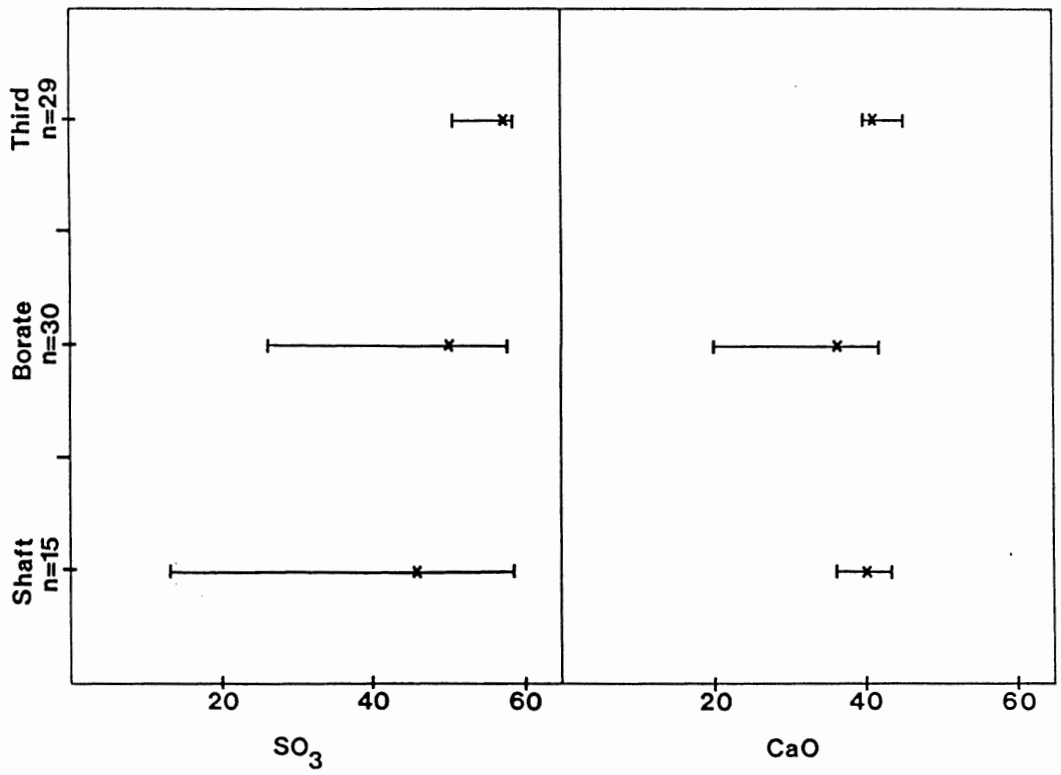

Figure 3-1 - Mean values and ranges of SO_3 and CaO for the shaft, borate, and third anhydrite units (x = mean, ⊢—⊣ = range).

Chloride

Figure 3-2 illustrates the variation in means and ranges of Cl between the three units. Mean Cl concentrations in the shaft and third units are less than 1%. In the borate unit the mean Cl concentration is 5 % and range of concentrations is much greater. The significantly higher mean concentration of Cl in the borate unit is due to abundant secondary halite.

MgO

Figure 3-2 illustrates the variation in means and ranges of MgO between the three units. The shaft anhydrite has approximately 15 times as much MgO as the third anhydrite and approximately 3 times as much as the borate anhydrite. Sample P-886-10 influences the range with an anomalously high MgO value. However, the shaft anhydrite range has a range 15 times that of the third. It must be considered that mean values for all units are close to detection limits and may be inaccurate.

Na_2O

Figure 3-2 illustrates the variation in means and ranges of Na_2O between the three units. The mean Na_2O concentration in the borate anhydrite is approximately 8 times that in the shaft anhydrite and approximately 193 times that in the third anhydrite. The range of Na_2O values in the borate anhydrite is approximately 8 times that in the shaft anhydrite and approximately 700 times that in the third anhydrite. The borate

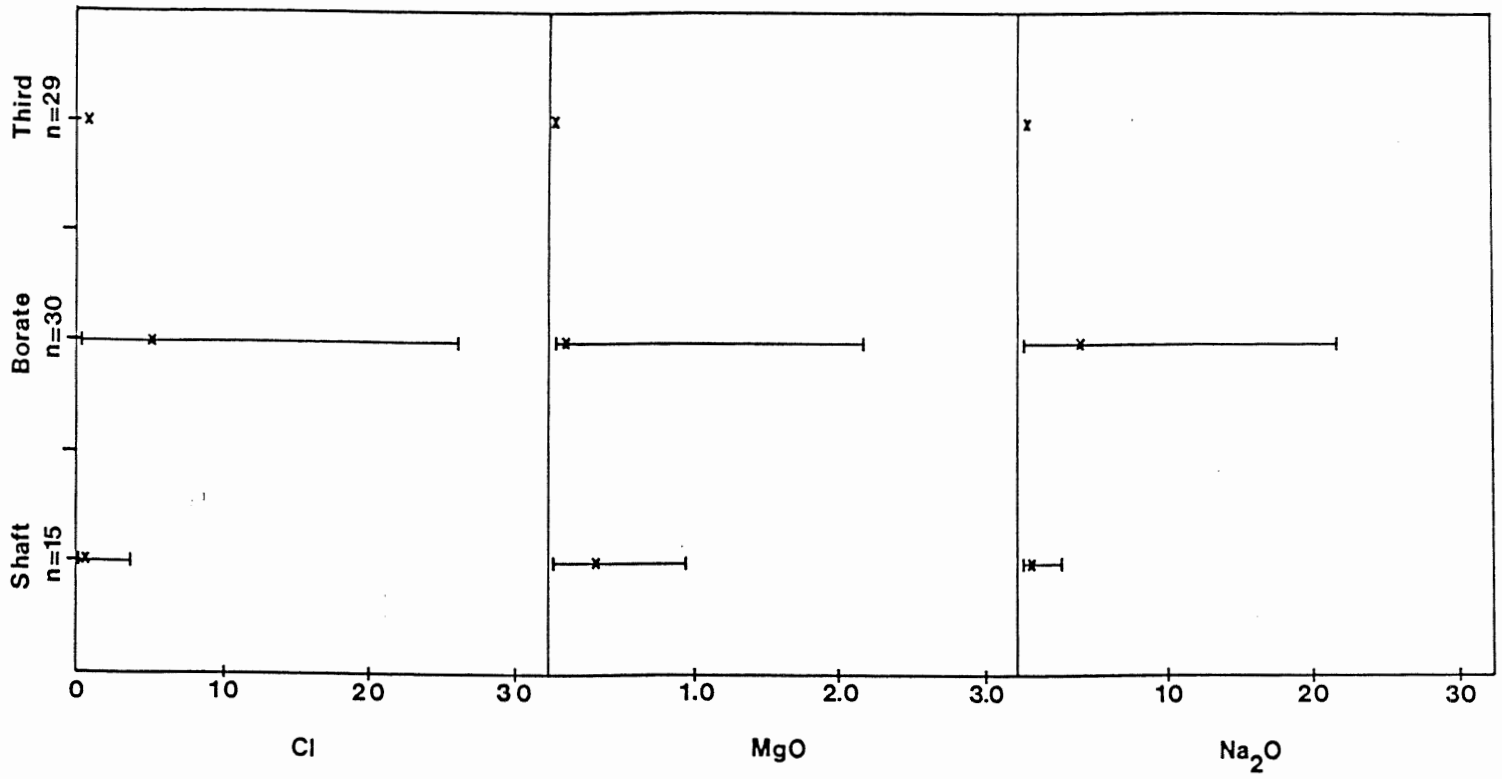

Figure 3-2 - Mean values and ranges of Cl, MgO, and Na_2O for the shaft, borate, and third anhydrite units (x = mean, ⊢—⊣ = range).

anhydrite shows a significantly greater mean Na_2O value and a much greater range of values because it has abundant secondary halite. The shaft anhydrite contains some minor primary and secondary halite and therefore shows somewhat lower values. The third anhydrite is almost completely lacking in halite and therefore has the lowest values.

MnO

Mean MnO concentrations and ranges are low for all units. The data from the all three units are very close to detection limits and it is not possible to accurately predict their reliability.

Fe_2O_3

Figure 3-3 illustrates the variation in means and ranges of Fe_2O_3 between the three units. The shaft anhydrite contains 3 times as much Fe_2O_3 as the third anhydrite. The borate anhydrite has a range approximately 15 times that of the shaft and third anhydrites, but this range has been influenced by an anomalously high value in P-886-10. The shaft anhydrite has the greatest mean value for Fe_2O_3 because it contains organic-rich detrital material. Pyrite replaces organic material in this unit and may also influence iron concentrations.

K_2O

Figure 3-3 shows the variation in means and ranges of K_2O

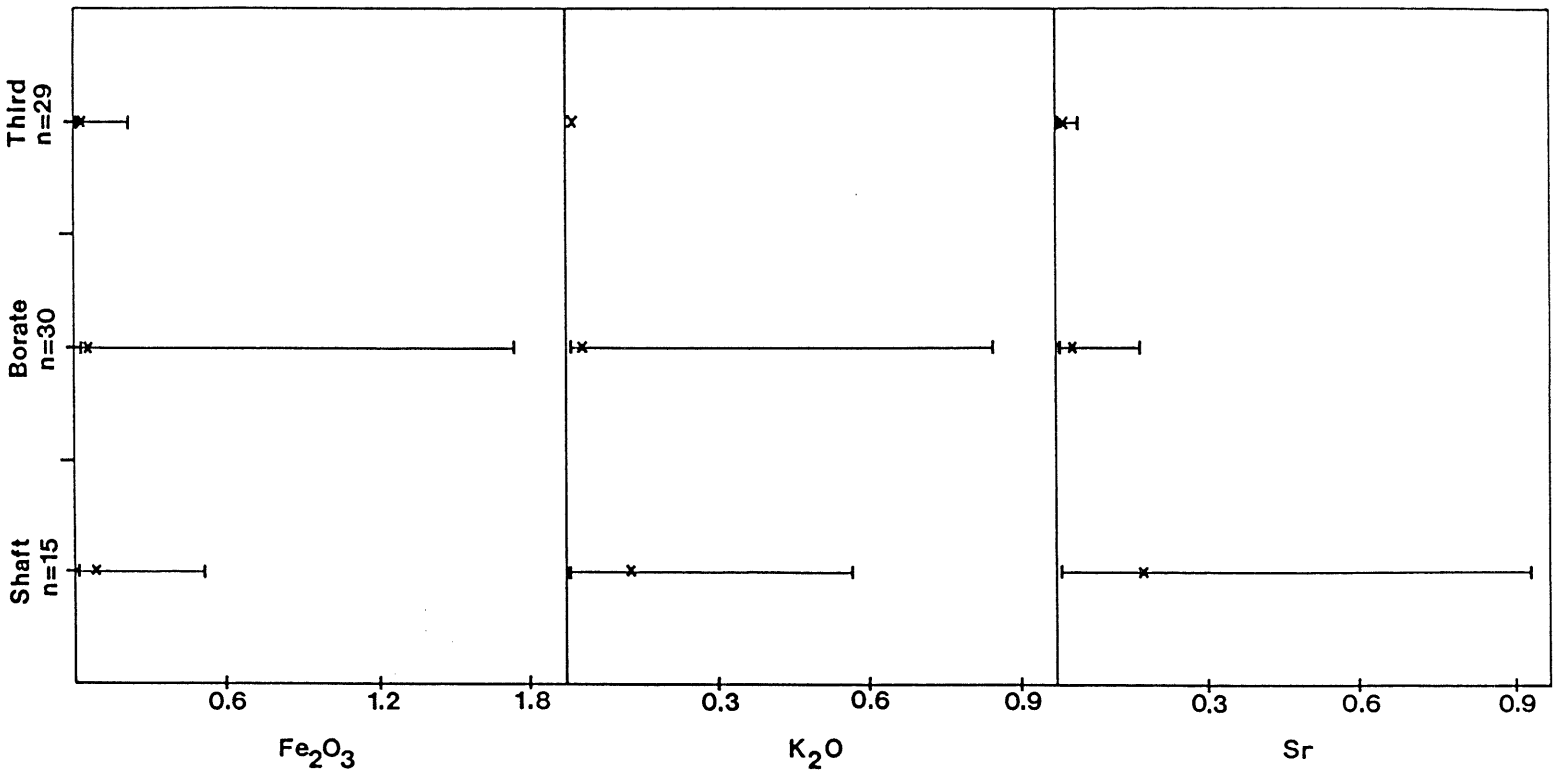

Figure 3-3 - Mean values and ranges of Fe_2O_3, K_2O and Sr for the shaft, borate, and third anhydrite units (x = mean, ⊢—⊣ = range).

values between the three units. The shaft anhydrite has 3 times as much K_2O as the borate anhydrite and 4 times as much K_2O as the third anhydrite. The shaft anhydrite has 18 times the range of the third anhydrite. The borate anhydrite shows the greatest range of K_2O values but this has been influenced by an anomalously high value in P-886-10.

Strontium

Figure 3-3 shows the variation in means and ranges of strontium between three units. The shaft anhydrite has approximately 3 times more strontium than the borate anhydrite and approximately 5 times more than the third anhydrite. The range of strontium in the shaft anhydrite is 7 times that in the borate anhydrite and 23 times that in the third. Sample P-816-90 has an anomalously high Sr value of 9500 ppm.

Elemental Sulfur

Only the third anhydrite unit contains visible elemental sulfur. Therefore, all samples from this unit were analyzed for sulfur. Three samples each from the borate and shaft anhydrites were analyzed as controls. Results presented in Figure 3-4 indicate that the third anhydrite has 3 times as much sulphur as the shaft anhydrite and 1.5 times as much sulphur as the borate anhydrite. Sulfur values in the third anhydrite have ranges 21 times that of the shaft anhydrite and 8 times that of the borate anhydrite. Elemental sulfur content should be carefully

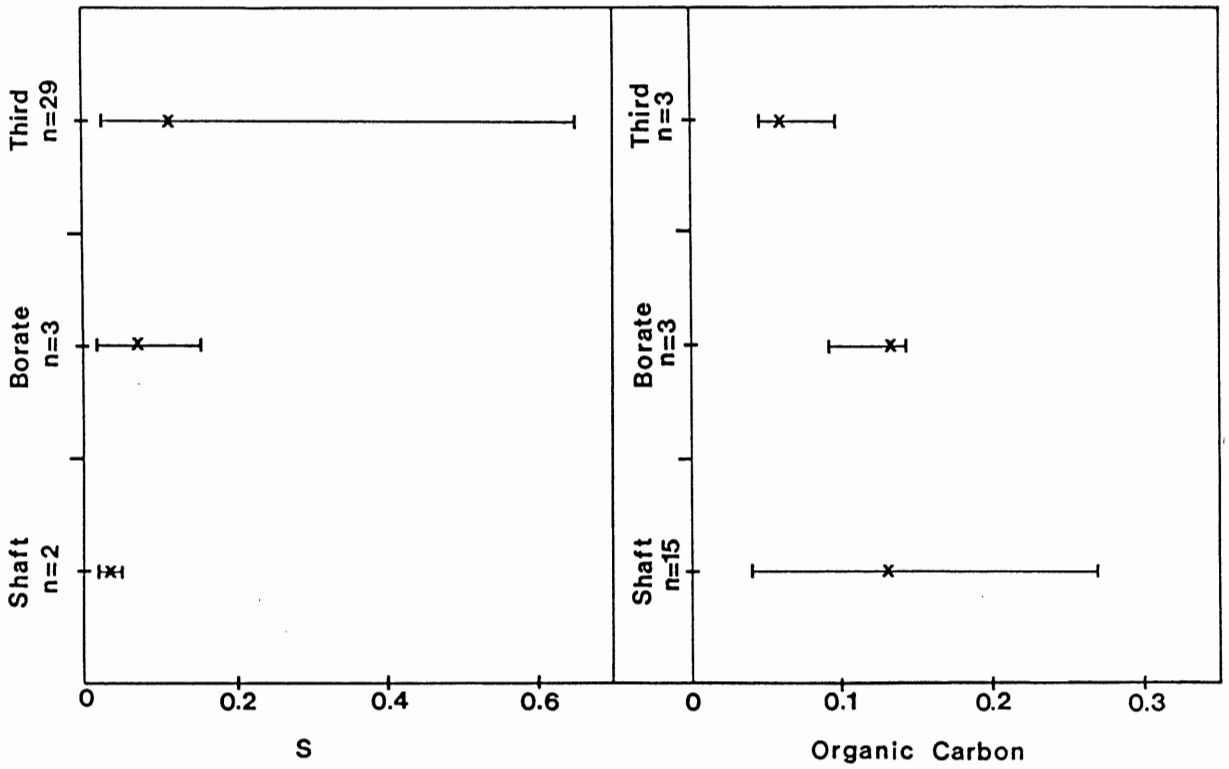

Figure 3-4 - Mean values and ranges of elemental sulfur and organic carbon for the shaft, borate, and third anhydrite units (x = mean, ⊢—⊣ = range).

considered when comparing the three units because it is a late diagenetic component that formed after the unit itself was formed.

Organic Carbon

All samples from the shaft anhydrite were analyzed for organic carbon because abundant organic-rich laminae were observed in thin section and hand specimen. Organic material is not abundant in the borate and third anhydrites and three samples from each of these units were analyzed as controls. Results shown in Figure 3-4 indicate that the shaft anhydrite has approximately twice as much organic carbon as the third anhydrite. Ranges of organic carbon values in the shaft anhydrite are approximately 5 times that of the borate and third anhydrite units.

The analyses were also used to calculate percentage values for gypsum, anhydrite, carbonate and halite for each sample. Gypsum values were calculated using results of combined water analyses. Anhydrite values were calculated using SO_3 and combined water analyses. Carbonate was calculated using CaO analyses. Halite content was determined from % water soluble NaCl. Specifics of calculation methods are included in Appendix I. Results shown in Table 1 indicate that, based on these four main constituents, there are significant differences in the shaft, borate, and third anyhdrite units. The shaft anhydrite shows the lowest anhydrite content, the highest carbonate content, and is

TABLE 1

Mean Concentrations (%) of Major Constituents in the Shaft, Borate, and Third Anhydrite Units

	Shaft	Borate	Third
Gypsum	2.13	2.56	3.28
Anhydrite	76.73	83.06	95.16
Carbonate	14.36	3.98	1.74
Halite	0.85	7.21	0.05
	n=15	n=30	n=29

Table 2

Significant results of Student t-tests

Shaft and Borate Anhydrite Units

MnO	t=3.37
Organic Carbon	t=3.21

Degrees of Freedom = 43

Shaft and Third Anhydrite Units

Cl	t=3.09
MnO	t=4.58
Fe_2O_3	t=2.81
MgO	t=4.89
Na_2O	t=2.99
K_2O	t=2.89
Sr	t=3.14
NaCl	t=2.99

Degrees of Freedom = 42

Borate and Third Anhydrite Units

Cl	t=4.00
Na_2O	t=3.81
Sr	t=4.84
$CaCO_3$	t=3.01
NaCl	t=3.82

Degrees of Freedom = 57

easily distinguished from the other two units. The borate and third anhydrites are also readily separated based on their four main constituents. The- borate anhydrite contains 14 % less anhydrite than the third anhydrite but contains 7 % more halite than the third anhydrite.

IV. v. Results of T-tests

In addition to basic statistics, t-tests were applied to geochemical data. T-tests were used to check for significant differences in mean elemental values between the three anhydrite units. Results acceptable at the 95% confidence level are shown in Table 2. Conclusions from T-tests are: 1) the shaft and third anhydrites have the greatest number of significant differences in mean elemental values; this result is related to the heterogeneity of the shaft anhydrite and the homogeneity of the third anhydrite; 2) the shaft and borate anhydrites show significant differences due to the presence of organic material in the shaft anhydrite; and 3) differences between the borate and third anhydrite are related to the occurence of halite in the borate anhydrite and the more homogeneous nature of the third anhydrite.

IV. vi. Inter-element Relationships

Correlation coefficients were also calculated for geochemical data. Pearson correlation coefficients are useful because they indicate what variables are related or vary together

within each anhydrite unit. The method is formally referred to as "Pearson's product moment of linear correlation" or "r". Spearman rank correlation coefficient is used where the product moment correlation; r, is unsuitable because the population is not normally distributed (Till, 1974). Complete Pearson and Spearman correlation matrices for each anhydrite unit are provided in Appendix 1. All elements in each of the three units approximate lognormal distributions. Therefore, Pearson correlations were computed for each unit using logarithms of measured concentrations. Plots of correlation coefficients significant at the 95% confidence level are provided in Appendix 1. As an additional check for significant correlations Spearman correlation coefficients were computed for each unit using original, non-normally distributed data. According to Cheeny (1983), the Spearman correlation coefficient has no available test for significance. Based on small sample populations and the possible introduction of statistical errors, correlations greater than 0.7 were arbitrarily selected as significant. In all three units logarithmic transformation of original data improves correlations, suggesting that the processes that incorporated these elements possibly happened in a non-linear fashion. This conclusion must be carefully considered because logarithmic transforms may make almost any distribution appear normal.

Shaft Anhydrite

The shaft anhydrite has the largest number of significant

correlations. It is possible that the small sample population (n=15) influenced correlations and/or that the number and variety of correlations may be related to the heterogeneity of this unit. The most significant positive correlations are between Cl and Na_2O; MnO and MgO; Fe_2O_3 and Na_2O; and Fe_2O_3 and K_2O. The most significant negative correlations are between SO_3 and Na_2O, and SO_3 and Sr. Plots of these correlations are included in Appendix I.

Borate Anhydrite

In this unit the sample population (n=30) is probably large enough to prevent the introduction of significant errors into correlation coefficients. Significant positive correlations include: SO_3 and CaO; Cl and Na_2O; Fe_2O_3 and MgO; Fe_2O_3 and K_2O; Fe_2O_3 and MgO; and K_2O and MgO. Significant negative correlations include SO_3 and Fe_2O_3, Na_2O and SO_3, and K_2O and SO_3. Plots of these correlations are included in Appendix I.

Third Anhydrite

In this unit the sample population (n=29) is probably large enough to prevent the introduction of significant errors. Original concentrations of elements do not show any significant correlations. Logarithmic transformation of the data yields significant positive correlations between: MnO and MgO; Na_2O and Cl; Fe_2O_3 and Na_2O and; Mgo and K_2O. Significant negative correlations occur between SO_3 and Sr. Correlations are weaker

and fewer in this unit possibly due to the homogeneity of the unit.

IV. vii. Conclusions

1. The three anhydrite units have unique chemical characteristics and may be separated based on the abundance of major constituents (see Table 2).

2. The shaft anhydrite unit has the most impurities. It has the highest concentration of several elements (MnO, Fe_2O_3, MgO, K_2O, Sr and Organic carbon). It also has the lowest anhydrite content and the highest carbonate content. The shaft anhydrite unit is readily distinguished from the borate and third anhydrite units on the basis of geochemical data.

3. The borate anhydrite unit has fewer impurities than the shaft anhydrite. It has the highest halite content and an intermedite anhydrite content, between the shaft and borate units. Based on the high halite content and the intermediate anhydrite content this unit is readily distinguished from the third anhydrite.

4. The third anhydrite has the fewest impurities among the three anhydrite units. It has the highest anhydrite and gypsum contents, lacks high concentrations of trace and minor elements, and has low contents of carbonate and halite. The third anhydrite

is readily distinguished from the borate on the basis of geochemical data.

5. Several inter-element correlations are present in each unit. Most interelement correlations are improved by logarithmic transforms suggesting that elemental incorporation processes may be non-linear.

IV. viii. Suggestions for Further Study

The geochemical study discussed above provides significant insight into the chemical characteristics of the three anhydrite units. However, the study is not based on sample populations that are large enough to eliminate the possibility of the introduction of statistical errors. Sample populations should all be in excess of thirty in order to provide statistically meaningful results. With larger sample population it would also be possible to use multivariate statistics to analyze the data. Techniques such as factor analysis or discriminant analysis would be useful to the description of the units.

V. DIAGENESIS

V. i. Introduction

This chapter proposes an approximation of the complex diagenetic processes that produced the shaft, borate and third anyhdrite units. Each unit has been extensively altered by diagenetic processes and the composition of original sediments is difficult to recognize. In particular, diagenetic processes make it difficult to predict the original nature of sediments that were the precursors for the borate and third anhydrite units.

V. ii. Diagenesis of the Shaft Anhydrite

The diagenetic interpretations of Evans (1972) form the basis for this discussion. Diagenetic processes that formed the shaft anhydrite unit are postulated to have occurred in the following order:

(1) formation of displacive gypsum crystals within pre-exsisting carbonate and organic material;

(2) replacement of gypsum by anhydrite, to form anhydrite pseudomorphs;

(3) replacement of anhydrite by pale to clear calcite, to form calcite pseudomorphs after gypsum;

(4) destruction of organic material by bacterial action and precipitation of pyrite in place of organic matter;

(5) recrystallization and minor dolomitization of original carbonate to form massive, microcrystalline carbonate;

(6) pervasive growth of anhydrite by:

i) complete replacment of carbonate laminae, to form coalescing nodules and laminated anhydrite;

ii) displacive growth of nodules within carbonate and organic material creates nodular anhydrite; and

(7) development and subsequent corrosion of dolomite rhombs within carbonate.

V. iii. Explanation of diagenesis: Shaft Anhydrite

The first stage in the diagenesis of the shaft anhydrite was the formation of gypsum along organic laminae. Evans (1972) suggested that organic matter may have acted as a conduit or aquiclude for the transport of a gypsum-rich brine. Gypsum was subsequently pseudomorphed by anhydrite. Some anhydrite nodules exhibit a lenticular shape characteristically observed in gypsum. The growth of gypsum crystals and the subsequent growth of anhydrite displaced the host carbonate sediment. This implies that gypsum growth occurred early in the formation of the shaft anhydrite unit. According to data obtained from Central Europe, in brines saturated with NaCl, gypsum is only stable at a depths less than 125 m, but in brines saturated with SO_4 it is readily stable at depths of 650 m and more. In pure water gypsum may also be found below 700 m. Therefore anhydrite can only occur in deeper-lying formations (Langbein, 1987). According to Fairbridge (1983) the dehydration from gypsum to anhydrite most commonly

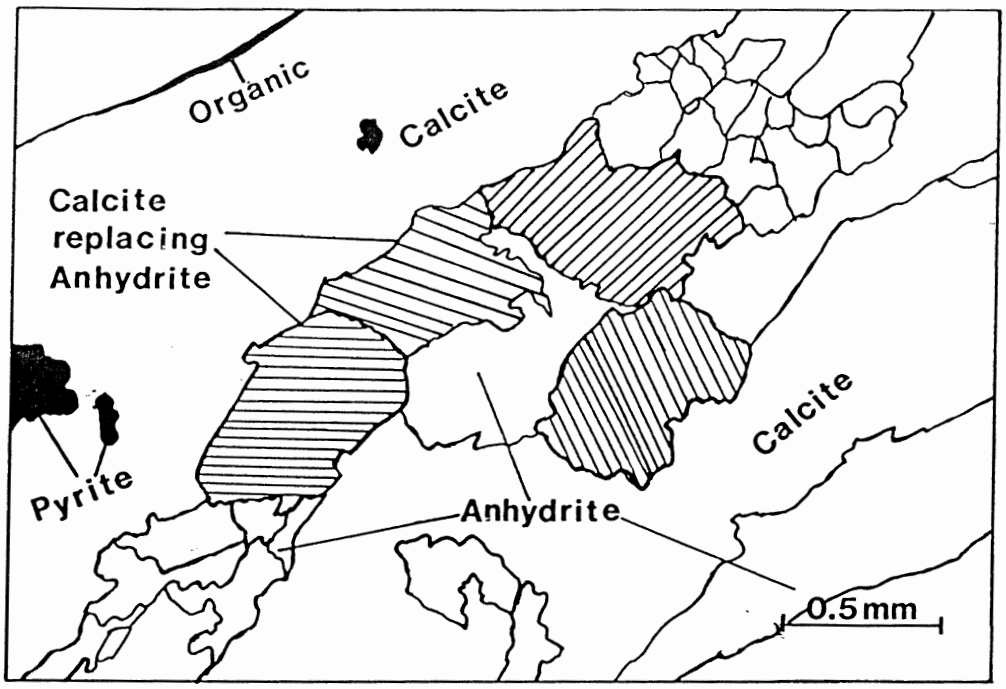
Organic
Calcite
Calcite
replacing
Anhydrite
Pyrite
Anhydrite
Calcite
0.5mm

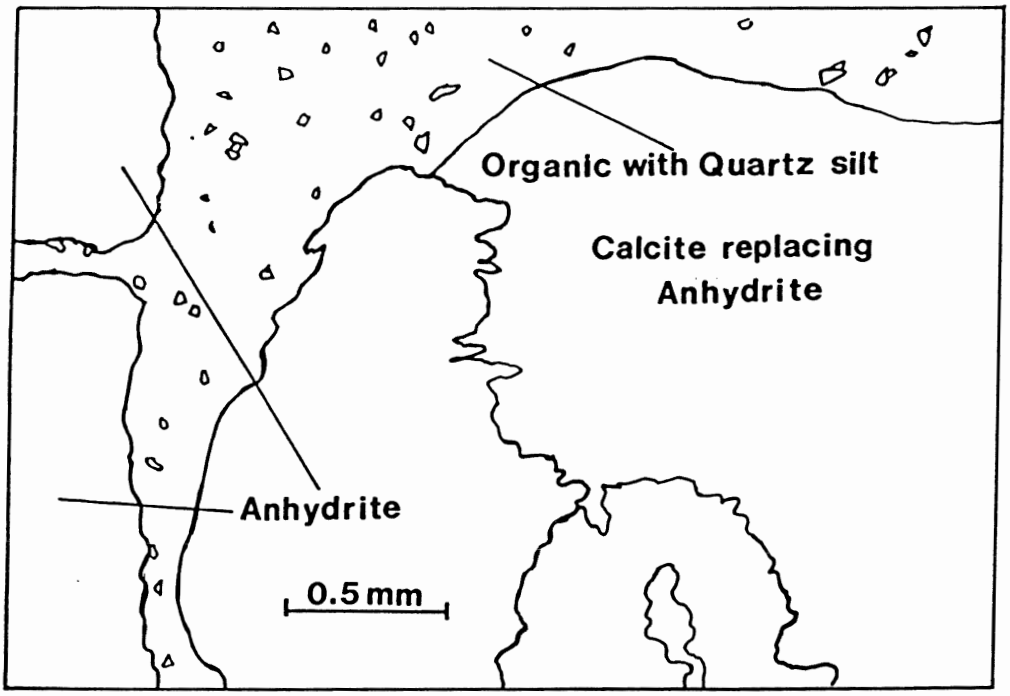
Organic with Quartz silt
Calcite replacing
Anhydrite
Anhydrite
0.5mm

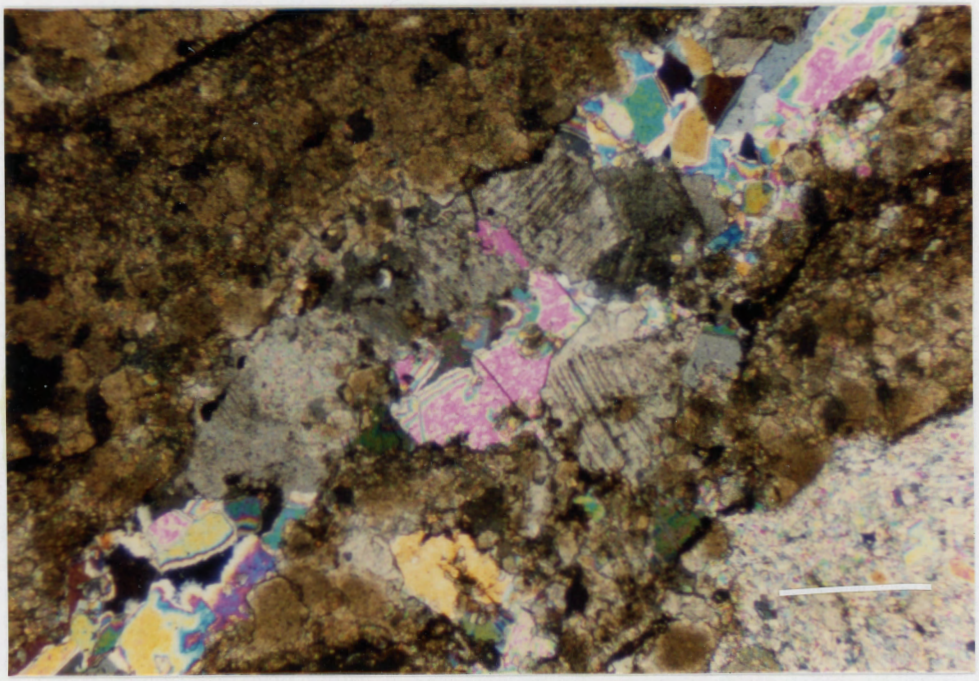

Plate 5-1 - Thin section 918-36; Shaft anhydrite unit; note calcite replacing anhydrite; crossed nicols; bar scale is 0.5 mm.

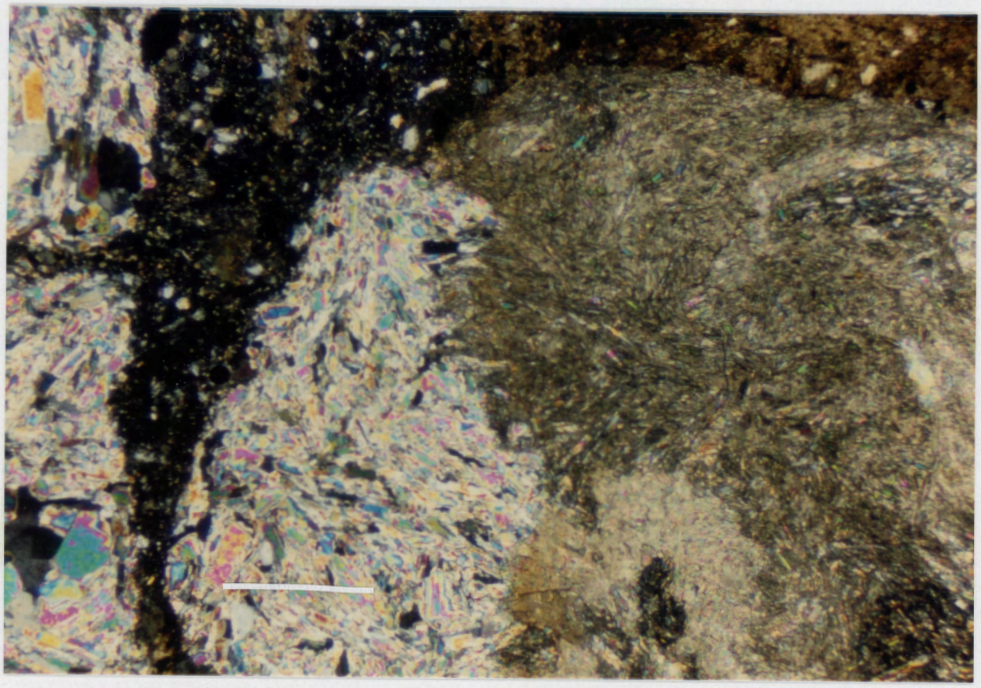

Plate 5-2 - Thin section 816-90; Shaft anhydrite unit; note calcite replacing anhydrite; crossed nicols; bar scale is 0.5 mm.

takes place at depths of about 100 m, at confining pressures of approximately 50 kg/cm^2. The replacement of anhydrite by calcite was the next stage of diagenesis. (Plates 5-1 and 5-2). Pale brown, subhedral to euhedral calcite is observed overgrowing anhydrite nodules and individual anhydrite grains. The next stage was the conversion of organic matter to pyrite. According to Berner (1970) the major steps in the formation of sedimentary pyrite are : 1) bacterial sulfate reduction; 2) reaction of H_2S with iron minerals to form FeS; 3) reaction of FeS with elemental sulphur to form pyrite. Upon the removal of dissolved oxygen from associated waters by aerobic metabolism of organic matter, anaerobic bacteria reduce sulfate within sediments. As a result of sulfate reduction, H_2S is formed. Dissolved H_2S reacts with the most reactive forms of iron present to form black, non-crystalline FeS. If sulfate reduction continues, H_2S concentration increases and additional detrital iron is converted to FeS. Some H_2S is oxidized either by organic processes or by sulfur oxidizing bacteria to elemental sulfur. Part of this sulfur is subsequently oxidized by bacteria to dissolved sulfate. Remaining elemental sulfur slowly reacts with FeS to form pyrite.

The pervasive growth of anhydrite, replacing calcite, forms laminated and nodular textures during the next stage of diagenesis. Evans (1972) did not propose a mechanism to explain why diagenetic processes would produce such different end-products. Why laminated anhydrite did not continue to evolve into a nodular texture is very hard to predict. Two possible

explanations are: 1) sediment in laminated portions was more cohesive or elastic; and 2) compactional forces were exerted by overlying layers and imparted a confining pressure. Evans (1972) suggested that the overall process of pervasive anhydrite growth resulted from increased concentrations of calcium and sulphate in brines.

The final stage of diagenesis (dolomitization) produced minor amoumts of euhedral dolomite. Hardie (1986) notes that the formation of contemporaneous dolomite in modern environments has been widely reported but that the nature of dolomite formation (primary or secondary) has yet to be clearly resolved. In the shaft anyhdrite unit dolomite always is a replacement product. In the presence of a high salinity brine enriched in magnesium, conditions would be suitable for dolomite formation. Dolomite is mainly observed around the rims of anhydrite nodule that have cores of secondary calcite. The calcite in turn contains inclusion of earlier-formed anhydrite.

V. iv. Diagenesis of the Borate Anhydrite

Diagenetic events producing the borate anhydrite are postulated to have occurred in the following order:

(1) displacive growth of gypsum crystals within pre-existing carbonate sediment and organic material;

(2) replacement of gypsum by anhydrite pseudomorphs;

(3) minor replacement of anhydrite by calcite;

(4) destruction of organic material, formation of minor

pyrite;

(5) recrystallization and minor dolomitization of carbonate;

(6) pervasive growth of anhydrite nodules, replacement and fragmentation of carbonate and organic material; recrystallization of anhydrite and development of:

i) nodular and stylolitic textures and;

ii) fibroradiate clusters of bladed, acicular crystal in a microcrystalline groundmass;

(7) dissolution of some primary halite and/or anhydrite followed by the deposition of clear, euhedral, vug-filling secondary anhydrite;

(8) recrystallization of anhydrite around halite-filled vugs;

(9) deposition of minor dolomite around periphery of vugs; and

(10) formation of danburite nodules, displacing anhydrite, organic material and carbonate.

V. vi. Explanation of diagenesis: borate anhydrite

The first stage in the diagenesis of the borate anhydrite was the formation of gypsum within host carbonate sediments and organic material. The original volume of carbonate and organic material appears to have been less than in the shaft anhydrite. Reduced carbonate formation was probably a result of increased salinity at the time of depostion.

The next stage of diagenesis was the replacement of gypsum

by anhydrite. Characteristic spindle-shaped gypsum crystals were pseudomorphed by anhydrite. Anhydrite was then replaced by secondary calcite. Next, organic material was consumed by bacterial action to form minor amounts of pyrite. Carbonate material was then: 1) recrystallized forming brown, microcrystalline calcite; and 2) dolomitized, forming minor euhedral dolomite.

The next stage was the pervasive growth of anhydrite. This stage formed the nodular and stylolitic textures. Most nodules exhibit a microcrystalline or aphanitic texture. Recrystallization of the microcrystalline anhydrite formed masses of felted crystals and fibroradiate clusters. A similar diagenetic process has been noted from the Middle Carboniferous of Spitsbergen, the upper Permian of the north of England and the upper Jurassic of Sussex (Holliday, 1973). Primary halite and/or some anhydrite was then dissolved and later replaced by clear, euhedral secondary halite. The growth of the secondary halite seems to have caused a recrystallization of anhydrite. There are three possible explanations: 1) the growth and volumetric expansion of the halite displaced pre-exsisting anhydrite, with resulting pressures that caused anhydrite to recrystallize; 2) brines that formed the secondary halite may have been enriched in calcium and sulphate resulting in the formation of secondary anhydrite; and 3) halite may have dissolved and recrystallized in situ and left an anhydrite rim as a residue. At or about this time danburite nodules were deposited. Borate nodules formed

within anhydrite, displacing carbonate and organic material, at the border of anhydrite and halite-filled vugs and within the halite-filled vugs. Borate occurrences in other localities have been explained in two ways: 1) concentration of brines enriched boron which is precipitated and subsequently altered by digenetic processes; and 2) hydrothermal solutions rich in boron are derived from and concentrated by volcanic activity. In New Brunswick an extensive borate mineral assemblage has been reported by Ralston and Waugh (1981). They point out that it is theoretically possible but rather unlikely that the borate minerals formed as a result of evaporative processes. Modern seawater, with an average concentration of 0.026% H_3BO_3, is considered an unlikely source for large concentrations of boron. In addition, volcanism of approximatley the same age as evaporite deposits has been reported in New Brunswick. Raup and Madsen (1986) have interpreted danburite occurences in the Paradox Basin of southeastern Utah to have formed diagenetically from the interaction of high salinity brines rich in boron and constituents of the anhydrite host rock. This explanation appears the most valid for the deposit at Pugwash. This conclusion is based on the following facts: 1) the number of borate minerals reported from Pugwash is very limited, unlike the New Brunswick occurences; and 2) all the constituents for the formation of borate nodules are present within the Pugwash deposit. Ca could be derived from anhydrite, Si from clay and quartz silt, and B from high-order salts associated with carnallite. The only

problem with this interpretation is that units with the required constituents are not presently in contact. It is possible that the intense deformation resulting from diapirism has changed the original stratigraphy of the deposit. However this is probably not necessary given fluid movement and brine concentrations as well as diagenetic processes. The most important fact is that all the constituents are present.

V. vii. Diagenesis of the Third Anhydrite

The diagenetic history of the third anhydrite unit is very difficult to reconstruct. The proximity of the third anhydrite to the edge of the diapir may explain the apparent lack of features in this unit compared to the shaft and borate anhydrites. The circulation of fluids from clastics in contact with the unit at the edge of the diapir may have removed halite, and contact between anhydrite and the clastics may have resulted in extensive recrystallization. Diagenetic processes that formed the borate anhydrite are postulated to have occurred in the following order:

(1) displacive growth of gypsum within organic material and minor carbonate sediment;

(2) replacement of gypsum by anhydrite pseudomorphs;

(3) pervasive development of anhydrite forming nodular and stylolitic textures;

(4) deposition of elemental sulphur.

V. viii. Explanation of diagenesis: third anhydrite

The first stage of diagenesis was the growth of gypsum within organic material and minor carbonate sediments. Gypsum was subsequently replaced by anhydrite pseudomorphs. Much of the replacement anhydrite consists of coarse, euhedral laths with a well-aligned fabric. In some portions faint outlines of gypsum crystals, defined by organic matter, surround coarse anhydrite. The formation of anhydrite in the third anhydrite appears to have been much more intense than in other units. As was mentioned above the position of the third anhydrite unit may also have influenced its present appearance. Recent work by Carter (1985, 1986) suggests that the Pugwash diapir may have been partially eroded by groundwater percolation. The third anhydrite occurs on the northern mining limit of the deposit on the uppermost level (630 ft.). A complete section of cap rock has not been reported from development drilling and no showings of elemental sulfur are noted. However, the presence of minor amounts of sulfur that replaces organic material indicates conditions that deposit elemental sulfur within salt dome cap rocks were present, at least on a limited scale. Therefore, the emplacement of elemental sulphur appears to be a late stage of diagenesis. Hydrocarbons from the nearby clastics provide a food source for sulfate reducing bacteria. These bacteria procure energy from the oxidation of hydrocarbons to CO_2 by the breakdown of SO_4 ions, releasing CO_2 and H_2S as by-products (Carter et al., 1989). The sulfur replaced organic material that surrounds nodules because this material probably provided an aquiclude for fluids.

V.ix. Conclusions

The three anhydrite units have been subjected to a series of complex, multi-stage diagenetic processes. The diagenetic sequence and resulting products are very different in all three units. The diagenetic sequence is most easily reconstructed in the shaft anhydrite because it has retained some features that appear to be primary. Original composition of sediments was probably a combination of carbonate and organic material (cyanobacteria). Subsequent growth and replacement of sulphate and carbonate produced textures and mineralogies that are presently observed.

VI. Paleoenvironmental Interpretation

VI. i. Introduction

This chapter is a brief account of paleoenvironments that were present at the time of formation of the three anhydrite units. Definitive models for the deposition of evaporites are lacking (Handford, 1981). Kendall (1979) summarized reasons for this. They include: 1) evaporites have traditionally been considered chemical precipitates rather than sedimentary rocks; 2) areas of recent evaporite deposition are not comparable in size to ancient saline giants; 3) modern evaporite sequences are difficult to observe due to remoteness of locations, relative lack of core and lack of surface outcrops of halite; and 4) diagenetic processes may extensively alter evaporites.

Diagenesis has extensively altered all units. It is possible that widespread bulk mineral replacements have occurred and anhydrite may replace calcite, or vice versa, on a much greater scale than is recognized. Therefore, what is presently observed in the three anhydrite units is not really a true representation of original composition of sediments. In particular, diagenetic processes make it very difficult to reconstruct depostional environments for the borate and third anhydrite units. However, the shaft anhydrite has retained some features that make it possible to reconstruct an approximation of depositional conditions.

VI. ii. Paleosalinity

Paleosalinity is a very useful tool when reconstructing environments of deposition. The sequence of evaporites has been interpreted to have formed in a maine environment (Bell). The concept of paleosalinity is most readily applied to the shaft anhydrite. According to Pounder (1970), theoretically, carbonate minerals will be the first to form in an evaporite sequence. They form from a point of zero evaporation to where about 72 % of the water has been removed. The deposition of carbonate beds in the shaft anhydrite may represent periods of moderate salinity. The deposition of sulfate and halite represents periods of more saline conditions. In a theoretical evaporation sequence calcium sulfate begins to form at a point where about 72 % of the water has evaporated. The first halite begins to form when about 91 % of the water has evaporated. A probable explanation for the interbedded sulfate-carbonate is a periodic incursion of normal marine water into the depositional basin. Based on the limited scale of the observations in the shaft anhydrite it is very hard to quantify this theory. A second possible cause may be a periodic climatic change that may have increased the inflow of meteoric water, reduced salinity and/or decreased the rate of evaporation.

Salinity conditions during the deposition of the borate anhydrite are much harder to reconstruct. Most halite in this unit is secondary. However, the unit does contain minor amounts

of primary calcite. There are two possible explanations for this fact: 1) carbonate was not a volumetrically important component of primary deposition; and 2) development of anhydrite has progressed to such a stage that nearly all carbonate has been replaced. Therefore, based on the occurrence of primary halite and the apparent lack of carbonate, it is probable that the borate anhydrite was deposited under higher salinity, less ephemeral condtions than the shaft anhydrite.

The third anhydrite unit has been extensively altered by diagenetic processes. No primary or secondary halite is observed. The invasion of connate waters from nearby clastics probably removed all traces of halite. Carbonate is a very minor component and, if originally present, appears to have been almost totally replaced by anhydrite. The third anhydrite unit may also be the result of cap rock development (although a complete section of cap rock has yet to be reported) and the incorporation into the halite by halokinetic movement. With this limited information it is practically impossible to predict the conditions at the time of deposition.

VI. iii Petrographic Observations

Diagenetic processes have obliterated many of the primary features in the borate and third anhydrites. However, the shaft anhydrite has retained several features that appear to be original.

During deposition of the shaft anhydrite original material

consisted of large amounts of organic matter. In portions of laminated anhydrite, coalescing nodules exhibit poorly developed enterolithic deformation that is generally contained by organic layers. A sedimented deposit would likely have been fragmented and broken by nodule development. The cohesive and elastic characterictics of the organic material suggest a living material such as an algal mat. Shearman and Fuller (1969) observed similar features in the Devonian Winnipegosis Formation of Saskatchewan. They interpreted these features to represent an algal mat. Another feature supporting the algal mat conclusion is the fractured and fragmented nature of some laminated portions. Algal mats are not usually very continuous laterally and are often very fragmented. Additional features with environmental significance are erosional surfaces overlain by clastic material (in sections showing stratigraphic top) indicating possible subaerial exposure and subsequent inundation by "fresh" or normal marine waters. In addition small fractures that are filled with coarse secondary anhydrite may represent periods of subaerial exposure.

Nodular anhydrite, occuring in all three units, also has great significance as an indicator of paleoenvironmental conditions. With the discovery in the late 1960's of nodular, mosaic and contorted anhydrite forming in Recent sabkhas along the Trucial Coast of the Persian Gulf (Butler, 1969; Kinsman, 1966, 1969; Shearman, 1966) a number of papers were published invoking a sabkha diagenetic model to explain ancient carbonate-sulphate facies sequences (Fuller and Porter, 1969; Schenk, 1969; and

others). According to Handford (1981) the sabkha hypothesis has not been universally accepted to explain the formation of nodular anhydrite. There has been a great deal of controversy over the significance of nodular and evenly laminated anhydrite (Dean et al., 1975) due to the widespread uncritical use of the nodular anhydrite = sabkha hypothesis. The presence of abundant nodular anhydrite does not alone justify the conclusion that the shaft, borate, and possibly the third anhydrite units represent sabkha deposits.

VI. iv. Conclusions

The complexity and extent of diagenetic processes in all three anhydrite units makes it very difficult to determine the depositional conditionss. The presence of carbonate in the shaft anhydrite may represent periodic conditions of moderate salinity. Evans (1972) concluded that the shaft anhydrite was deposited in a subaqueous environment. The presence of dissolution surfaces, possible subaerial exposure features and algal material indicate that water may have been relatively shallow. The borate anhydrite was possibly deposited under slightly more saline conditions than the shaft anhydrite. At the present time it is extremely difficult to propose an accurate reconstruction of the depositional environment that formed the third anhydrite unit.

VII. CONCLUSIONS

1. Mineralogical and textural features observed in thin sections indicates the presence of three distinct anhydrite units.

2. Interpretation of geochemical data also suggests three distinct anhydrite units.

3. Each of the three anhydrite units has undergone a complex series of diagenetic processes that have severely altered the orginal composition and mineralogy.

4. The shaft anhydrite was probably deposited in shallow water, under salinity conditions that were by times moderate, and was possibly subjected to periods of subaerial exposure. The borate anhydrites was probably deposited under slightlty more saline conditions. At the present time it is impossible to accurately reconstruct the depositional evironment that formed the third anhydrite.

VIII. References

Aitchison, J. A. 1984a. The statistical analysis of geochemical compositions. Mathematical Geology, **16**: 529-540.

———————— 1984b. Reducing the dimensionality of compositional data. Mathematical Geology, **16**: 617-650.

Aumento, F. 1964. Authigenic minerals and preliminary investigations of the evporite deposit at Pugwash, Nova Scotia. Nova Scotia Research Foundation, Unpublished Report 13-64, 39 p.

Barr, C. A. 1966. Report on the first phase geochemical investigation for the potash exploration project; Nova Scotia Research Foundation; Report Number 2-66: 40p.

Bell, W. A. 1929. Horton Windsor District, Nova Scotia; Geological Survey of Canada, Memoir 155: 268p.

———————— 1944. Carboniferous rock and fossil floras of northern Nova Scotia; Geological Survey of Canada, Memoir 238: 277p.

———————— 1958. Possibilities for the occurence of petroleum reservoirs in Nova Scotia; Nova Scotia Department of Mines: 177p.

Berner, R. A. 1970. Sedimentary pyrite formation. American Journal of Science. **268**: 1-23.

Boehner, R. C.; Ryan, R. J.; and Carter, D. C. 1985. Cumberland Basin Project - A progress report; In: Program and Summaries, Ninth Annual Open House and Report of Activities, Nova Scotia Department of Mines and Energy, 41-43.

Boehner, R. C. 1986. Salt and Potash in Nova Scotia ; Nova Scotia Department of Mines and Energy; Bulletin Number 5, 346p.

Butler, G. P. 1969. Modern evaporite deposits and the geochemitry of coexsisting brines, the sabkha, Trucial Coast, Arabian Gulf. Journal of Sedimentary Petrology, **39**, 70-89.

Butler, J. C. and Woronow, A. 1986. Discrimination among tectonic settings using trace element abundances of basalts. Journal of Geophysical Research. **91**, Number B10, 10,289-10,300

Carter, D. C. 1985. Geology of the Pugwash Mine - A Progress Report; In: Program and Summaries, Ninth Annual Open House and Report of Activities, Nova Scotia Department of Mines and Energy, 47-49.

Carter, D. C. 1986. Geology of the Pugwash Mine - An update; In: Program and Summaries, Tenth Annual Open House and Report of

Activities, Nova Scotia Department of Mines and Energy, 65-71.

Carter, D. C. and Pickerill, R. K. 1985. Algal swamp and shallow evaporitic lacustrine lithofacies from the late Devonian-early Carboniferous Albert Formation, southeastern New Brunswick, Canada, Maritime Sediments and Atlantic Geology. **21**, 69-86.

Carter, D. C.; Boehner, R. C. and Adams, G. In Press. Sulphur in Nova Scotia: Geological setting of native sulfur occurrences in Nova Scotia, Nova Scotia Department of Mines and Energy, Open File Report 88-01, 14 p.

Cheeny, R. F. 1983. Statistical methods in geology for field and lab decisions; George, Allen and Unwin, London, 169 p.

Dean, W. E.; Davies, G. R. and Anderson, R. Y. 1975. Sedimentological significance of nodular and laminated anhydrite. Geology, **3**, 367-372.

Evans, R. E., 1965. Studies in the evaporites of the Maritime provinces of Canada; unpublished M. Sc. thesis, Dalhousie University, Halifax, Nova Scotia; Nova Scotia Department of Mines and Energy, Thesis 102, 110 p.

---------- 1967. The structure of the Mississippian evaporite deposit at Pugwash, Cumberland County, Nova Scotia. Economic

Geology, 62, 262-273.

---------- 1972.Studies in the evaporites of the Maritime provinces of Canada; unpublished Ph. D. thesis, University of Kansas, Lawrence, Kansas; Nova Scotia Department of Mines and Energy, Thesis 103, 115 p.

---------- 1974. Geometry and Devlopment of structures within the Pugwash diapir, Nova Scotia, In: Fourth International Symposium on Salt, Northern Ohio Geological Society Inc., p. 251.

Fairbridge, R. E. 1983. Syndiagenesis-Anadiagenesis-Epidiagenesis: Phases in lithogenesis, In: Developments in Sedimentology, 25B, Diagenesis in sediments and sedimentary rocks, 2, Eds. Larsen, G. and Chilingar, G. V., Elsevier, Amsterdam, The Netherlands, 17-114.

Faribault, E. R. and Fletcher, H. 1905. Pugwash Sheet, Nova Scotia Old Series Maps, Number 61.

Fuller, J. G. C. M. and Porter, J. W. 1969. Evaporitic formations and petroleum reserviors in the Devonian and Mississippian of Alberta, Saskatchewan, and North Dakota. A. A. P. G. Bulletin, 53, 909-926.

Goodman, N. R. 1985. All evaporite deposits are the same. Or are

they ?, In: Sixth International Symposium on Salt, Eds. B. C. Schreiber and H. C. Hanes, Volume 1, 131-138.

Handford, C. R. 1981. Coastal sabkha and salt pan deposition of the Lower Clear Fork Formation (Permian) Texas. Journal of Sedimentary Petrology, **51**, No. 3, 761-778.

Hardie, L. A. 1986. Dolomitization: A critical view of some current models. Journal of Sedimentary Petrology, **57**, No. 1, 166-183.

Hayes, A. O. 1931. Report on the potash possibilities of Nova Scotia, In: Annual Report in the Mines, 1930, Part 2, Nova Scotia Department of Mines, 147p.

Holliday, D. W. 1973. Early diagenesis in nodular anhydrite rocks. Inst. of Min. and Metall., Section B, Applied Earth Sciences, B81-B84.

Kendall, A. C. 1979. Facies Models 13: Continental and supratidal (sabkha) evaporites, In: Facies Models: Geoscience Canada, Reprint Series No. 1, Ed. R. G. Walker, 159-174.

Keppie, J. D. 1982a. The Minas Geofracture; In: Major Structural Zones and Faults of the northern Appalachians, Eds. P. St. Julien and J. Beland, Geological Association of Canada, Special Paper

24, 263-280.

Keppie, J. D. 1982b. Tectonic Map of the Province of Nova Scotia, Nova Scotia Department of Mines and Energy, Scale 1:500,000.

Kinsman, D. J. J. 1966. Gypsum and anhydrite of Recent Age; Trucial Coast, Persian Gulf, In: Second Symposium on Salt, Ed. Rau, J. L., Volume 1: Cleveland, Northern Ohio Geological Society, 302-326.

---------- 1969. Modes of formation, sedimentary association and diagnostic features of shallow-water supratidal evaporites, A. A. P. G. Bulletin, **53**, 830-840.

Knight, I. 1983. Geology of the Carboniferous Bay St. George Subbasin, Western Newfoundland, Mineral Development Division, Department of Mines and Energy, Government of Newfoundland and Labrador, Memoir 1, 357p.

Langbein, R. 1986. The Zechstein evaporites: the state of the art. In: Lecture Notes in Earth Sciences, 10, The Zechstein Facies in Europe, Ed. Peryt, T. M.; Springer-Verlag, Berlin, 143-188.

McCutcheon, S. R. 1981. Stratigraphy and paleogeography of the Windsor Group in southern New Brunswick, New Brunswick Department

of Natural Resources, Mineral Resources Division, Open File Report, 81-31, 210p.

Pounder, D. A. 1970. Principles of the origin, deposition, and alteration of evaporite rocks. Notes to accompany a lecture given at the Corporation Stratigraphic Seminars, Chevron Standard Limited, Calgary Alberta. 59 p.

Ralston, B. V. and Waugh, D. C. E. 1981. A borate mineral assemblage from the Penobsquis and Salt Springs evaporite deposits of southern New Brunswick, Canadian Mineralogist, **19**, 291-301.

Raup, O. B. and Madsen B. M. 1986. Danburite in evaporites from the Paradox Basin, Utah. Journal of Sedimentary Petrology, **56**, No. 2, 248-251.

Roliff, W. A. 1962. The Maritimes Carboniferous Basin of Eastern Canada. Proc. Geol. Assoc. Can., Volume 14, 21-41.

Schenk, P. E. 1969. Carbonate-sulphate-redbed facies and cyclic sedimentation of the Windsorian Stage (Middle Carboniferous), Maritime provinces. Canadian Journal of Earth Sciences, **6**, No. 5, 1037-1066.

Shearman, D. J. 1966. Origin of marine evaporites by diagenesis.

Trans. Inst. Min. Metall., Volume B-75, 208-215.

Shearman, D. J. and Fuller J. G., 1969. Anhydrite diagenesis, calcitization and organic laminites, Winnepegosis Formation, Middle Devonian Saskatchewan, Bull. Canadian Petroleum Geology, **35**, 496-525.

Skala, W. 1979. Some effects of the constant-sum closure problem in geochemistry, Chemical Geology, **27**, 1-9.

Till, R. 1974. Statistical Methods for the earth scientist: An Introduction. MacMillan, Hong Kong, 154 p.

Appendix I Geochemical Data

Geochemical data consisted of 74 samples each analyzed for 14 variables. Data was analyzed using "Systat 2.1", a statistical software package designed for the IBM PC. This appendix contains all information generated during the statical analysis of the data.

Appendix I

Calculation of major constituents in the shaft, borate, and third anhydrite units.

Gypsum = Combined Water * 4.778

Anhydrite = SO_3 * 1.7004 - Combined Water * 3.7186

$CaCO_3$ = CaO * 1.7845 - SO_3 * 1.25

NaCl = % Water Soluble Nacl

SHAFT ANHYDRITE

		SAMPLE$	MOIST	COMBH2O	SO3	CAO
CASE	1	P-816-10	0.020	0.200	48.570	41.120
CASE	2	P-816-30	0.030	0.380	58.130	41.170
CASE	3	P-816-40	0.060	0.380	51.660	40.450
CASE	4	P-816-50	0.070	0.300	47.900	42.060
CASE	5	P-816-60	0.070	0.310	57.030	40.210
CASE	6	P-816-70	0.030	0.400	52.790	40.550
CASE	7	P-816-80	0.020	0.430	53.010	40.630
CASE	8	P-816-90	0.005	0.590	14.500	43.570
CASE	9	P-816-100	0.005	0.410	35.890	36.310
CASE	10	P-816-110	0.050	0.480	52.080	42.570
CASE	11	P-816-120	0.060	0.520	28.360	37.530
CASE	12	P-816-130	0.040	0.380	51.210	40.460
CASE	13	P-816-140	0.020	0.570	56.600	41.910
CASE	14	P-816-150	0.030	0.610	58.370	41.230
CASE	15	P-816-160	0.040	0.730	28.310	37.350

		CL	MNO	FE2O3	MGO	NA2O
CASE	1	0.130	0.001	0.030	0.027	0.092
CASE	2	0.055	0.001	0.022	0.014	0.064
CASE	3	0.007	0.001	0.010	0.004	0.034
CASE	4	0.025	0.007	0.040	0.090	0.054
CA	5	0.032	0.013	0.034	0.480	0.046
C	6	0.033	0.025	0.060	0.920	0.055
CASE	7	0.016	0.006	0.036	0.320	0.042
CASE	8	2.950	0.018	0.540	0.770	2.650
CASE	9	1.380	0.010	0.170	0.220	0.950
CASE	10	0.007	0.003	0.056	0.100	0.049
CASE	11	1.870	0.013	0.370	0.590	1.300
CASE	12	0.020	0.003	0.064	0.160	0.051
CASE	13	0.007	0.003	0.049	0.130	0.043
CASE	14	0.064	0.001	0.017	0.013	0.051
CASE	15	1.890	0.012	0.360	0.570	1.270

		K2O	SR	S	ORGC	GYP
CASE	1	0.016	0.057	.	0.041	0.950
CASE	2	0.013	0.075	.	0.073	1.810
CASE	3	0.002	0.051	.	0.230	1.810
CASE	4	0.028	0.072	.	0.073	1.430
CASE	5	0.016	0.065	.	0.180	1.480
CASE	6	0.025	0.100	0.050	0.180	1.910
CASE	7	0.015	0.072	.	0.180	2.050
CASE	8	0.550	0.950	.	0.180	2.810
CASE	9	0.085	0.320	.	0.040	1.950
CASE	10	0.034	0.166	.	0.260	2.290
CASE	11	0.470	0.168	.	0.044	2.480
CASE	12	0.052	0.059	0.025	0.140	1.820
CASE	13	0.032	0.047	.	0.270	2.720
CASE	14	0.013	0.055	.	0.047	2.910
CASE	15	0.450	0.157	.	0.046	3.480

		ANH	CACO3	NACL
CASE	1	81.630	12.670	0.170
CASE	2	98.020	0.800	0.120
CASE	3	86.020	7.610	0.064
CASE	4	80.010	15.180	0.100
CA	5	95.490	0.470	0.087
CA	6	87.850	6.370	0.100
CASE	7	88.080	6.240	0.079
CASE	8	21.830	59.620	5.000
CASE	9	59.060	19.930	1.790
CASE	10	86.260	10.870	0.092
CASE	11	46.250	31.520	2.450
CASE	12	85.260	8.190	0.096
CASE	13	93.520	4.030	0.075
CASE	14	96.330	0.610	0.096
CASE	15	45.370	31.260	2.390

TOTAL OBSERVATIONS: 15

	MOIST	COMBH2O	SO3	CAO	CL
N OF CASES	15	15	15	15	15
MINIMUM	0.005	0.200	14.500	36.310	0.007
MAXIMUM	0.070	0.730	58.370	43.570	2.950
MEAN	0.037	0.446	46.294	40.475	0.566
STANDARD DEV	0.022	0.138	13.237	1.998	0.960

	MNO	FE2O3	MGO	NA2O	K2O
N OF CASES	15	15	15	15	15
MINIMUM	0.001	0.010	0.004	0.034	0.002
MAXIMUM	0.025	0.540	0.920	2.650	0.550
MEAN	0.008	0.124	0.294	0.450	0.120
STANDARD DEV	0.007	0.164	0.300	0.766	0.194

	SR	S	ORGC	GYP	ANH
N OF CASES	15	2	15	15	15
MINIMUM	0.047	0.025	0.040	0.950	21.830
MAXIMUM	0.950	0.050	0.270	3.480	98.020
MEAN	0.161	0.038	0.132	2.127	76.732
STANDARD DEV	0.230	0.018	0.085	0.659	22.752

	CACO3	NACL
N OF CASES	15	15
MINIMUM	0.470	0.064
MAXIMUM	59.620	5.000
MEAN	14.358	0.847
STANDARD DEV	15.949	1.446

TOTAL OBSERVATIONS: 15

	MOIST	COMBH2O	SO3	CAO	CL
N OF CASES	15	15	15	15	15
RANGE	0.065	0.530	43.870	7.260	2.943
VARIANCE	0.000	0.019	175.218	3.993	0.922

	MNO	FE2O3	MGO	NA2O	K2O
N OF CASES	15	15	15	15	15
RANGE	0.024	0.530	0.916	2.616	0.549
VARIANCE	0.000	0.027	0.090	0.587	0.037

	SR	S	ORGC	GYP	ANH
N OF CASES	15	2	15	15	15
RANGE	0.903	0.025	0.230	2.530	76.190
VARIANCE	0.053	0.000	0.007	0.434	517.651

	CACO3	NACL
N OF CASES	15	15
RANGE	59.150	4.936
VARIANCE	254.376	2.090

PEARSON CORRELATION MATRIX

	SO3	CAO	CL	MNO	FE2O3
SO3	1.000				
CAO	0.146	1.000			
CL	-0.835	-0.514	1.000		
MNO	-0.547	-0.296	0.518	1.000	
FE2O3	-0.866	-0.368	0.814	0.738	1.000
MGO	-0.502	-0.248	0.445	0.941	0.770
NA2O	-0.922	-0.462	0.958	0.558	0.907
K2O	-0.811	-0.312	0.799	0.674	0.973
SR	-0.879	-0.122	0.741	0.607	0.816
ORGC	0.196	0.580	-0.639	0.006	-0.238

	MGO	NA2O	K2O	SR	ORGC
MGO	1.000				
NA2O	0.509	1.000			
K2O	0.733	0.866	1.000		
SR	0.533	0.842	0.738	1.000	
ORGC	0.090	-0.459	-0.318	-0.098	1.000

UMBER OF OBSERVATIONS: 15

Signifcant values at 95 %, r > 4.41

MATRIX OF SPEARMAN CORRELATION COEFFICIENTS

	SO3	CAO	CL	MNO	FE2O3
SO3	1.000				
CAO	0.207	1.000			
CL	-0.538	-0.254	1.000		
MNO	-0.458	-0.204	0.452	1.000	
FE2O3	-0.732	-0.161	0.487	0.751	1.000
MGO	-0.432	-0.268	0.434	0.939	0.800
NA2O	-0.668	-0.127	0.917	0.492	0.645
K2O	-0.769	-0.097	0.483	0.648	0.966
SR	-0.586	-0.105	0.585	0.711	0.742
ORGC	0.379	0.456	-0.733	-0.060	-0.166

	MGO	NA2O	K2O	SR	ORGC
MGO	1.000				
NA2O	0.450	1.000			
K2O	0.673	0.653	1.000		
SR	0.627	0.708	0.677	1.000	
ORGC	-0.011	-0.677	-0.201	-0.287	1.000

NUMBER OF OBSERVATIONS: 15

Significant values > .7

CL

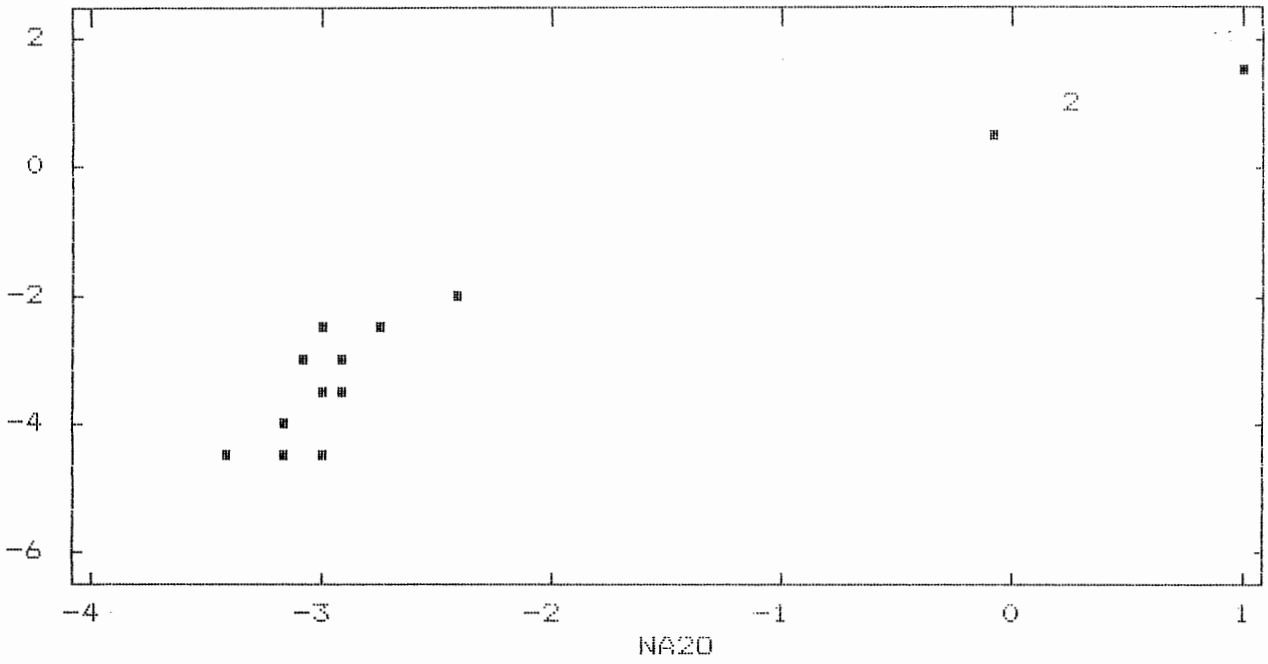

MNO

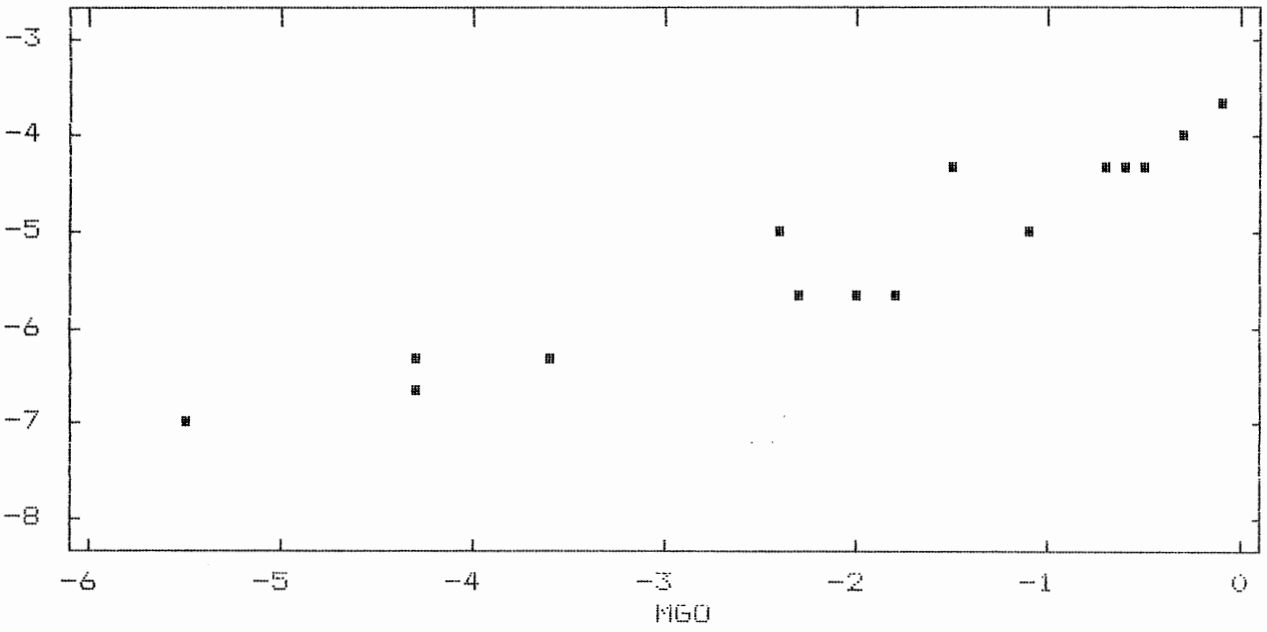

FE2O3

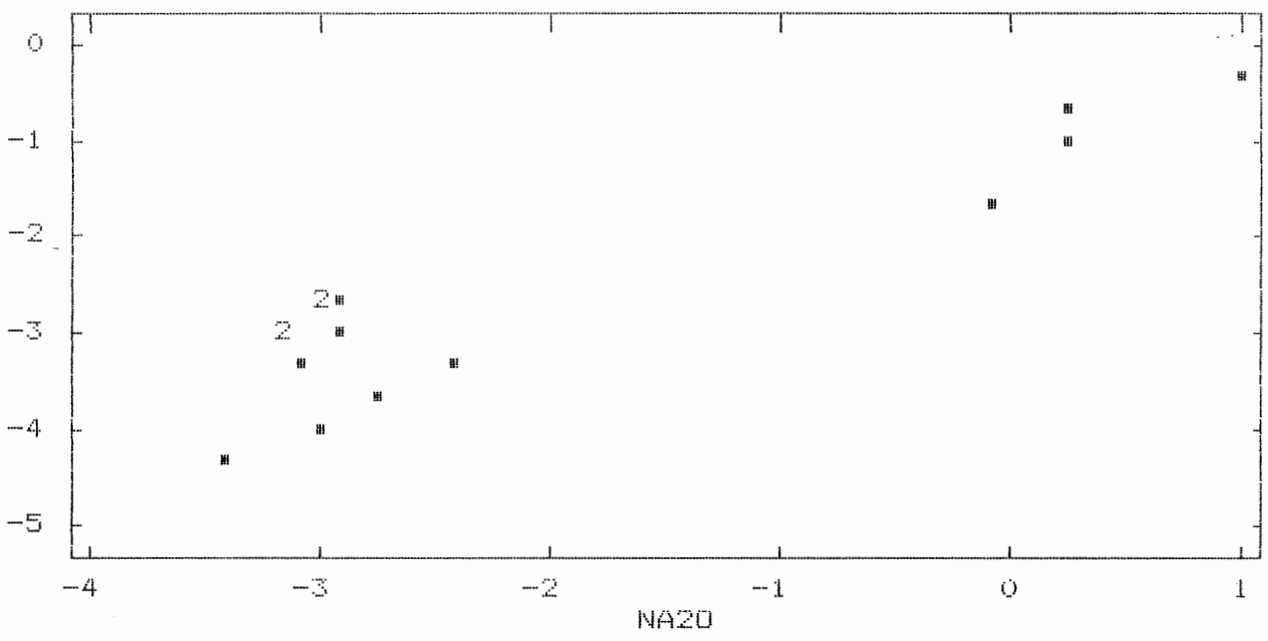

FE2O3

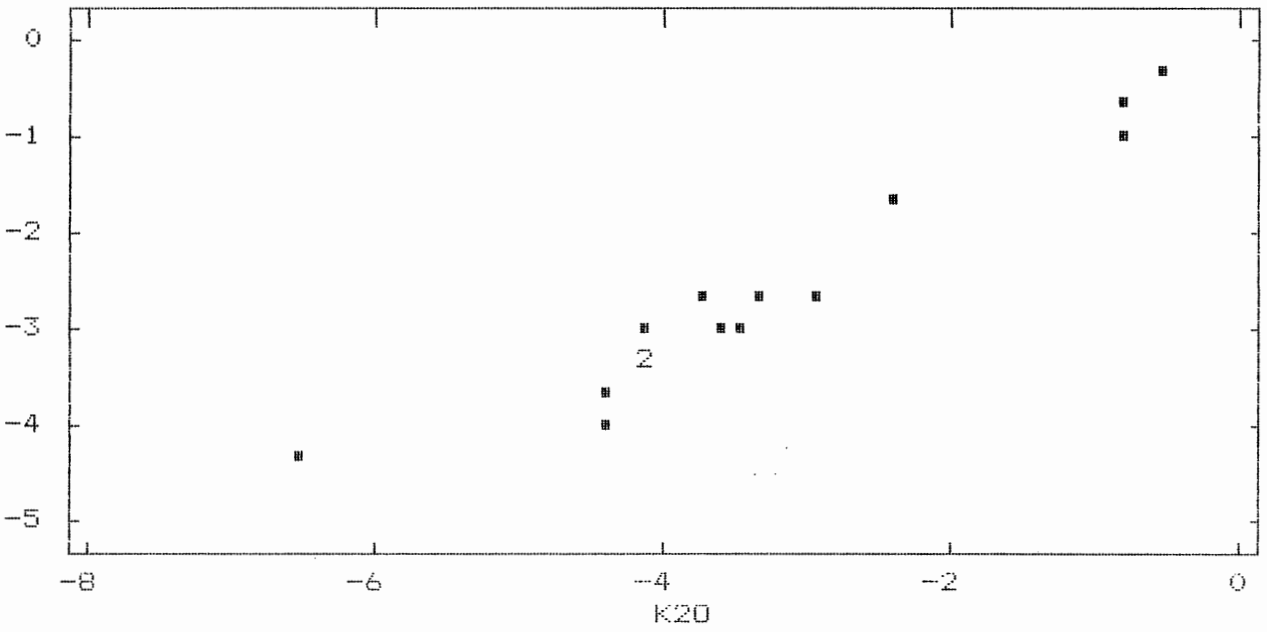

Borate Anhydrite

		SAMPLE$	MOIST	COMBH2O	SO3	CAO
CASE	1	P-886-10	0.020	1.120	26.740	20.560
CASE	2	P-886-20	0.005	0.630	44.040	32.130
CASE	3	P-886-30	0.020	0.680	50.480	39.030
CASE	4	P-886-40	0.005	0.540	51.220	37.350
CASE	5	P-886-50	0.040	0.510	51.420	38.020
CASE	6	P-886-60	0.030	0.530	58.330	41.050
CASE	7	P-886-70	0.020	0.500	56.390	40.630
CASE	8	P-886-80	0.050	0.490	54.600	39.030
CASE	9	P-886-90	0.050	0.540	53.890	38.700
CASE	10	P-886-100	0.040	0.520	50.250	36.850
CASE	11	P-886-110	0.005	0.350	50.480	36.510
CASE	12	P-886-120	0.020	0.460	56.110	40.170
CASE	13	P-886-130	0.005	0.590	57.450	41.350
CASE	14	P-886-140	0.020	0.560	53.550	38.860
CASE	15	P-886-150	0.110	0.540	56.840	41.300
CASE	16	P-886-160	0.040	0.540	47.230	34.000
CASE	17	P-886-160a	0.010	0.500	54.480	40.210
CASE	18	P-886-170	0.005	0.530	50.700	39.120
CASE	19	P-886-170a	0.030	0.460	50.740	37.180
CASE	20	P-886-180	0.010	0.460	55.970	41.050
CASE	21	P-886-190	0.005	0.610	51.930	41.050
CASE	22	P-886-200	0.080	0.550	49.170	40.880
CASE	23	P-886-210	0.005	0.280	47.680	41.130
CASE	24	P-886-220	0.080	0.190	52.930	40.380
CASE	25	P-886-230	0.030	0.640	56.180	40.630
CASE	26	P-886-240	0.050	0.490	31.310	23.720
CASE	27	P-886-240a	0.060	0.530	50.260	38.360
CASE	28	P-886-250	0.005	0.730	54.110	41.170
CASE	29	P-886-260	0.010	0.450	48.770	36.590
CASE	30	P-886-270	0.040	0.530	31.320	23.410
CASE	31		.	.	.	.

		CL	MNO	FE203	MGO	NA20
CASE	1	1.100	0.014	1.750	2.190	1.160
CASE	2	11.490	0.001	0.016	0.018	7.830
CASE	3	2.600	0.001	0.011	0.025	2.650
CASE	4	7.310	0.001	0.014	0.020	5.520
CASE	5	0.550	0.001	0.019	0.017	0.280
CASE	6	0.058	0.001	0.019	0.018	0.031
CASE	7	1.310	0.001	0.019	0.018	0.890
CASE	8	3.100	0.001	0.016	0.018	2.170
CASE	9	3.200	0.002	0.017	0.027	2.250
CASE	10	6.780	0.001	0.011	0.037	5.480
CASE	11	7.260	0.001	0.010	0.022	5.410
CASE	12	1.510	0.001	0.011	0.025	1.010
CASE	13	0.300	0.001	0.020	0.030	0.220
CASE	14	1.800	0.003	0.037	0.075	1.260
CASE	15	0.420	0.002	0.019	0.032	0.300
CASE	16	10.610	0.002	0.019	0.023	8.090
CASE	17	1.930	0.003	0.042	0.052	1.320
CASE	18	4.160	0.003	0.016	0.045	3.240
CASE	19	5.770	0.004	0.022	0.037	4.320
CASE	20	0.640	0.003	0.014	0.030	0.450
CASE	21	1.650	0.015	0.034	0.065	1.160
CASE	22	1.590	0.007	0.054	0.089	1.160
CA	23	2.650	0.007	0.040	0.072	2.120
CA	24	3.280	0.003	0.037	0.048	2.880
CASE	25	1.430	0.003	0.024	0.130	0.930
CASE	26	26.860	0.002	0.022	0.032	21.500
CASE	27	4.680	0.003	0.026	0.057	3.480
CASE	28	1.320	0.003	0.023	0.053	0.089
CASE	29	7.060	0.001	0.014	0.022	5.350
CASE	30	26.930	0.002	0.020	0.032	21.870
CASE	31	.	.	.	.	.

		K2O	SR	S	ORGC	GYP
CASE	1	0.840	0.061	.	.	5.350
CASE	2	0.007	0.039	.	.	3.010
CASE	3	0.007	0.040	.	.	3.240
CASE	4	0.007	0.042	.	.	2.580
CASE	5	0.010	0.043	0.025	0.092	2.430
CASE	6	0.011	0.036	.	.	2.530
CASE	7	0.009	0.044	.	.	2.380
CASE	8	0.009	0.040	.	.	2.340
CASE	9	0.009	0.039	.	.	2.580
CASE	10	0.007	0.069	.	.	2.480
CASE	11	0.006	0.040	.	.	1.670
CASE	12	0.007	0.065	.	.	2.200
CASE	13	0.012	0.046	.	.	2.810
CASE	14	0.025	0.059	.	.	2.670
CASE	15	0.009	0.073	0.150	0.140	2.580
CASE	16	0.006	0.053	.	.	2.590
CASE	17	0.028	0.059	.	.	2.390
CASE	18	0.008	0.065	.	.	2.530
CASE	19	0.010	0.049	.	.	2.200
CASE	20	0.008	0.069	.	.	2.200
CASE	21	0.017	0.160	.	.	2.910
CASE	22	0.039	0.135	.	.	2.630
CA	23	0.024	0.056	.	.	1.330
CA	24	0.022	0.050	0.050	0.140	0.910
CASE	25	0.035	0.032	.	.	3.060
CASE	26	0.015	0.039	.	.	2.340
CASE	27	0.018	0.044	.	.	2.530
CASE	28	0.017	0.047	.	.	3.490
CASE	29	0.012	0.032	.	.	2.150
CASE	30	0.013	0.040	.	.	2.530
CASE	31	.	.	.	.	.

		ANH	CACO3	NACL
CASE	1	41.230	3.260	2.190
CASE	2	72.500	2.280	14.760
CASE	3	83.260	6.550	5.000
CASE	4	84.670	2.620	10.410
CASE	5	85.510	3.570	0.530
CASE	6	96.990	0.340	0.058
CASE	7	93.990	2.010	1.680
CASE	8	90.990	1.400	4.090
CASE	9	89.590	1.690	4.240
CASE	10	83.480	2.940	10.330
CASE	11	84.570	2.050	10.200
CASE	12	93.670	1.540	1.900
CASE	13	95.450	1.970	0.420
CASE	14	88.930	2.410	2.370
CASE	15	94.600	2.650	0.560
CASE	16	78.260	1.630	15.260
CASE	17	90.740	3.650	2.490
CASE	18	83.680	6.430	6.100
CASE	19	84.080	2.920	8.160
CASE	20	92.970	3.290	0.850
CASE	21	85.380	8.340	2.190
CASE	22	80.980	11.480	2.190
CASE	23	79.780	13.720	4.000
CASE	24	89.090	5.890	5.430
CASE	25	92.470	2.270	1.750
CASE	26	50.890	3.190	40.540
CASE	27	82.930	6.520	5.560
CASE	28	89.240	5.830	1.680
CASE	29	81.230	4.330	10.090
CASE	30	50.720	2.630	41.240
CASE	31	.	.	.

TOTAL OBSERVATIONS: 31

	MOIST	COMBH2O	SO3	CAO	CL
N OF CASES	30	30	30	30	30
MINIMUM	0.005	0.190	26.740	20.560	0.058
MAXIMUM	0.110	1.120	58.330	41.350	26.930
MEAN	0.030	0.535	50.152	37.347	4.978
STANDARD DEV	0.027	0.153	7.693	5.500	6.666

	MNO	FE2O3	MGO	NA2O	K2O
N OF CASES	30	30	30	30	30
MINIMUM	0.001	0.010	0.017	0.031	0.006
MAXIMUM	0.015	1.750	2.190	21.870	0.840
MEAN	0.003	0.080	0.112	3.814	0.042
STANDARD DEV	0.003	0.316	0.393	5.352	0.151

	SR	S	ORGC	GYP	ANH
N OF CASES	30	3	3	30	30
MINIMUM	0.032	0.025	0.092	0.910	41.230
MAXIMUM	0.160	0.150	0.140	5.350	96.990
MEAN	0.055	0.075	0.124	2.555	83.062
STANDARD DEV	0.028	0.066	0.028	0.732	13.358

	CACO3	NACL
N OF CASES	30	30
MINIMUM	0.340	0.058
MAXIMUM	13.720	41.240
MEAN	3.980	7.209
STANDARD DEV	3.008	10.063

TOTAL OBSERVATIONS: 31

	MOIST	COMBH2O	SO3	CAO	CL
N OF CASES	30	30	30	30	30
RANGE	0.105	0.930	31.590	20.790	26.872
VARIANCE	0.001	0.023	59.184	30.249	44.442

	MNO	FE2O3	MGO	NA2O	K2O
N OF CASES	30	30	30	30	30
RANGE	0.014	1.740	2.173	21.839	0.834
VARIANCE	0.000	0.100	0.155	28.642	0.023

	SR	S	ORGC	GYP	ANH
N OF CASES	30	3	3	30	30
RANGE	0.129	0.125	0.048	4.440	55.760
VARIANCE	0.001	0.004	0.001	0.536	178.430

	CACO3	NACL
N OF CASES	30	30
RANGE	13.380	41.182
VARIANCE	9.051	101.267

PEARSON CORRELATION MATRIX

	SO3	CAO	CL	MNO	FE2O3
SO3	1.000				
CAO	0.970	1.000			
CL	-0.495	-0.480	1.000		
MNO	-0.277	-0.125	-0.082	1.000	
FE2O3	-0.563	-0.494	-0.163	0.711	1.000
MGO	-0.504	-0.422	-0.105	0.776	0.917
NA2O	-0.526	-0.503	0.996	-0.049	-0.114
K2O	-0.527	-0.450	-0.169	0.714	0.964
SR	0.062	0.183	-0.171	0.663	0.269

	MGO	NA2O	K2O	SR
MGO	1.000			
NA2O	-0.050	1.000		
K2O	0.947	-0.122	1.000	
SR	0.309	-0.153	0.200	1.000

NUMBER OF OBSERVATIONS: 30

Sigificant values at 95 %, r > .306

MATRIX OF SPEARMAN CORRELATION COEFFICIENTS

	SO3	CAO	CL	MNO	FE2O3
SO3	1.000				
CAO	0.734	1.000			
CL	-0.699	-0.723	1.000		
MNO	-0.190	0.205	-0.106	1.000	
FE2O3	-0.095	0.216	-0.226	0.774	1.000
MGO	-0.171	0.204	-0.108	0.864	0.731
NA2O	-0.741	-0.776	0.980	-0.108	-0.230
K2O	-0.031	0.239	-0.293	0.677	0.905
SR	0.055	0.345	-0.295	0.506	0.258

	MGO	NA2O	K2O	SR
MGO	1.000			
NA2O	-0.098	1.000		
K2O	0.733	-0.306	1.000	
SR	0.479	-0.248	0.103	1.000

NUMBER OF OBSERVATIONS: 30

Signicant values $>$ .7

SO3

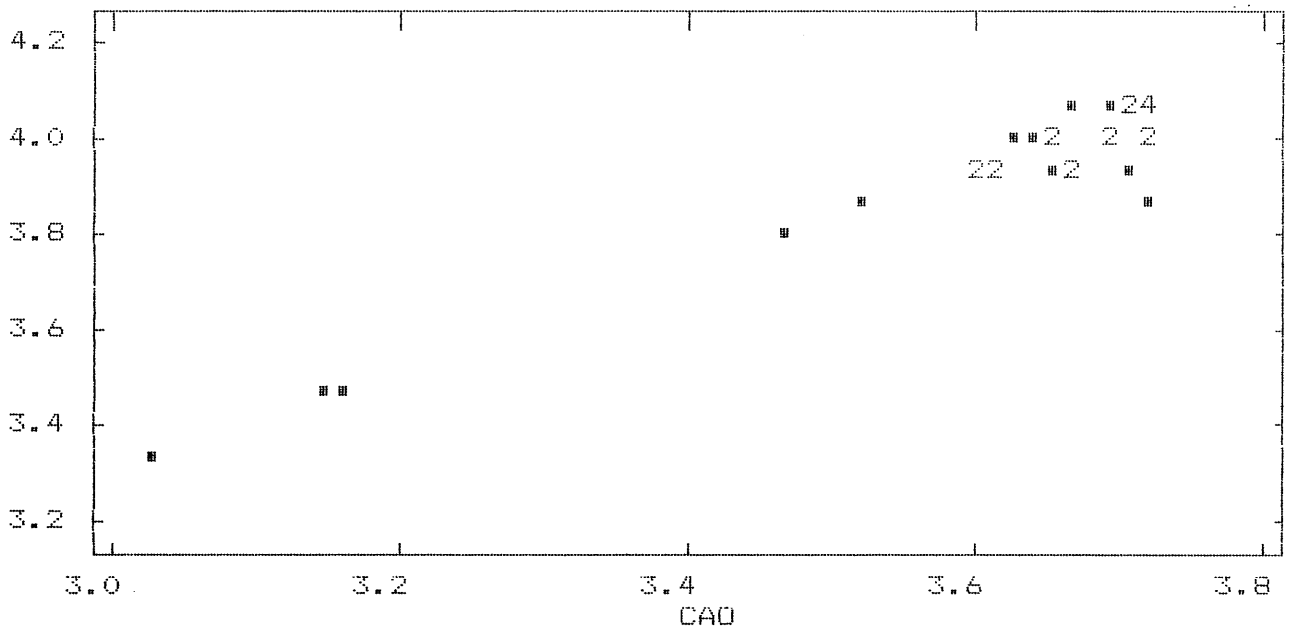

FE203

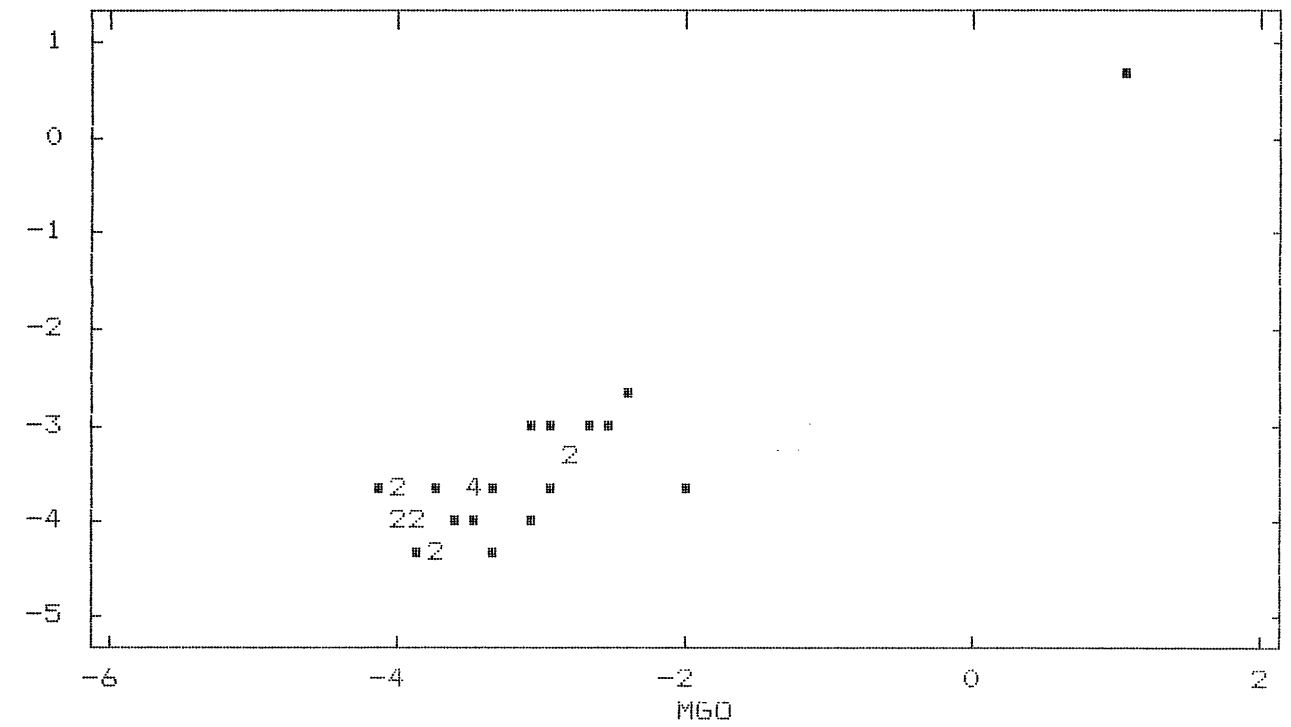

FE203

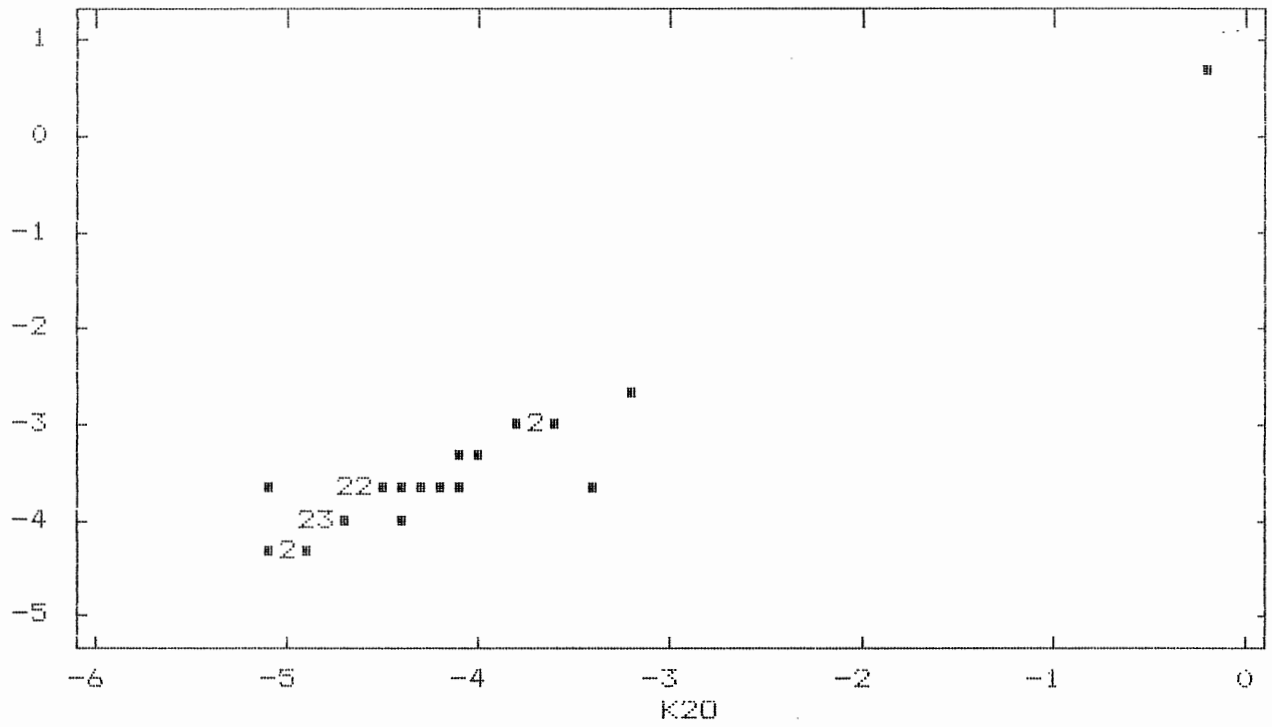

FE203

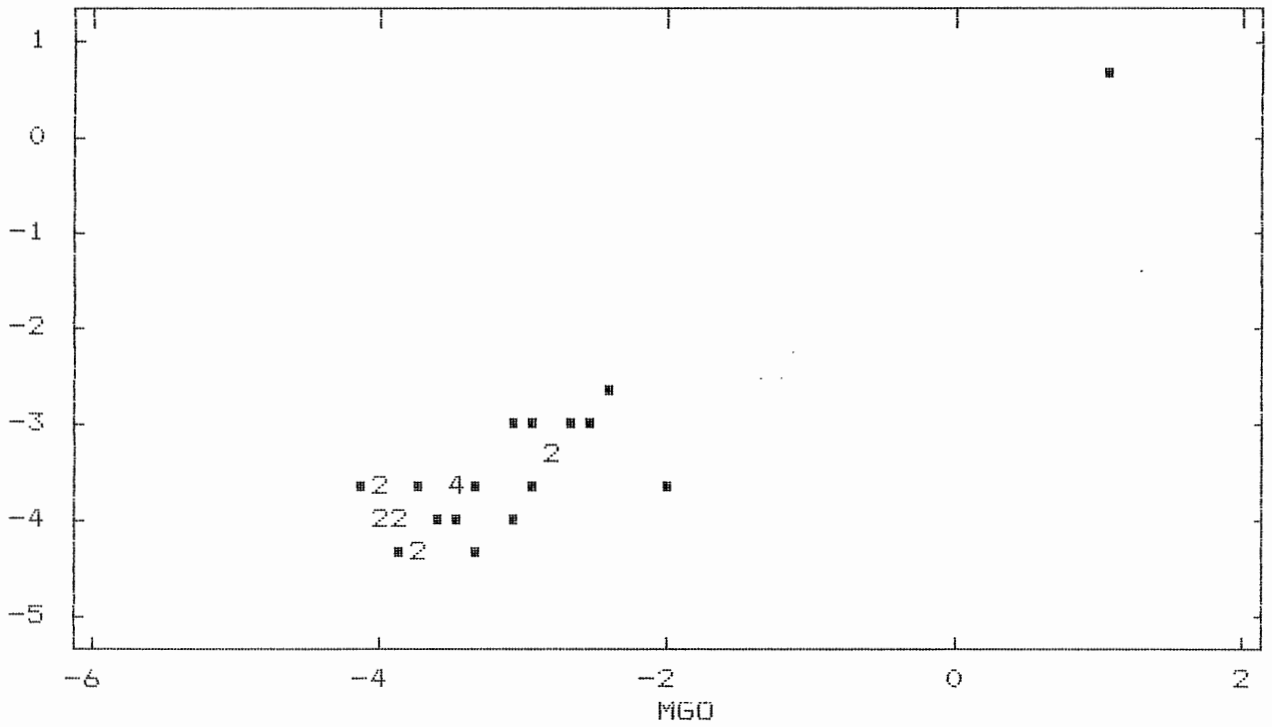

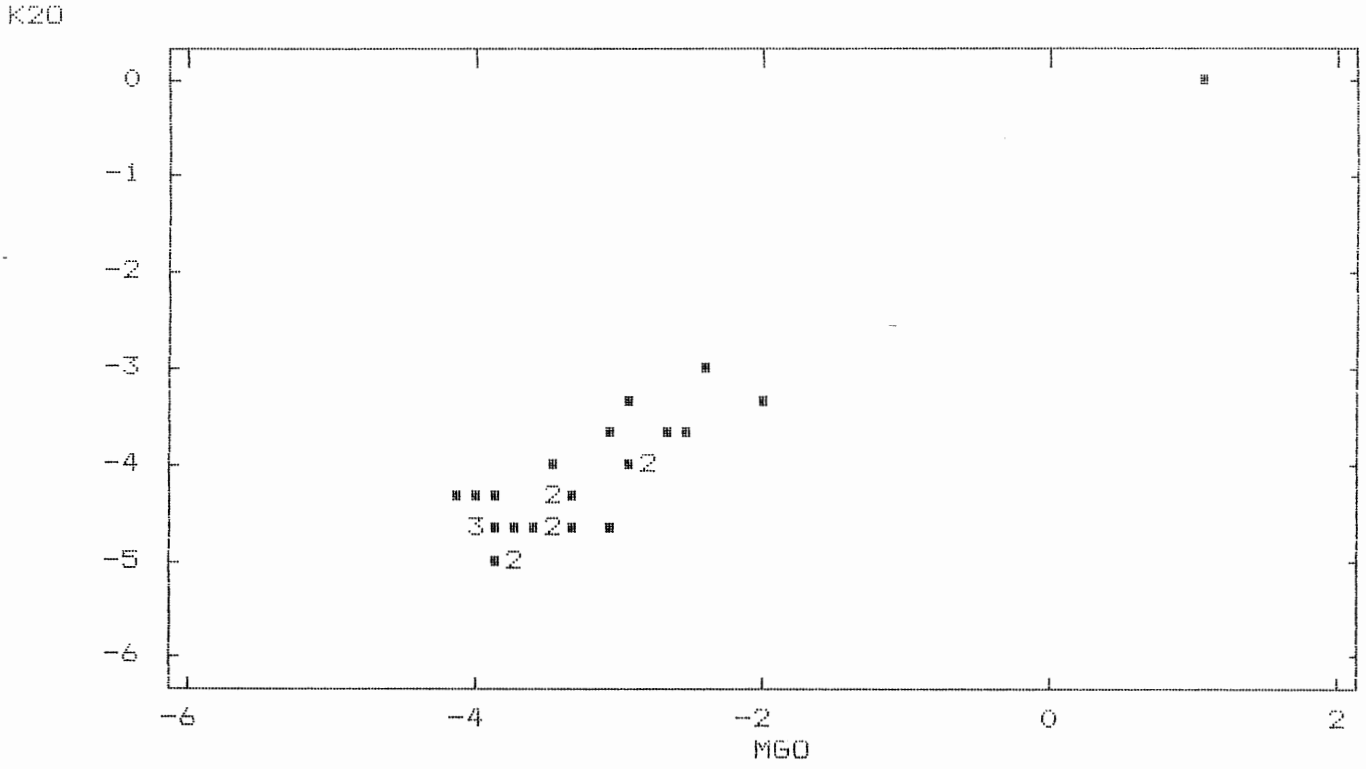
K2O
0
-1
-2
-3
-4
-5
-6
-6
-4
-2
0
2
MGO

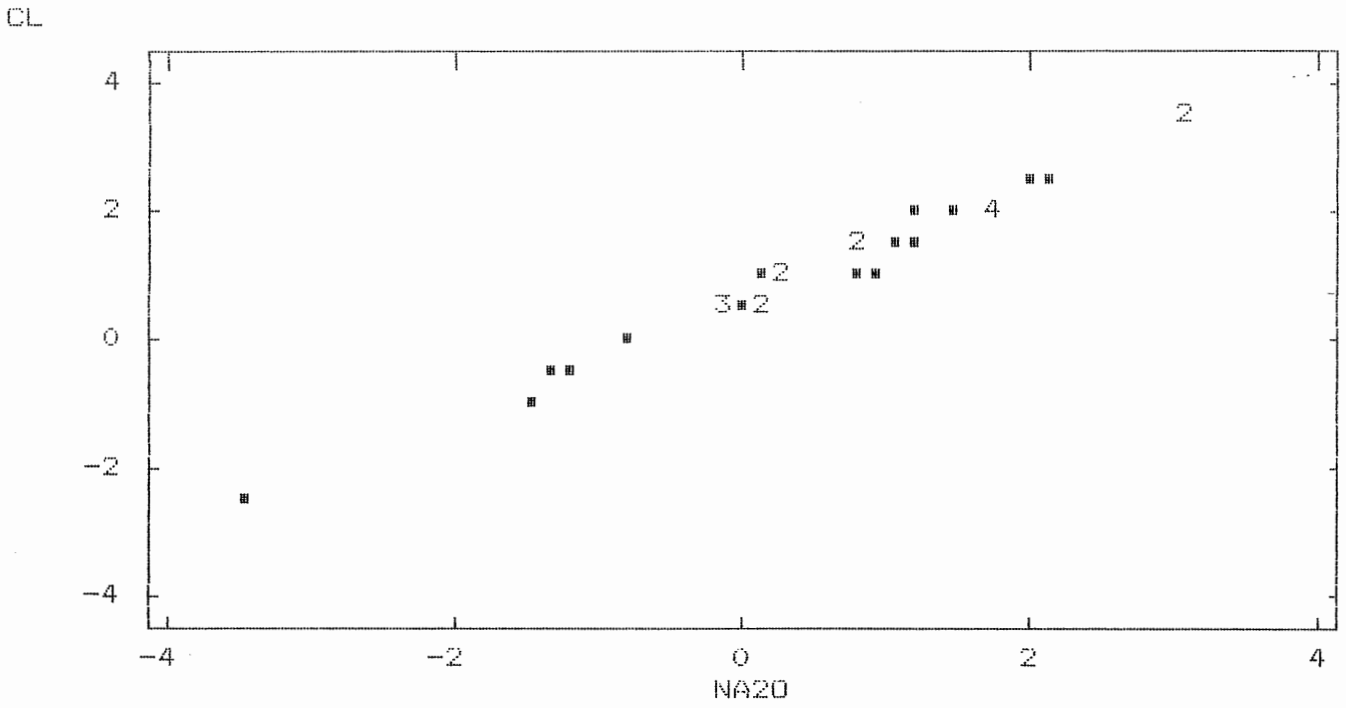
CL
4
2
0
-2
-4
-4
-2
0
2
4
NA2O
2
4
2
2
3 2

Third Anhydrite

		SAMPLE$	MOIST	COMBH2O	SO3	CAO
CASE	1	P-158-63	0.030	0.550	53.480	41.720
CASE	2	P-158-64	0.020	0.610	54.950	41.560
CASE	3	P-158-65	0.005	0.610	52.040	41.300
CASE	4	P-158-66	0.010	0.660	53.030	41.560
CASE	5	P-158-67	0.050	0.550	53.370	41.150
CASE	6	P-158-68	0.005	0.032	58.830	41.220
CASE	7	P-158-69	0.005	0.680	56.810	41.470
CASE	8	P-158-70a	0.005	0.710	57.330	41.390
CASE	9	P-158-71	0.005	0.630	57.860	41.220
CASE	10	P-158-72	0.010	0.037	58.860	45.090
CASE	11	P-158-73	0.005	0.430	58.460	41.140
CASE	12	P-158-74	0.005	0.480	58.920	41.300
CASE	13	P-158-75	0.005	0.360	58.530	41.050
CASE	14	P-158-76	0.005	0.460	58.110	40.780
CASE	15	P-158-77	0.005	1.020	58.410	40.970
CASE	16	P-158-78	0.005	0.860	57.350	40.320
CASE	17	P-158-79	0.005	0.820	58.710	41.220
CASE	18	P-158-80	0.005	0.910	58.280	41.050
CASE	19	P-158-81	0.005	0.950	58.720	41.190
CASE	20	P-158-82.2	0.005	0.750	57.780	41.160
CASE	21	P-158-85.2	0.005	0.770	58.220	41.280
CASE	22	P-158-90.2	0.005	0.780	58.850	41.300
CA	23	P-158-91	0.005	0.880	58.410	41.120
CA	24	P-158-92a	0.005	0.910	58.850	41.220
CASE	25	P-158-93	0.010	0.750	57.260	41.140
CASE	26	P-158-94	0.005	0.730	58.710	41.150
CASE	27	P-158-95	0.005	0.790	58.860	41.740
CASE	28	P-158-98	0.005	0.360	58.770	41.150
CASE	29	P-158-99	0.005	0.710	58.820	41.350

		CL	MNO	FE2O3	MGO	NA2O
CASE	1	0.044	0.003	0.024	0.030	0.035
CASE	2	0.046	0.004	0.024	0.052	0.035
CASE	3	0.023	0.002	0.024	0.027	0.030
CASE	4	0.017	0.002	0.024	0.025	0.028
CASE	5	0.012	0.003	0.026	0.037	0.024
CASE	6	0.012	0.002	0.026	0.037	0.022
CASE	7	0.018	0.002	0.020	0.028	0.020
CASE	8	0.016	0.002	0.022	0.020	0.022
CASE	9	0.014	0.002	0.020	0.023	0.020
CASE	10	0.016	0.002	0.047	0.033	0.023
CASE	11	0.016	0.002	0.042	0.030	0.035
CASE	12	0.011	0.002	0.022	0.018	0.020
CASE	13	0.016	0.001	0.011	0.011	0.020
CASE	14	0.023	0.003	0.064	0.057	0.028
CASE	15	0.083	0.001	0.039	0.017	0.050
CASE	16	0.047	0.002	0.160	0.062	0.054
CASE	17	0.027	0.001	0.023	0.011	0.031
CASE	18	0.014	0.002	0.054	0.022	0.031
CASE	19	0.031	0.001	0.029	0.011	0.035
CASE	20	0.011	0.001	0.073	0.023	0.030
CASE	21	0.013	0.005	0.039	0.010	0.031
CASE	22	0.012	0.001	0.019	0.003	0.022
CA	23	0.010	0.004	0.034	0.010	0.027
C	24	0.011	0.001	0.017	0.007	0.023
CASE	25	0.014	0.001	0.047	0.022	0.031
CASE	26	0.012	0.001	0.044	0.018	0.023
CASE	27	0.019	0.001	0.026	0.011	0.022
CASE	28	0.016	0.002	0.030	0.038	0.022
CASE	29	0.025	0.001	0.029	0.010	0.030

		K2O	SR	S	ORGC	GYP
CASE	1	0.019	0.027	0.050	.	2.620
CASE	2	0.017	0.038	0.025	.	2.910
CASE	3	0.015	0.052	0.060	.	2.910
CASE	4	0.015	0.048	0.090	.	3.150
CASE	5	0.029	0.039	0.025	.	2.620
CASE	6	0.017	0.040	0.050	.	1.530
CASE	7	0.015	0.037	0.050	0.093	3.240
CASE	8	0.017	0.036	0.050	.	3.390
CASE	9	0.017	0.038	0.025	.	3.010
CASE	10	0.017	0.034	0.100	.	1.770
CASE	11	0.023	0.038	0.080	.	2.480
CASE	12	0.025	0.032	0.025	.	2.290
CASE	13	0.017	0.027	0.110	.	1.720
CASE	14	0.009	0.015	0.025	.	2.200
CASE	15	0.036	0.016	0.025	0.047	4.870
CASE	16	0.023	0.017	0.025	.	4.100
CASE	17	0.011	0.016	0.025	.	3.910
CASE	18	0.023	0.014	0.090	.	4.340
CASE	19	0.012	0.018	0.070	.	4.530
CASE	20	0.029	0.018	0.080	.	3.580
CASE	21	0.010	0.020	0.500	.	3.680
CASE	22	0.004	0.023	0.150	0.046	3.720
CASE	23	0.012	0.020	0.130	.	4.200
CASE	24	0.007	0.018	0.130	.	4.340
CASE	25	0.022	0.023	0.580	.	3.580
CASE	26	0.021	0.024	0.650	.	3.480
CASE	27	0.010	0.024	0.150	.	3.770
CASE	28	0.017	0.038	0.025	.	3.720
CASE	29	0.009	0.017	0.110	.	3.390

		ANH	CACO3	NACL
CASE	1	88.860	7.600	0.066
CASE	2	91.130	5.470	0.066
CASE	3	86.180	8.650	0.056
CASE	4	87.670	7.880	0.053
CASE	5	88.670	6.710	0.045
CASE	6	98.820	0.019	0.041
CASE	7	94.020	2.990	0.038
CASE	8	94.790	2.200	0.041
CASE	9	96.000	1.230	0.038
CASE	10	98.880	0.480	0.043
CASE	11	97.770	0.330	0.066
CASE	12	98.370	0.050	0.038
CASE	13	98.670	0.090	0.038
CASE	14	97.070	0.130	0.052
CASE	15	95.460	0.100	0.095
CASE	16	94.260	0.260	0.100
CASE	17	96.130	0.170	0.058
CASE	18	95.660	0.400	0.058
CASE	19	96.250	0.100	0.066
CASE	20	95.410	1.220	0.056
CASE	21	96.080	0.890	0.058
CASE	22	96.650	0.014	0.041
CA	23	95.990	0.360	0.051
CA	24	96.620	0.005	0.043
CASE	25	94.520	1.830	0.058
CASE	26	97.070	0.040	0.043
CASE	27	96.650	0.910	0.041
CASE	28	98.570	0.020	0.041
CASE	29	97.330	0.260	0.056

TOTAL OBSERVATIONS: 29

	MOIST	COMBH2O	SO3	CAO	CL
N OF CASES	29	29	29	29	29
MINIMUM	0.005	0.032	52.040	40.320	0.010
MAXIMUM	0.050	1.020	58.920	45.090	0.083
MEAN	0.008	0.648	57.468	41.356	0.022
STANDARD DEV	0.010	0.242	2.021	0.767	0.016

	MNO	FE2O3	MGO	NA2O	K2O
N OF CASES	29	29	29	29	29
MINIMUM	0.001	0.011	0.003	0.020	0.004
MAXIMUM	0.005	0.160	0.062	0.054	0.036
MEAN	0.002	0.037	0.024	0.028	0.017
STANDARD DEV	0.001	0.028	0.015	0.008	0.007

	SR	S	ORGC	GYP	ANH
N OF CASES	29	29	3	29	29
MINIMUM	0.014	0.025	0.046	1.530	86.180
MAXIMUM	0.052	0.650	0.093	4.870	98.880
MEAN	0.028	0.121	0.062	3.278	95.157
STANDARD DEV	0.011	0.164	0.027	0.868	3.428

	CACO3	NACL
N OF CASES	29	29
MINIMUM	0.005	0.038
MAXIMUM	8.650	0.100
MEAN	1.738	0.053
STANDARD DEV	2.703	0.016

TOTAL OBSERVATIONS: 29

	MOIST	COMBH2O	SO3	CAO	CL
N OF CASES	29	29	29	29	29
RANGE	0.045	0.988	6.880	4.770	0.073
VARIANCE	0.000	0.058	4.083	0.589	0.000

	MNO	FE2O3	MGO	NA2O	K2O
N OF CASES	29	29	29	29	29
RANGE	0.004	0.149	0.059	0.034	0.032
VARIANCE	0.000	0.001	0.000	0.000	0.000

	SR	S	ORGC	GYP	ANH
N OF CASES	29	29	3	29	29
RANGE	0.039	0.625	0.047	3.340	12.700
VARIANCE	0.000	0.027	0.001	0.753	11.753

	CACO3	NACL
N OF CASES	29	29
RANGE	8.645	0.062
VARIANCE	7.307	0.000

ARSON CORRELATION MATRIX

	SO3	CAO	CL	MNO	FE2O3
SO3	1.000				
CAO	0.010	1.000			
CL	-0.231	-0.087	1.000		
MNO	-0.427	0.140	-0.077	1.000	
FE2O3	0.125	-0.095	0.189	0.135	1.000
MGO	-0.398	0.041	0.287	0.573	0.453
NA2O	-0.181	-0.267	0.735	0.017	0.609
K2O	-0.223	-0.055	0.184	0.214	0.343
SR	-0.527	0.283	-0.194	0.444	-0.428
S	0.200	0.126	-0.437	-0.171	0.038

	MGO	NA2O	K2O	SR	S
MGO	1.000				
NA2O	0.245	1.000			
K2O	0.612	0.290	1.000		
SR	0.362	-0.420	0.188	1.000	
S	-0.485	-0.139	-0.263	-0.180	1.000

NUMBER OF OBSERVATIONS: 29

Significant values, $r > .317$

MATRIX OF SPEARMAN CORRELATION COEFFICIENTS

	SO3	CAO	CL	MNO	FE2O3
SO3	1.000				
CAO	0.040	1.000			
CL	-0.272	0.107	1.000		
MNO	-0.450	0.087	-0.017	1.000	
FE2O3	-0.059	-0.467	0.065	0.105	1.000
MGO	-0.447	-0.072	0.290	0.512	0.334
NA2O	-0.342	-0.261	0.523	0.089	0.547
K2O	-0.271	-0.346	-0.059	0.071	0.361
SR	-0.266	0.437	-0.126	0.344	-0.395
S	0.259	0.117	-0.402	-0.343	0.084

	MGO	NA2O	K2O	SR	S
MGO	1.000				
NA2O	0.142	1.000			
K2O	0.448	0.214	1.000		
SR	0.418	-0.397	0.136	1.000	
S	-0.601	-0.089	-0.339	-0.150	1.000

NUMBER OF OBSERVATIONS: 29

MNO

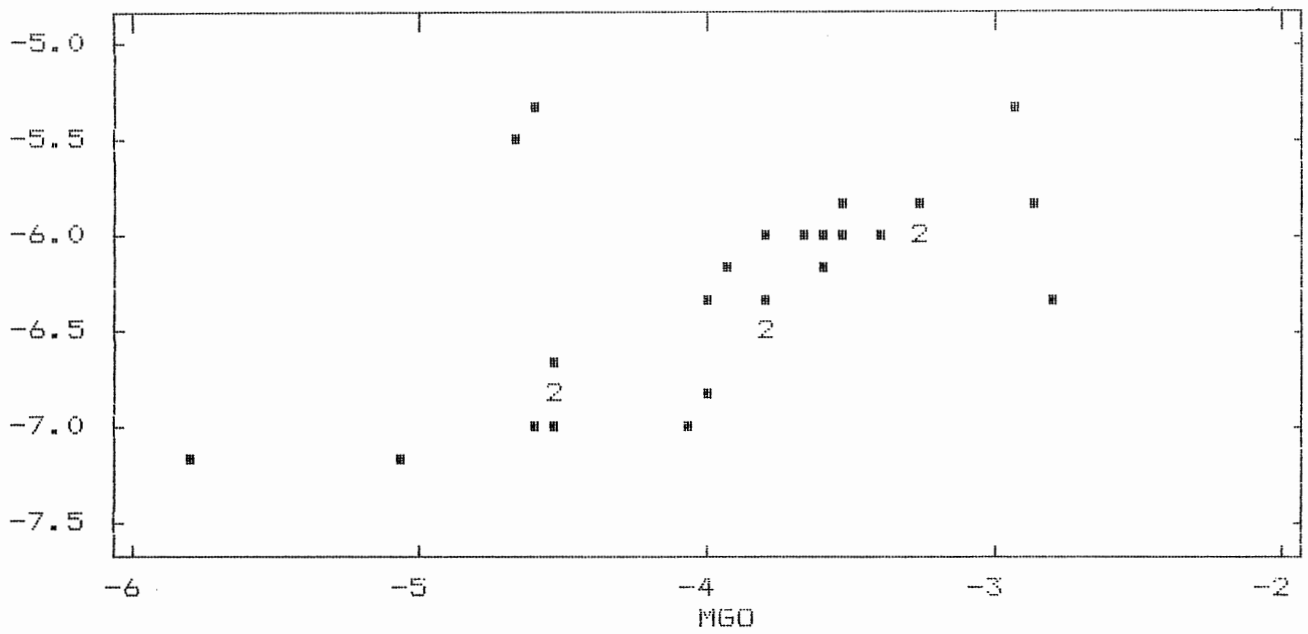

MGO

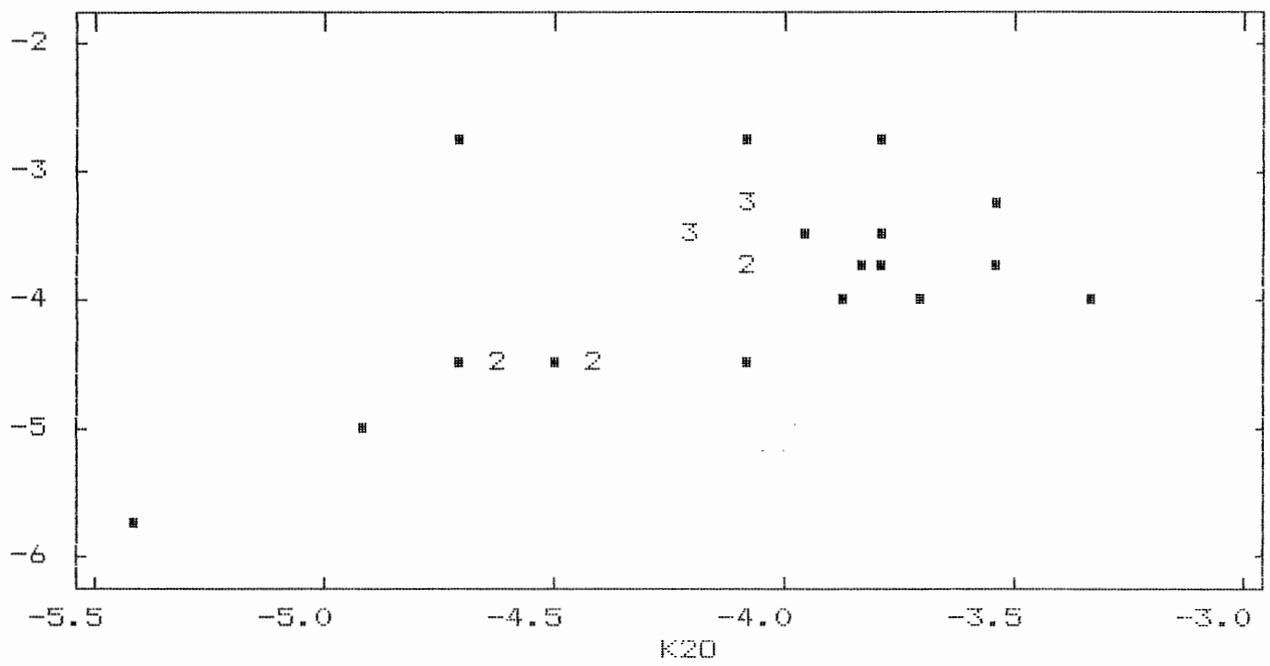

CL

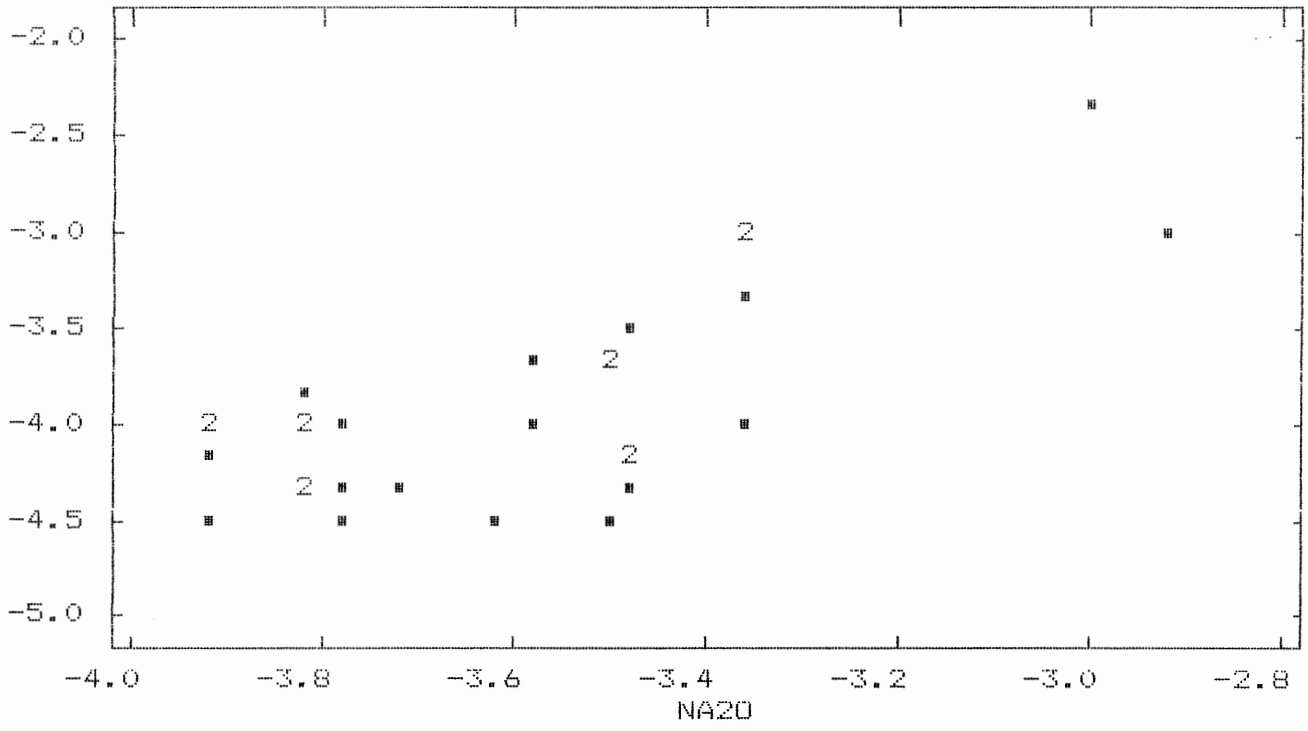
-2.0
-2.5
-3.0
-3.5
-4.0
-4.5
-5.0
-4.0
-3.8
-3.6
-3.4
-3.2
-3.0
-2.8
NA2O

FE2O3

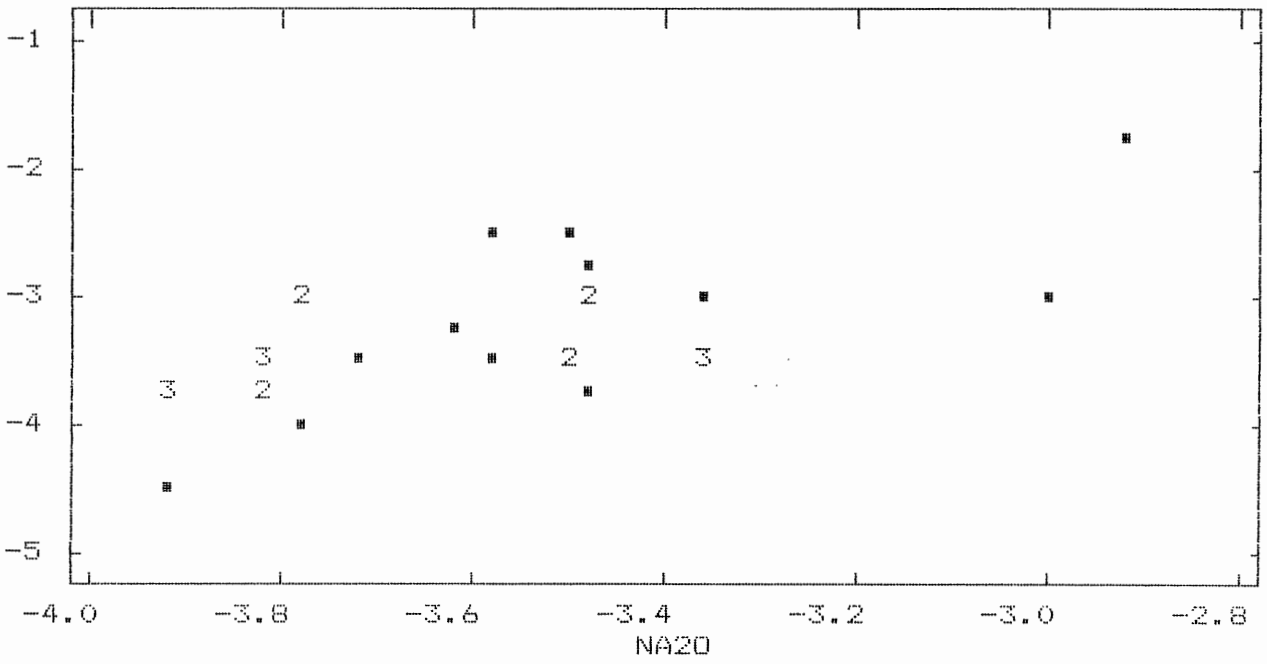
-1
-2
-3
-4
-5
-4.0
-3.8
-3.6
-3.4
-3.2
-3.0
-2.8
NA2O

Appendix II Thin Section Descriptions

Stratigraphic top was known only in hole P-918. Thin section descriptions are from apparent top to apparent bottom in this hole. In all other holes thin sections are described in order from the beginning to the end of anhydrite in the borehole.

The sampling code for thin sections is: P-158-76. The abbreviation P stands for Pugwash. In this particular example the sample was taken from borehole number 158 at a depth of approximately 76 feet.

Thin sections were described and classified on the basis of texture and mineralogy. Textural descriptions were based on the scheme of Maiklem et al. (1969).

Borehole 816

250 m (830 foot) level

Coordinates: N 1631 ft. E 4516 ft.

Strike: 181 degrees grid

Dip: 0 degrees

Total depth: 250 feet

P-816-10 Anhydrite - nodular, texture microcrystalline; isolated lath-shaped grains; calcite 15 %, organic 5 %; veinlets of coarse, secondary anhydrite crosscut calcite; anhydrite pseudomorphs after gypsum.

P-816-30 Anhydrite - nodular, texture microcrystalline to felted and aligned-felted; isolated blocky patches < 5 %; 1 % carbonate; minor halite filled vugs, < 1 %; < 1 % organic; recrystallized anhydrite around vugs.

P-816-40 Anhydrite - nodular contorted; texture microcrystalline to blocky; carbonate 5 %; organics < 1 %.

P-816-50 Anhydrite - nodular; texture microcrystalline to blocky; organic < 5 %, dark brown, internodular; secondary anhydrite crosscuts calcite, 1-2 mm wide, grey-brown, recrystallized; pyrite < < 1 %.

P-816-60 Anhydrite - nodular to stylolitic; texture microcrystalline; organics, dark brown, internodular, 5 %;

Pyrite, associated with organic layers, < < 1 %.

P-816-70 Anhydrite - nodular to stylolitic; texture microcrystalline with isolated blocky and lath-shaped grains; carbonate 5 %; organics < 5 %; pyrite < < 1%.

P-816-80 Anhydrite - nodular to stylolitic; texture; microcrystalline with isolated blocky and lath-shaped grains; carbonate 5 %; organics 5 %, discontinuous, pulled apart by nodule growth; pyrite < 1%.

P-816-90 Laminated carbonate with anhydrite nodules- calcite 60 %, reddish-brown, recrystallized, continuous laminae up to 0.5 mm wide, displaced by the growth of anhydrite nodules, calcite replaces anhydrite; anhydrite 20 %, nodules with sub-felted to blocky textures; organic 20 %, with 5 % to abundant quartz silt; pyrite < 5 %.

P-816-100 Anhydrite with laminated carbonate - nodular; texture microcrystalline; calcite 20 %, brown, recrystallized, continuous; organics 10 %; pyrite < 1 %; secondary anhydrite crosscuts laminations, coarse, blocky, no inclusions of organic material, high birefringence under crossed nicols.

P-816-110 Anhydrite - nodular; texture microcrystalline; calcite 10 %, brownish-yellow, laminations and single grains which replace anhydrite; organics < 5 %; pyrite < < 1 %; veinlet

filled with secondary anhydrite crosscuts laminated calcite.

P-816-120 Anhydrite with laminated carbonate - laminated and nodular anhydrite; texture microcrystalline; dolomite 3 %, corroded grains in anhydrite nodules; calcite 35 %, brownish-yellow, laminated and replaces anhydrite; organics 10 %, associated with laminated carbonate; pyrite < 5 %; veinlets filled with secondary anhydrite crosscut laminated calcite and anhydrite.

P-816-130 Anhydrite - nodular; texture microcrystalline to blocky; dolomite < 1%, corroded grains in anhydrite nodules; calcite 10 %; organics 5 %, internodular; pyrite < 5 %; veinlets filled with blocky, secondary anhydrite crosscut laminations.

P-816-140 Anhydrite - nodular; texture microcrystalline; calcite 5%; dolomite < 1%; organics < 5 %; veinlets filled with coarse, blocky anhydrite crosscut carbonate.

Borehole 918

250 m (830 foot) level

Coordinates: N 1108 ft. E 2716 ft.

Dip: < 10 degrees

Total depth: 250 feet

P-918-12 Laminated anhydrite with carbonate - laminated to nodular anhydrite; texture; microcrystalline; anhydrite 45 %; calcite 30 %; organic 15 %; calcite laminated and replaces anhydrite; pyrite < < 1 %; secondary anhydrite fills fractures that crosscut laminations.

P-918-21.5 Anhydrite - nodular; texture microcrystalline with isolated blocky; calcite 30 %, laminated and replaces anhydrite; organic 5 %, streaky, < 1 % quartz; < 1 % pyrite; secondary anhydrite fills veinlets which crosscut laminations; anhydrite pseudomorphs after gypsum.

P-918-23.5 Biomicrite - biomicrite crosscut by veinlets filled with coarse, acicular anhydrite; organic < 5 %; pyrite < 1 %; foraminifera and ostracod remains.

P-918-25.5 Laminated carbonate with anhydrite; in contact with siltstone and biomicrite - biomicrite overlies siltstone, laminated quartz silt and carbonate with anhydrite nodules; biomicrite, fossiliferous, ostracod and foraminifera remains, crosscut by sparry calcite veinlet, continues into underlying

siltstone; siltstone 50 % quartz, 25 %, sericitized clay 15 %; underlying layer: laminated quartz silt and organic material, grades downward into laminated calcite with anhydrite nodules; erosional contact between laminated quartz silt and siltstone; laminated quartz silt and laminated carbonate are crosscut by veinlets filled with coarse, secondary anhydrite.

P-918-27.5 Laminated carbonate with anhydrite nodules- anhydrite 30 %; texture microcrystalline; calcite 50 %; texture recrystallized, yellowish-brown; organics 15 %; pyrite < 5 %.

P-918-32 Anhydrite - nodular mosaic; texture microcrystalline; irregular patches of calcite 15 %; replaces anhydrite; organic < 5 %; pyrite < 2 %; fractures filled with blocky anhydrite crosscut calcite.

P-918-33.5 Anhydrite - nodular anhydrite associated with clastic material; microcrystalline anhydrite 50 %; silt-sized quartz 35 %; organics 15 %; pyrite 5 %; clastics crosscut by veinlets filled with secondary anhydrite.

P-918-34 Anhydrite - nodular; texture micocrystalline; isolated blocky and lath-shaped grains; calcite 20 %; primary laminated; secondary replaces anhydrite; organics 10 %; pyrite < 5%; fractures filled with secondary anhydrite crosscut carbonate laminae.

P-918-36 Laminated carbonate with anhydrite nodules- calcite 70 %; laminated and replaces anhydrite; anhydrite 20 %; texture microcrystalline; nodules displace carbonate and organic laminae; organics 5-10 %; pyrite < 1 %.

P-918-38 Laminated carbonate with anhydrite nodules- calcite 60 %; laminated and replace anhydrite; nodular anhydrite 25 %; texture microcrystalline; displaces carbonate and organic laminae; organics 10 %; disrupted, with 10 % quartz; pyrite < 1 %; fractures filled with coarse blocky anhydrite crossscut laminations.

P-918-42 Laminated carbonate with anhydrite nodules- calcite 50 %; laminated and replaces anhydrite; anhydrite 40 %; texture microcrystalline; nodules grow displacively within calcite and organic laminae; organics 5 %; pyrite < 1%.

P-918-43.5 Carbonate with anhydrite nodules - calcite 75 %; anhydrite 15 %; texture microcrystalline with isolated blocky; nodules displace calcite; organics 5 %; pyrite 1 %.

P-918-45 Anhydrite - laminated to nodular; texture microcrystalline; calcite 40 %, laminated and replaces anhydrite; organic 5 %, streaky, with 10 % silt-sized quartz; pyrite 5 %.

P-918-49 Laminated anhydrite with calcite - anhydrite 55 %; laminated; texture microcrystalline; calcite 30 %; replaces

anhydrite; organics 5 %; pyrite < 1 %.

P-918-51 Anhydrite - laminated to nodular; texture blocky with microcrystalline nodules; calcite 25 %; laminated and replaces anhydrite; organics 10 %; pyrite < 1%; anhydrite pseudomorph after gypsum, euhedral, 5 mm x 2 mm, yellow in cross nicols, with inclusions of microcrystalline anhydrite and calcite; calcite replaces pseudomorph; veinlets of coarse, secondary anhydrite crosscut calcite laminae.

P-918- 58 Anhydrite - nodular; texture blocky with laminations and nodules of microcrystalline; calcite 15 %; replaces anhydrite; organics 5-10 %; pyrite < 1 %; veinlets of coarse, secondary anhydrite crosscut calcite laminae.

P-918-59 Anhydrite with micrite - contact between coarse, blocky anhydrite and distorted, laminated micrite with anhydrite nodules; erosional contact; micrite: laminae terminated abruptly, anhydrite nodules eroded and truncated; organics < 5 %; pyrite < 1%; veinlets of coarse, secondary anhydrite crosscut micrite; intrclasts in micrite.

P-918-60.5 Anhydrite with fragmented laminated carbonate- nodular; texture blocky; calcite 20 %; fragmented and contorted by anhydrite growth; organics 5 %, with 10 % quartz silt; pyrite < 5 %.

P-918-64 Anhydrite - laminated; texture microcrystalline; calcite 10 %; laminated and replaces anhydrite; organics < 5 %; veinlets of coarse, secondary anhydrite crosscut calcite laminae.

P-918-66 Anhydrite - laminated; texture microcrystalline; calcite 5 %, laminated, recrystallized; organics < 5 %; veinlets of coarse, secondary anhydrite crosscuts calcite laminae.

P-918-67 Anhydrite - laminated; texture microcrystalline; calcite 40 %, laminated; organics 5 %; veinlets of coarse, secondary anhydrite crosscut calcite laminae.

P-918-68 Anhydrite - laminated; texture microcrystalline; calcite 20 %; laminated; organics 10 %, streaky; veinlets of coarse, secondary anhydrite crosscut calcite laminae.

P-918-69.5 Anhydrite - laminated; texture microcrystalline; organics 5 %, thin, continous laminations; anhydrite contains cubic halite, < 1 mm.

Borehole P-886

250 m (830 foot) level

Coordinates: N 1071 ft. E 4142 ft.

Strike: 138 degrees grid

Dip: 0 degrees

Total depth: 845 ft.

P-886-10 Siltstone with anhydrite - fine grained, grey-brown silt, 60 %, anhydrite 35 %; organics < 5%.

P-886-20 Anhydrite - massive; texture microcrystalline with fibroradiate clusters; organics < 5 %; halite 15 %; anhydrite pseudomorphs after gypsum.

P-886-30 Anhydrite - nodular; texture microcrystalline with 5-10 % lath-shaped and blocky; anhydrite recrystallized around halite-filled vugs; carbonate 5 %; halite < 5 %; organics < 1 %; anhydrite pseudomorphs after gypsum.

P-886-40 Anhydrite - nodular, contorted; texture microcrystalline to blocky with fibroradiate clusters; carbonate 5 %; halite 10 %; anhydrite pseudomorphs after gypsum.

P-886-50 Anhydrite - nodular; texture microcrystalline to blocky with isolated fibroradiate clusters; recrystallized anhydrite around halite-filled vugs; halite < 1 %; organics < 5 %; anhydrite pseudomorphs after gypsum.

P-886-60 Anhydrite - nodular; texture microcrystalline with lath-shaped and fibroradiate clusters; organics < 5 %; anhydrite pseudomorphs after gypsum.

P-886-70 Anhydrite - nodular; texture microcrystalline to fibroradiate; recrystallized, blocky anhydrite around vugs; halite 1 %; organics < 5 %; anhydrite pseudomorphs after gypsum.

P-886-80 Anhydrite - nodular; texture microcrystalline to felted and aligned-felted with fibroradiate; recrystallized anhydrite around vugs; halite 5 %; organics < 5 %; anhydrite pseudomorphs after gypsum.

P-886-90 Anhydrite - nodular contorted; texture microcrystalline to felted and aligned-felted in fibroradiate groups; recrystallized anhydrite around vugs; carbonate 5%; halite 5 %; organics < 5 %; danburite nodule, 1 mm, oval-shaped, dark grey, colliform.

P-886-100 Anhydrite - nodular; texture microcrystalline to fibroradiate; recrystallized anhydrite around vugs; carbonate < 5 %, zoned dolomite rhombs around halite-filled vugs; halite 10 %; organics 5 %.

P-886-110 Anhydrite - nodular distorted; texture microcrystalline to fibroradiate; carbonate < 1 %; halite 10 %;

organics 5 %; anhydrite pseudomorphs after gypsum.

P-886-120 Anhydrite - nodular distorted; texture microcrystalline to fibroradiate; blocky anhydrite associated with vugs; halite < 5 %; carbonate < 1 %; anhydrite pseudomorphs after gypsum.

P-886-130 Anhydrite - massive to nodular; texture microcrystalline with isolated lath-shaped, blocky, and fibroradiate patches; halite 2 %; carbonate 2 %; organics < 1 %;.

P-886-140 Anhydrite - nodular; texture microcrystalline to fibroradiate; dolomite 2 %, euhedral, stained reddish-brown, associated with halite filled vugs; halite 2 %; organics 5-10 %; danburite nodule, 0.8 mm, displaces organic laminae; anhydrite pseudomorphs after gypsum.

P-886-150 Anhydrite - nodular; texture microcrystalline with fibroradiate clusters; dolomite < 1 %, associated with halite-filled vugs, halite < 1 %; organics < 3 %; anhydrite pseudomorphs after gypsum.

P-886-160 Anhydrite - nodular distorted; texture microcrystalline with fibroradiate clusters; minor blocky, < 5%, associated with halite-filled vugs; dolomite < 3 %; halite 20 %; organics < 5 %; danburite nodule, 1.5 mm, colliform, displaces and recrystallizes anhydrite.

P-886-160a Anhydrite - nodular distorted; texture microcrystalline with fibroradiate; coarse, blocky asoociated with halite-filled vugs; carbonate < 3 %; halite 3 %; organics < 5 %; several danburite nodules, 0.5 to 3 mm, colliform, displace organic laminae.

P-886-170 Anhydrite - nodular distorted; texture microcrystalline with fibroradiate; carbonate 5 %; halite 5 %; organics < 5 %; anhydrite pseudomorphs after gypsum.

P-886-170a Anhydrite - nodular, texture microcrystalline to fibroradiate; dolomite 3 %; halite 10 %; organics < 5 %; anhydrite pseudomorphs after gypsum.

P-886-180 Anhydrite - nodular; texture microcrystalline to fibroradiate; dolomite 5 %, halite < 1%; organics 5 %; anhydrite pseudomorphs after gypsum.

P-886-190 Anhydrite - nodular; texture microcrystalline with fibroradiate; carbonate 10 %; halite 3 %; oragnics < 5 %; anhydrite replacement of twinned gypsum crystal, 2 cm long, overgrowths separated by organic layers.

P-886-200 Anhydrite - nodular; texture microcrystalline; calcite 15 %, replaces anhydrite; halite 5 %; organics 5 %; pyrite < < 1%.

P-886-210 Anhydrite - nodular, texture microcrystalline; carbonate 15 %; halite 5 %; organics 5 %.

P-886-220 Anhydrite - nodular; texture microcrystalline; dolomite 5 %, associated with halite-filled vugs; halite 5 %; organics < 1 %.

P-886-230 Anhydrite - nodular distorted; texture microcrystalline; carbonate < 5 %; halite 1 %; organics < 1 %.

P-886-240 Anhydrite - nodular; texture microcrystalline; dolomite 5 %; associated with halite-filled vugs; halite 40 %; organics < 5 %.

P-886-240a Anhydrite - nodular; texture microcrystalline; carbonate 5 %; halite 5 %; organics < 1 %.

P-886-250 Anhydrite - nodular; texture microcrystalline; carbonate < 5 %; halite 3 %; organics < 1 %.

Borehole P-158 - Third Anhydrite Unit

192 m (630 foot) level

Coordinates: N 2666 ft. E 2802 ft.

Strike: 120 degrees grid

Dip: unknown

Total depth: 979 ft.

P-158-63 Anhydrite - massive; texture microcrystalline; lath shaped crystals 5 %; organics < 1 %, disseminated and wispy.

P-158-64 Anhydrite - massive to nodular; texture microcrystalline and aligned-felted; microcrystalline anhydrite forms nodules, surrounded by aligned-felted laths and minor organics < 5 %.

P-158-65 Anhydrite - nodular; texture microcrystalline; nodules surrounded by aligned-felted anhydrite; minor laminations of aligned-felted laths < 1 mm thick; carbonate 10 %; organics < 1 %.

P-158-66 Anhydrite - nodular; texture microcrystalline; nodules surorunded by << 1 mm thick organic layers and aligned-felted anhydrite laths; organics < 1%.

P-158-67 Anhydrite - nodular; texture microcrystalline; nodules surrounded by lath-shaped and aligned-felted anhydrite and extremely thin organic material (< 0.1 mm); minor laminations

of lath-shaped anhydrite; organics < 1 %.

P-158-68 Anhydrite - massive; texture microcrystalline with some blocky and lath-shaped grains; organics < 1%.

P-158-69 Anhydrite - nodular; texture microcrystalline; nodules surrounded by lath-shaped and aligned felted grains; 95 % anhydrite; organics < 1%.

P-158-70 Anhydrite - nodular; texture microcrystalline; nodules surrounded by aligned -felted grains and thin, <<1 mm organic layers; organics < 1%.

P-158-71 Anhydrite - nodular; texture microcrystalline; nodules surrounded by aligned-felted grains and thin, << 1mm, organic layers; organics < 1 %.

P-158-72 Anhydrite - nodular to weakly laminated; texture microcrystalline; nodules surrounded by aligned-felted and thin << 1 mm organic layers; weak banding produced by alternations of microcrystalline and aligned-felted grains seperated by organic material << 1mm thick; organics < 1 %.

P-158-73 Anhydrite - nodular to weakly laminated; texture microcrystalline; nodules surrounded by blocky, felted and aligned felted grains; laminated appearance as in previous slide; organics 1 %.

P-158-74 Anhydrite - nodular to laminated; texture blocky to lath-shaped; nodules surrounded by aligned-felted and sub-felted grains; organics, internodular < 5 %.

P-158-75 Anhydrite - nodular; texture sub-felted to aligned-felted; nodules surrounded by very aligned-felted and lath-shaped grains, alignment very well defined, grains arranged with long axes parallel; organics < 1%.

P-158-76 Anhydrite - nodular; texture aligned-felted to sub-felted, alignment very well defined by anhydrite laths up to 1 mm long; organics < 1 % with silt-sized quartz.

P-158-77 Anhydrite - nodular; texture microcrystalline with aligned felted and sub-felted; pseudomorphs after gypsum; organics 5 %, with 30 % quartz silt in portions.

P-158-78 Anhydrite - nodular; texture microcrystalline with felted and aligned-felted; pseudomorphs after gypsum; organics < 5 %.

P-158-79 Anhydrite - nodular; texture very similar to previous slide; well defined anhydrite pseudomorphs after gypsum; organics < 5 %.

P-158-80 Anhydrite - nodular; texture aligned-felted,

felted, and blocky, nodules surrouded by aligned-felted grains, nodules displace dark brown organic material; organics < 5 %, with 10 % angular, quartz silt.

P-158-81 Anhydrite - nodular; texture felted to aligned-felted; pseudomorphs after gypsum; organics < 5 %.

P-158-82.2 Anhydrite - nodular; texture microcrystalline with felted; pseudomorphs after gypsum; organics very dark brown, < 5 %.

P-158-85.2 Anhydrite - nodular; texture felted and aligned-felted with microcrystalline; well defined coarse, lath-shaped anhydrite pseudomorphs after gypsum, organics < 3 %.

P-158-90.2 Anhydrite - nodular to massive; texture microcrystalline to blocky; pseudomorphs after gypsum; organics < 5 %.

P-158-91 Anhydrite - nodular; texture coarse, lath-shaped; organics very dark brown, < 5 %, with quartz silt < 5%.

P-158-92 Anhydrite - nodular; texture microcrystalline with isolated lath-shaped grains; pseudomorphs after gypsum; organics < 5 %.

P-158-93 Anhydrite - nodular to laminated; texture aligned-

felted to felted; very well defined alignment of anhydrite laths; anhydrite "nodules" with blocky to lath-shaped textures in very well aligned portions; anhydrite pseudomorphs after gypsum; organics < 5 %, with quartz silt 30 to 40 %.

P-158-94 Anhydrite - nodular; texture aligned-felted to felted; pseudomorphs after gypsum; organics < 5 %.

P-158-95 Anhydrite - nodular; texture aligned-felted to felted; organics, very dark brown, with 10 % quartz silt.